CR-135185

NASA

Nasa Aeronautics and Space Administration

VARIABLE PITCH FAN SYSTEM

FOR

NASA/NAVY RESEARCH AND TECHNOLOGY AIRCRAFT

BY

W. P. RYAN, D. M. BLACK, A. F. YATES

(NASA-CR-135185) VARIABLE PITCH FAN SYSTEM FOR NASA/NAVY RESEARCH AND TECHNOLOGY AIRCRAFT (Hamilton Standard, Windsor Locks, Conn.) 29 p HC A03/MF A01 CSCL 21I

N77-23105

Unclas

G3/07 26128

HAMILTON STANDARD
DIVISION OF UNITED TECHNOLOGIES CORPORATION

PREPARED FOR

NATIONAL AERONAUTICS AND SPACE ADMINISTRATION

NASA LEWIS RESEARCH CENTER
CONTRACT NAS3-20033

MAY 1977
RECEIVED
NASA STI FACILITY
INPUT BRANCH

Nasa Aeronautics and
Space Administration

VARIABLE PITCH FAN SYSTEM

FOR

NASA/NAVY RESEARCH AND TECHNOLOGY AIRCRAFT

BY

W. P. RYAN, D. M. BLACK, A. F. YATES

HAMILTON STANDARD
DIVISION OF UNITED TECHNOLOGIES CORPORATION

PREPARED FOR

NATIONAL AERONAUTICS AND SPACE ADMINISTRATION

NASA LEWIS RESEARCH CENTER
CONTRACT NAS3-20033

1 Report No NASA CR 135185	2 Government Accession No.	3 Recipient's Catalog No
4 Title and Subtitle VARIABLE PITCH FAN SYSTEM FOR NASA/NAVY RESEARCH AND TECHNOLOGY AIRCRAFT		5 Report Date April 1977 6 Performing Organization Code
7 Author(s) W. P. Ryan, D. M. Black, A. F. Yates		8 Performing Organization Report No 10 Work Unit No
9 Performing Organization Name and Address Hamilton Standard Division of United Technologies Windsor Locks, Conn. 06096		11 Contract or Grant No. NAS3-20033
12 Sponsoring Agency Name and Address National Aeronautics and Space Administration Washington, D. C. 20546		13 Type of Report and Period Covered Contractor Report 14 Sponsoring Agency Code
15 Supplementary Notes Project Manager, Albert G. Powers, Propulsion Systems Project Office, NASA Lewis Research Center, Cleveland, Ohio 44135		

16 Abstract

Preliminary design of a shaft driven, variable-pitch lift fan and lift-cruise fan was conducted for a V/STOL Research and Technology Aircraft. The lift fan and lift-cruise fan employed a common rotor of 157.5 cm (62 inch) diameter, 1.18 pressure ratio variable-pitch fan designed to operate at a rotor tip speed of 284 mps (932 fps).

Preliminary definitions were coordinated for lift fan/aircraft and lift-cruise fan/engine interfaces.

Fan performance maps were prepared and detailed aerodynamic characteristics were established. Cost/weight/risk trade studies were conducted for the blade and fan case. Structural sizing was conducted for major components and weights determined for both the lift and lift-cruise fans.

17 Key Words (Suggested by Author(s)) Lift Fan Lift-Cruise Fan Variable Pitch V/STOL (Vertical/Short Takeoff and Landing) RTA (Research and Technology Aircraft)	18 Distribution Statement Unclassified - Unlimited		
19 Security Classif (of this report) Unclassified	20 Security Classif (of this page) Unclassified	21 No of Pages 90	22 Price*

* For sale by the National Technical Information Service, Springfield, Virginia 22161

NASA-C-168 (Rev. 10-75)

CONTENTS

ILLUSTRATIONS

ILLUSTRATIONS (Cont)

TABLES

SYMBOLS AND ABBREVIATIONS

B	chord
B/A1	Boron/Aluminum
BMAD (BAC)	Boeing Military Airplane Division
Cps	cycles per second
CA	Circular Arc
cm	centimeter
Df	diffusion factor
DCA	Double Circular Arc
DDA	Detroit Diesel Allison
deg	degree
fps	feet per second
FPR	fan pressure ratio
FOD	Foreign Object Damage
ft	feet
gpm	gallon per minute
Hz	hertz
in	inch
kg	kilogram
$K\theta$	circumferential distortion index
KR	radial distortion index
kw	kilowatt
KSI	thousand pounds per square inch
KN	thousand newtons
Kt	Knots
LeRC	Lewis Research Center
lb	pound
mps	meter per second
Mm	Meridianal mach number
Mr	relative mach number
Ma	absolute mach number
mm	millimeter
McAir	McDonnell Aircraft Company
M	Meter
$N/\sqrt{\theta}$	Corrected speed
NASA	National Aeronautics & Space Administration
N	newtons
P/P	Stagnation pressure ratio
P_R	Pressure ratio
P	Stagnation Pressure
psi	pound per square inch
RPM	Revolutions per minute
rad	radians

SYMBOLS AND ABBREVIATIONS (Cont)

R_c	Rockwell hardness
RTA	Research and Technology Aircraft
R/R_T	blade station/blade tip radius
s	second
SOTA	State-of-the-Art
sec	second
SHP	Shaft horsepower
t/b	blade thickness ratio
Ti	Titanium
T/T	Stagnation temperature ratio
Vo	freestream velocity
V/STOL	Vertical/Short Take-Off and Landing
VP	Variable Pitch
z	loss coefficient
α	absolute air angle
β	relative air angle
θ	Tamb/519°R
θ *	camber angle
η	efficiency
η ad	adiabatic efficiency
β	Beta (fan blade angle)
$W\sqrt{\theta}/\delta A$	Corrected specific airflow
τ	gap

SECTION 1.0
SUMMARY

This report presents the results of design studies of shaft driven, variable-pitch lift and lift-cruise fans for use in the NASA/NAVY "V/STOL Research and Technology Aircraft Program". The work was conducted between May and December 1976 under NASA LeRC contract NAS3-20033.

The objective of these studies was to provide technical and program information for use by NASA and designated engine and airframe contractors working on V/STOL propulsion system and aircraft studies; i.e.; Detroit Diesel Allison (DDA), Boeing Military Aircraft Division (BMAD) and McDonnell Aircraft (McAir).

This work described herein builds upon the results of design studies conducted during 1975 by Hamilton Standard under NASA contract NAS3-19414. The earlier studies were aimed at providing parametric and point design data on lift and lift-cruise fans to support Boeing's studies of a Navy V/STOL operational aircraft.

The fan design covered herein for the current program is a 157.5 cm (62 in) diameter, 1.18 pressure ratio variable pitch fan designed to operate at a tip speed of 284 mps (932 fps).

Under the current program Hamilton Standard coordinated preliminary interface definitions with Detroit Diesel Allison relative to the lift-cruise fan for the XT701 engine; and with Boeing Military Aircraft Division and McDonnell Aircraft relative to the lift fan for their respective V/STOL aircraft configurations. An Interface Document was published which covered both the lift and lift-cruise fans.

Fan performance maps were prepared and detailed aerodynamic characteristics were established. Cost/Weight/Risk trade studies were conducted for the blade and fan case. Structural sizing was conducted for major components and weights determined for both the lift and lift-cruise fans.

SECTION 2.0
INTRODUCTION

Aircraft capable of vertical and short take off and landing have been the subject of study over an extended period of time, due to their attractiveness for a variety of commercial and military applications. One such application is a multi-mission Navy airplane envisioned to meet an operational requirement in the 1990's. The Navy operational vehicle and its related propulsion system were the subject of studies by several contractors, including Hamilton Standard, during 1975.

During 1976, airframe and propulsion system contractors were funded by NASA to study a V/STOL research and technology aircraft (RTA) which could be used to investigate and demonstrate the technology associated with the operational V/STOL aircraft. Two airframe contractors, BMAD and McAir, studied aircraft employing shaft driven, variable pitch fans. Both Hamilton Standard, under NASA LeRC contract NAS3-20033, and DDA supported these contractors with propulsion system technical data, i.e., weight, performance, interfaces, etc., and program planning information.

The RTA was to employ state-of-the-art (SOTA) technology and existing engines. The contractors using shaft driven variable pitch fans focused on three fan - three engine aircraft.

Both BMAD's and McAir's concepts employed two lift cruise fans adjacent to the aft fuselage and a single lift fan in the vehicle's nose which was stopped during forward flight. A significant difference between the propulsion system approaches was that Boeing's concept involved rotation of the direct-connected lift-cruise fan and core engine to deflect the thrust vector; while McAir deflected the nozzle of the lift-cruise fan while leaving the nacelle stationary.

The variable pitch fan concept which provides the basis for these and prior studies has an extensive background as the result of efforts by Hamilton Standard and NASA. This concept has been explored through model, component and full scale hardware for both ground and flight testing over the past ten years. Several of the models and full scale variable pitch fans associated with the development of this technology, are shown in figure 2-1.

The work described herein was aimed at investigating the variable pitch fan conceptually designed in 1975 for the operational aircraft, and making such modification as necessary to accommodate the requirements of the RTA.

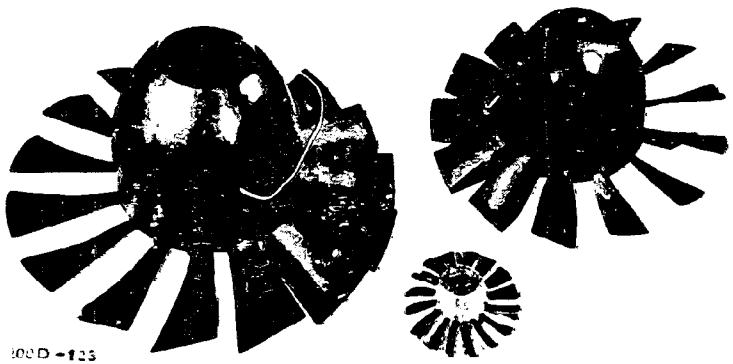

VARIABLE PITCH FANS

SIKORSKY BLACKHAWK
(FAN-IN-FIN)

C4164

Q-FAN® DEMONSTRATOR

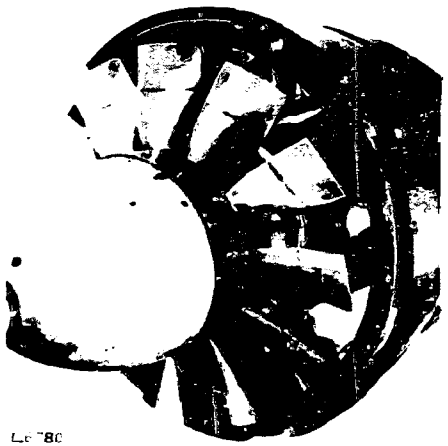

WINDTUNNEL TEST MODEL

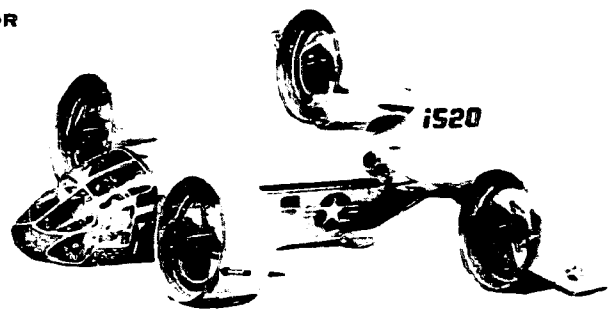

L4721

BELL X-22A

FIGURE 2-1. VARIABLE PITCH FAN BACKGROUND

2.0 (Continued)

For the RTA, three turboshaft engines will collectively drive three Variable Pitch (VP) fans through interconnecting shafting. Two fans, designed lift-cruise, are located on each side of the aft fuselage, directly coupled to the side mounted engines (figure 2-2). The third fan, designated lift fan, is remotely mounted in the aircraft nose and is driven by a third engine (not shown). As mentioned earlier the lift fan only operates during the V/STOL mode. Hamilton Standard has responsibility for the lift-cruise fan rotor assembly and rotor control regulators and the complete lift fan system.

The VP Lift Fan System is made up of four (4) major components:

- Rotor Assembly
- Beta Regulator
- Gear Reduction Assembly
- Fan Case

The Rotor Assembly consists of the blades, disc, variable pitch actuator, and spinner (figure 2-3). The Beta Regulator is an electrohydraulic control unit which changes the fan blade pitch according to a given input command. The Gear Reduction Assembly is incorporated in the lift fan and contains a bevel gear/cross shaft system to drive the fan from the aft mounted engines. The Fan Case is the structural mounting member of the fan assembly. The fan stators are attached to the outer shell and position the rotor housing.

This report contains preliminary technical data on the Variable Pitch Fans for the NASA/NAVY Research and Technology V/STOL Aircraft.

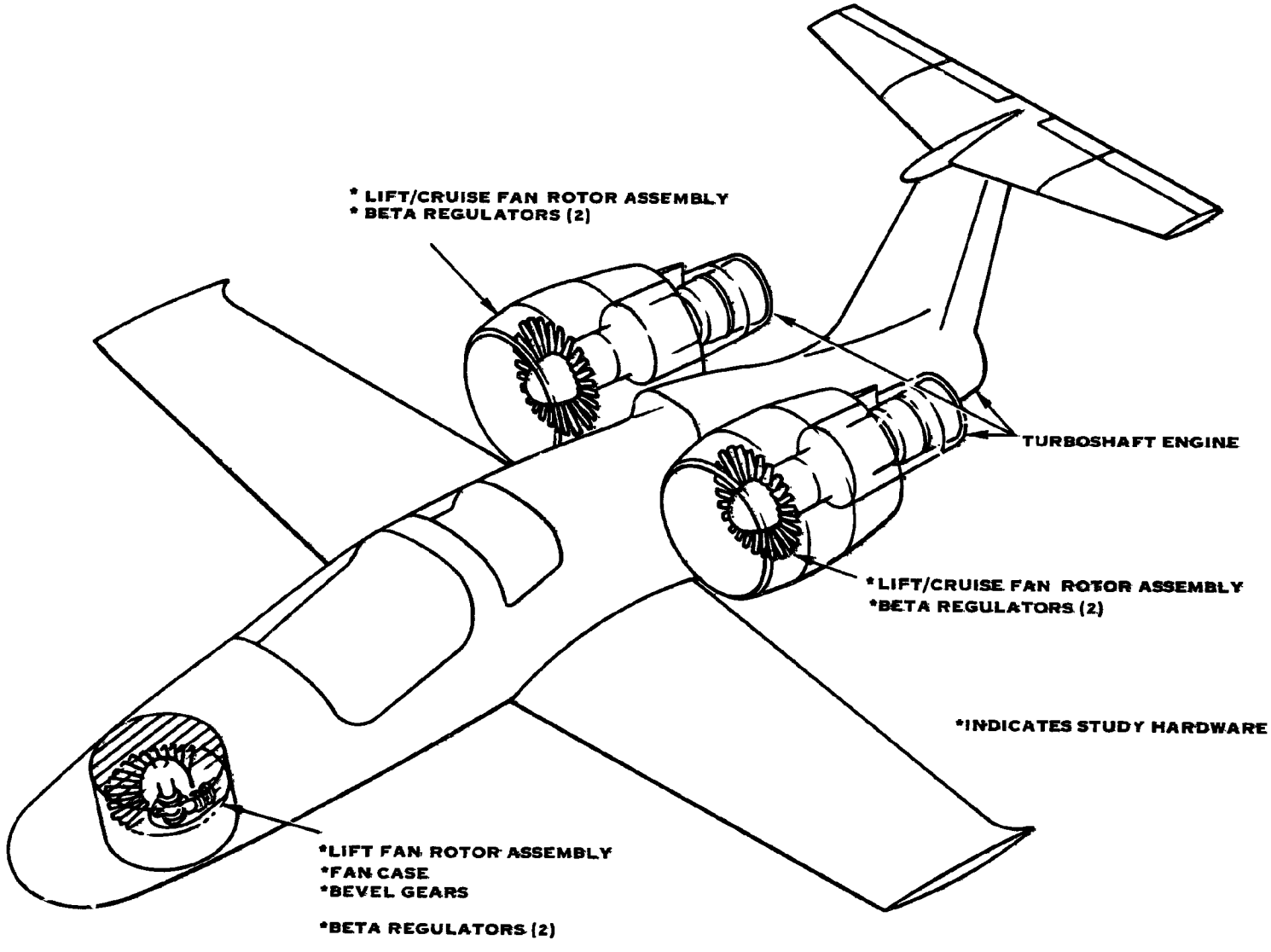

Figure 2-2. Conceptual PTA Design

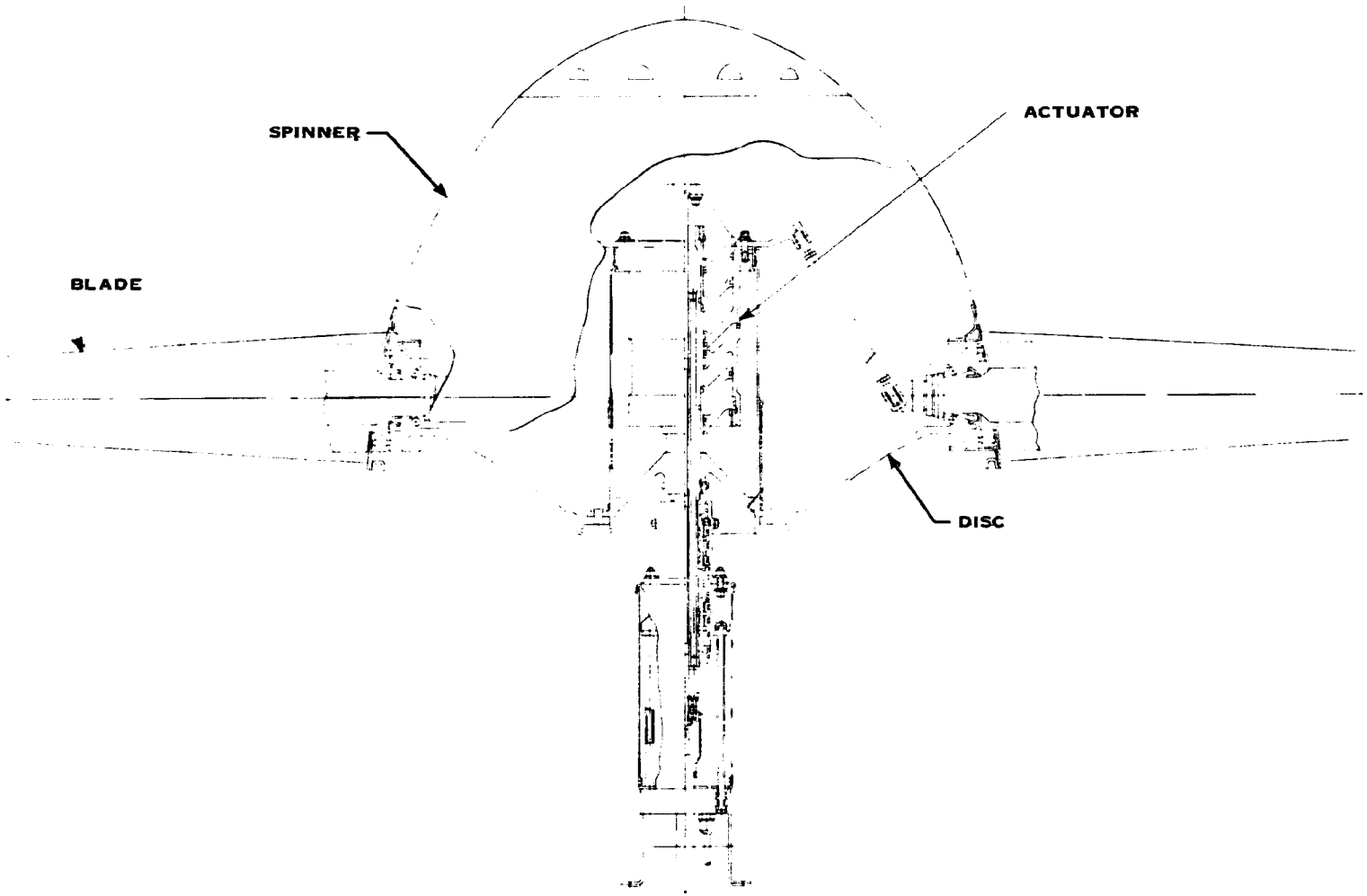

Figure 2-3. Fan Rotor Assembly

SECTION 3.0
INTERFACE DEFINITION - TASK I

The initial task conducted under the V/STOL fan study program was to identify and define the interfaces associated with the lift and lift-cruise fans, in areas such as performance, mounting, cooling, control requirements and mechanical, electrical and hydraulic interconnections. The lift-cruise fan-engine interface was coordinated with DDA; and lift fan-aircraft interfaces were coordinated with both BMAD and McAir.

Both Hamilton Standard and DDA (contract NAS3-20034) had contractual requirements to provide NASA with an Interface Document identifying interfaces and defining those interfaces which were established during the preliminary design study. An interface document was jointly prepared which covered both the lift-cruise and lift fans. The Interface Document which is contained in Appendix A, was preliminary in that all interfaces would not be defined during the design study. In this document the interfaces which were not finalized during the design study are indicated as "TBD".

During the study, agreement was reached on a number of specific interfaces which are defined on the three drawings noted below. Separate drawings were required for the respective Boeing and McAir lift fan installations because the drive shaft angle was different for their applications. A value of 105° was selected by McAir and 100° was selected by Boeing.

Figure	Item	Drawing No.
3-1	Lift Cruise Fan Rotor	SK 92250
3-2	Lift Fan - Boeing	SK 92252
3-3	Lift Fan - McAir	SK 92251

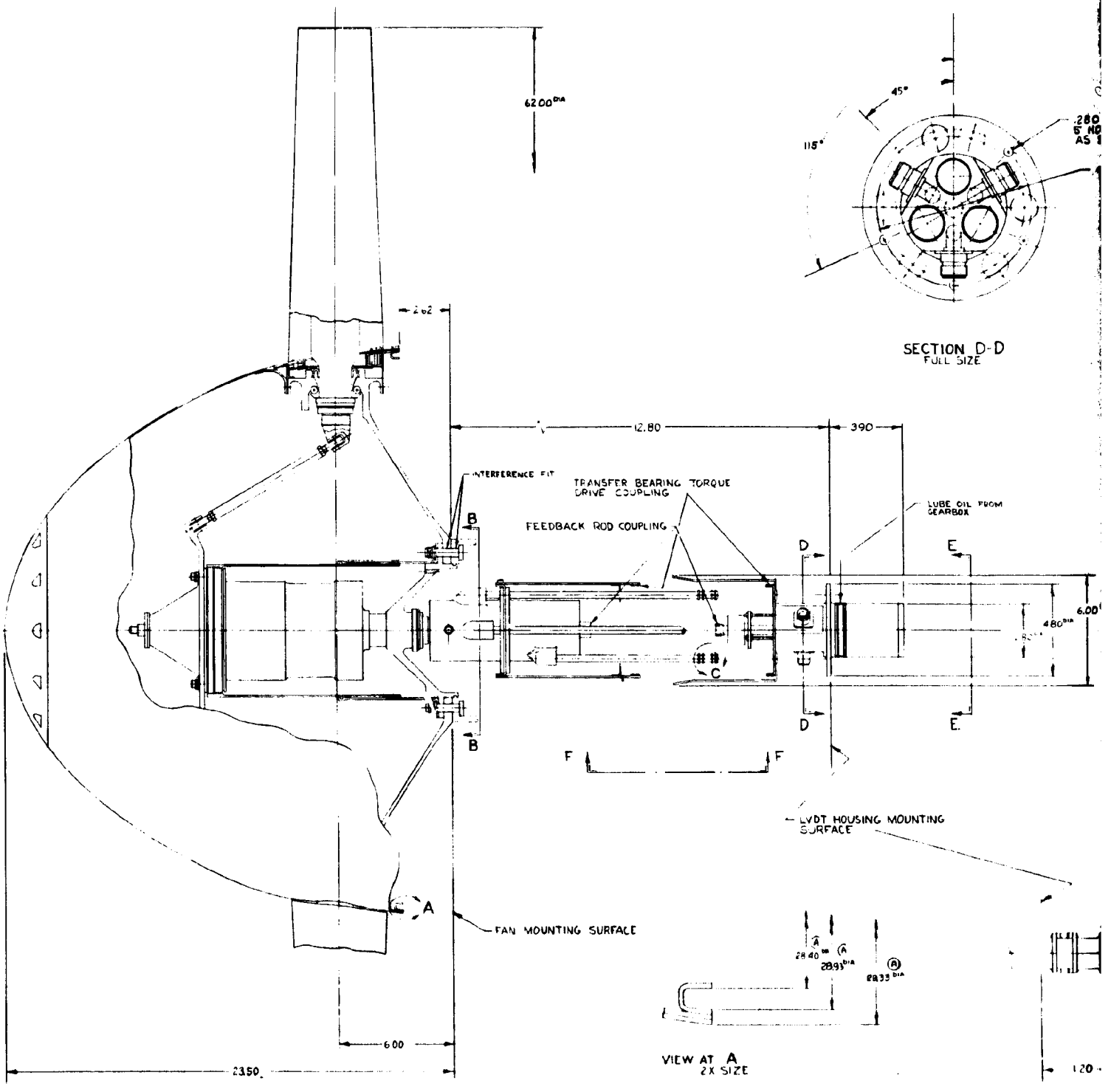

Figure 3-1. Lift Cruise Fan Rotor (HS Drwg SK92250)

FOLDOUT FRAME

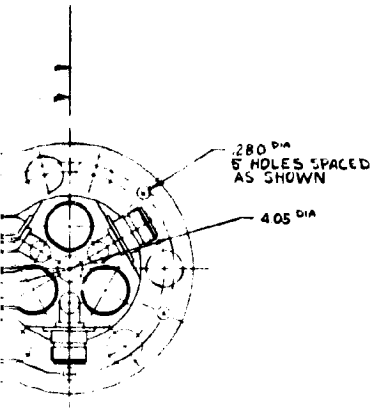

CTION D-D
FULL SIZE

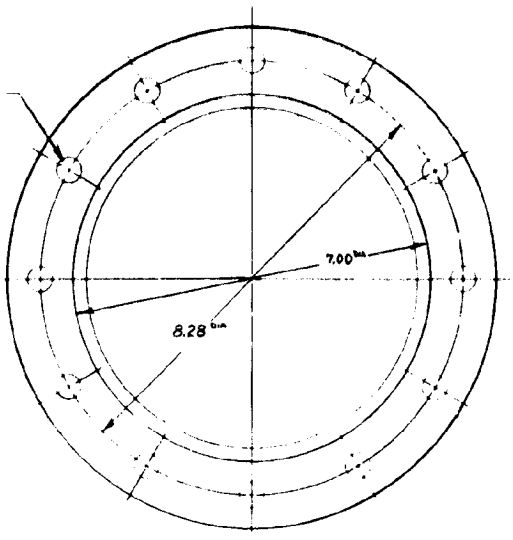

SECTION B-B

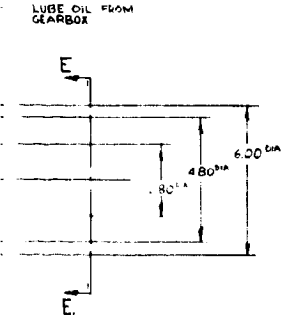

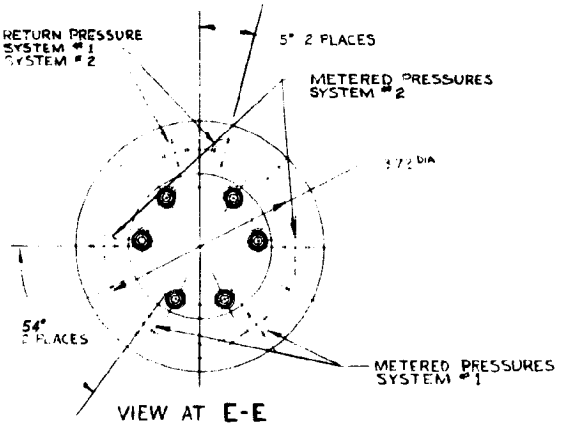

VIEW AT E-E

TING

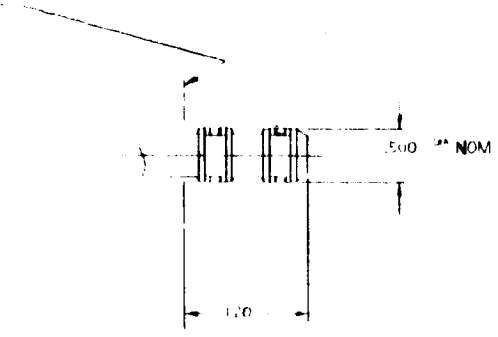

VIEW AT C
2X SIZE
6 PLACES

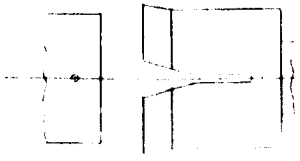

VIEW AT F-F
DETAIL OF ANGULAR POSITIONING
SLOT AND PIN

FOLDOUT FRAME 2

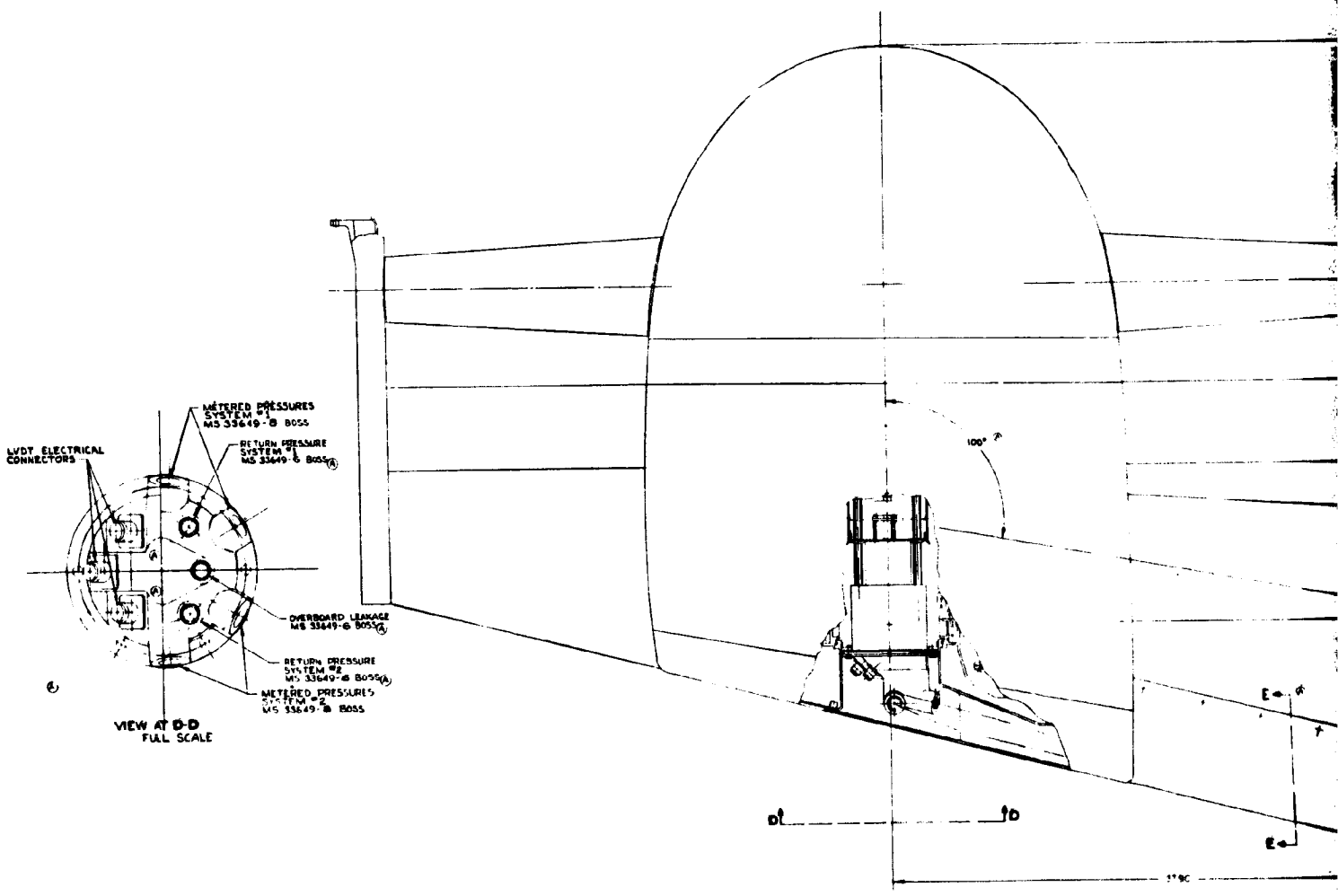

Figure 3-2. Lift Fan - Boeing (HS Drwg SK92252)

FOLDOUT FRAME

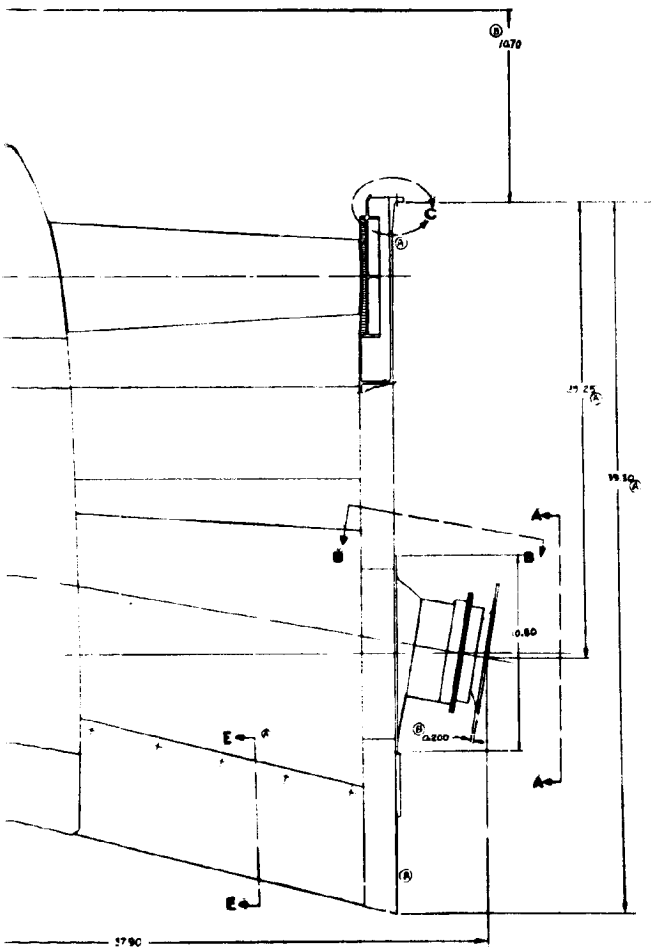

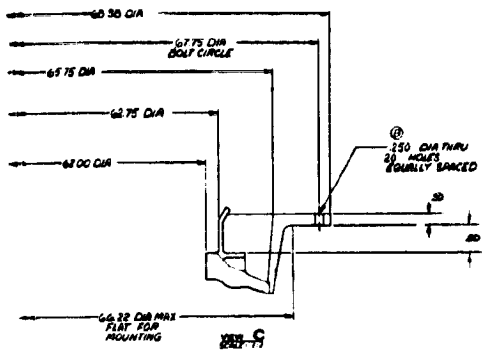

VIEW C

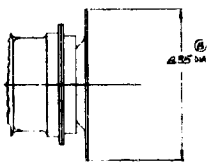

VIEW B-B

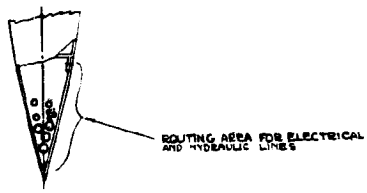

VIEW E-E

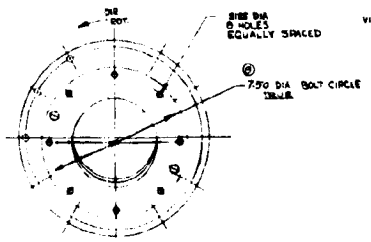

VIEW A-A

FOLDOUT FRAME

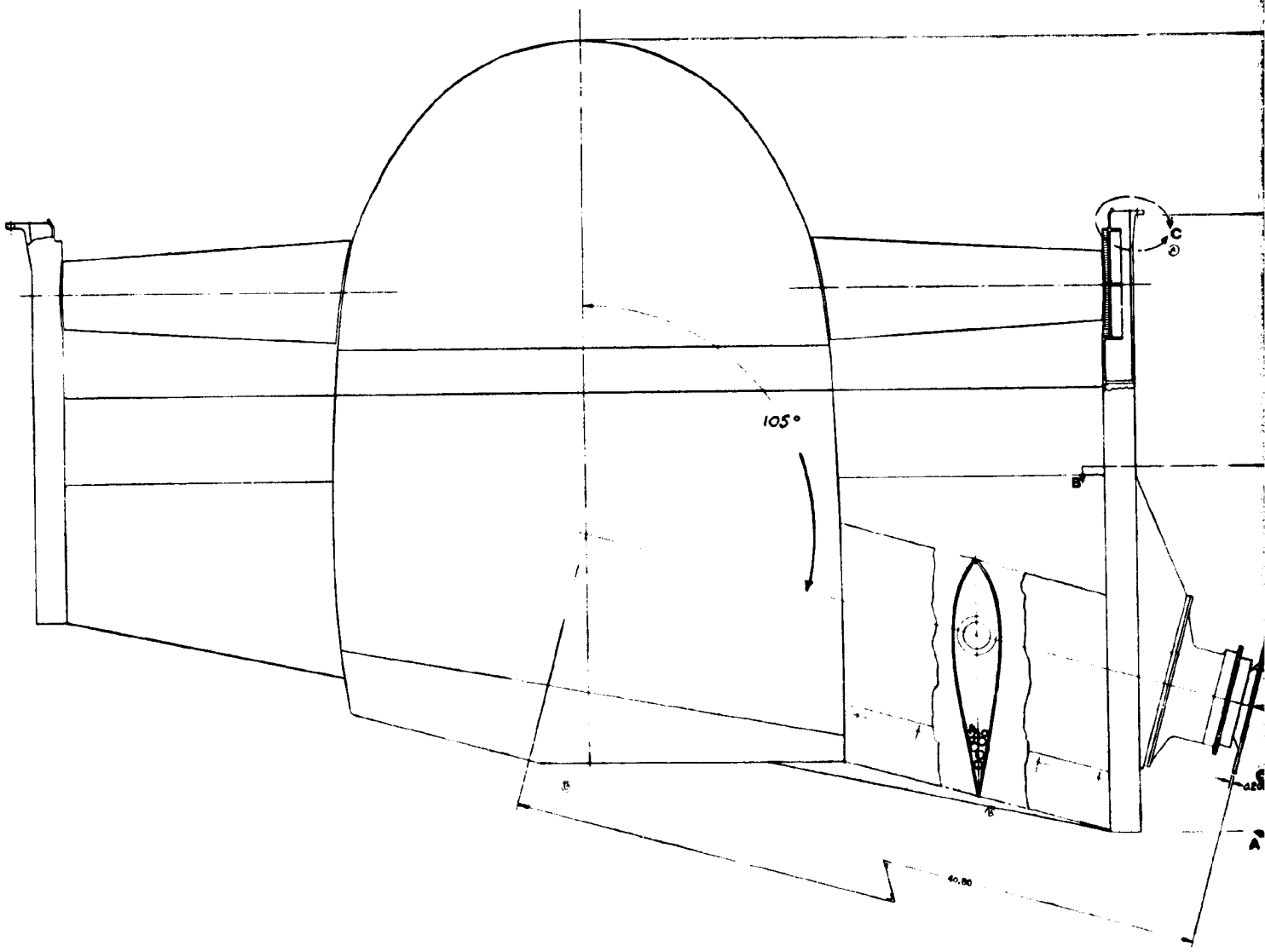

FOLDOUT FRAME 1

Figure 3-3. Lift Fan – McAir (HS Drwg SK92251)

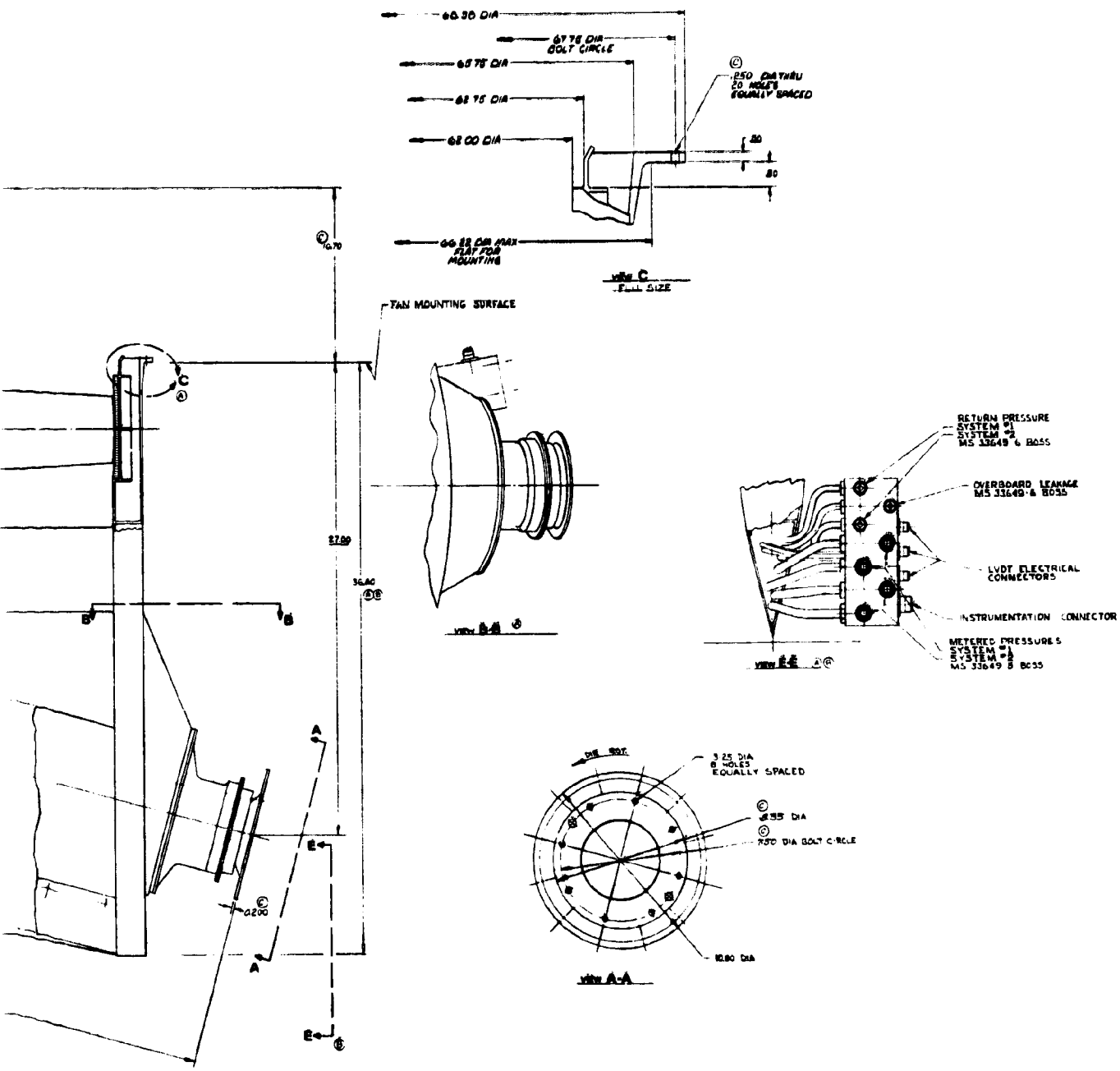
68.30 DIA
67.75 DIA BOLT CIRCLE
65.75 DIA
65.75 DIA
65.00 DIA
.250 DIA THRU 50 HOLES EQUALLY SPACED
.50
.80
64.52 DIA MAX FLAT FOR MOUNTING
VIEW C
FULL SIZE
FAN MOUNTING SURFACE
27.00
36.40
VIEW B-B
RETURN PRESSURE SYSTEM #1 SYSTEM #2 MS 33649-6 BOSS
OVERBOARD LEAKAGE MS 33649-6 BOSS
LVDT ELECTRICAL CONNECTORS
INSTRUMENTATION CONNECTOR
METERED PRESSURES SYSTEM #1 SYSTEM #2 MS 33649-8 BOSS
VIEW E-E
DRILL 90°
3.25 DIA 8 HOLES EQUALLY SPACED
.855 DIA
.750 DIA BOLT CIRCLE
10.80 DIA
VIEW A-A

FOLDOUT FRA

SECTION 4.0
PRELIMINARY DESIGN STUDY - TASK II

A preliminary design study was conducted to refine the 1.575 m (62 in.) diameter operational fan design concept (reference NASA CR-134988) to mee he requirements of the NASA/NAVY Research and Technology Aircraft (RTA).

This work consisted of three major subtasks. The initial item was a cost trade-off study to define where weight, life, risk or durability might be traded-off to reduce the program cost. The second item was to perform structural and aerodynamic analyses which would generate data needed by DDA, BMAD and McAir in their respective studies. The third item was to optimize the design configuration for the bevel gear/cross-shaft assembly with the objective of establishing commonality between the lift and lift-cruise fan's cross-shaft gearing.

4.1 COST TRADE-OFF STUDY

The lift and lift-cruise fans incorporate design features and materials aimed at providing the light weight, high structural integrity, reliability, safety and life required for a V/STOL application. While structural integrity, reliability and safety could not be compromised for a flight vehicle, development risk, weight and life were felt to offer viable trade-offs for a research and technology program.

The fan concepts were reviewed to identify areas where weight and/or life could be sacrificed to reduce cost. No areas were identified where cost/life or cost/risk trades would provide a significant program cost saving; however, two areas, the fan blades and fan case, were identified which offered promise of a significant cost saving at an increased weight.

The baseline fan blade construction incorporates a boron-aluminum (B/Al) shell and a solid titanium spar. This technology had been selected after a successful demonstration of its ability to meet the structural and environmental considerations of turbofan engines under several NASA and USAF-funded programs. The alternate constructions considered were: (1) composite blade with a fiberglass-epoxy shell, and a titanium spar; and (2) a solid titanium blade.

In the size of the V/STOL fan, the fiberglass shell did not have adequate bird strike tolerance. Its shell fabrication process is quite similar to that of the B/Al shell, and the titanium spar was common to both blades. The major cost difference between the two blade constructions was the higher tooling, process development and shell material cost of the B/Al composite blade. The cost savings were not large, however.

4.1 (Continued)

This blade construction had been developed for propeller blades of much larger size than the V/STOL fan blade where FOD is not a significant design consideration. Experimental work had demonstrated that for the much smaller fan blades the fiberglass shell had insufficient strength to transmit the loads associated with a bird strike to the spar. Therefore, for the V/STOL fan this blade would have an inadequate FOD tolerance. In light of low FOD tolerance and only modest program cost saving, this concept was discarded from consideration.

The solid titanium blade was initially evaluated as a direct replacement for the 26 composite blades. The titanium blade, however, did not have adequate stiffness resulting in critical speeds within the operating range as shown in figure 4-1. Reduction of the number of blades to 18 provided sufficient increased stiffness to remove the critical speeds from the operating range and this blade was used in the trade-off study. The loads associated with the 18 titanium fan blades were substantially increased over the B/Al blades. Centrifugal load was increased by 130% and the actuator loads increased by 480%. This increase resulted in major rotor mass increase of nearly 70% or 113 Kg (250 pounds). This value would be further compounded in the fan structural support weight.

The costs associated with each blade concept, including the unit blade cost, tooling and process development, were estimated. If was found that the solid titanium blade costs were significantly lower than those of the composite blade. As it was suspected that the large rotor weight increase associated with the titanium blade would affect the total fan cost, disc and actuator costs were estimated for a fan employing both solid titanium and B/Al blades. It was determined that the heavier disc and actuator associated with the solid titanium blade was considerably more expensive than similar hardware associated with the B/Al blades and essentially offset the savings of the blade.

The baseline fan case is a welded titanium structure employing the manufacturing technology which is used in current production turbofan engines. The design considered in the trade study was a fabricated aluminum structure which was riveted rather than welded. This concept resulted in a mass increase of 27 Kg (60 pounds). Unlike the blade, the fan case weight does not impact on other fan structure, therefore, the component weight increase is the total impact on the fan. Cost savings would result from the reduced tooling and manufacturing associated with the fabricated aluminum fan case.

Discussions were held with the airframe study contractors, Boeing and McDonnell, which indicated that the fan weights were critical and any increase in the fan weight would necessitate a weight reduction effort to remove a like amount from the airframe. Since identifiable lightweight concepts and materials had already been incorporated in the design, this would be a difficult and costly task. It was concluded that the lightweight concepts and materials, i.e., the B/Al fan blade and titanium fan case, selected during 1975's operational aircraft fan studies, contract no. NAS3-19414, were cost effective for a research and technology aircraft.

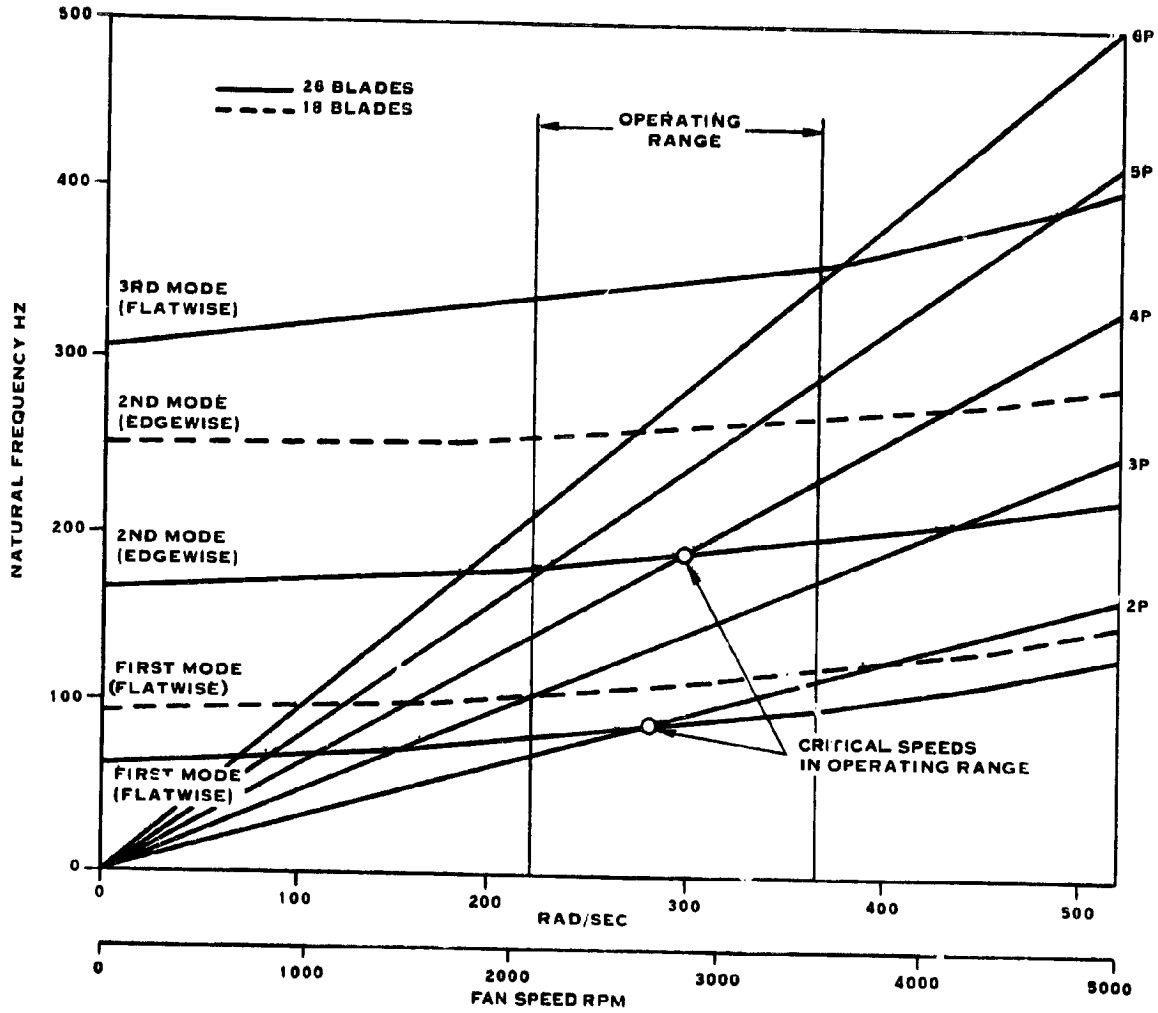

Figure 4-1. Solid Titanium Blade Critical Speeds

4.2 ROTOR PRELIMINARY DESIGN

The VP rotor preliminary design includes aerodynamic design and structural analyses. The variable pitch fan design selected during 1975 by BMAD for their V/STOL Operational Aircraft provided the basis for the rotor preliminary design. This fan as described in NASA report CR134988 had a pressure ratio of 1.2 and a diameter of 1.575 meters (62 in.).

4.2.1 Aerodynamic Analyses

The aerodynamic analysis was conducted to provide detail fan performance data to NASA V/STOL study contractors and to support the Hamilton Standard fan structural design with detail blade characteristics and aerodynamic loads. This analysis, as defined by the NASA Statement of Work, was to provide fan maps and supercharging performance at five different fan blade angles and to conduct a fan distortion analysis.

4.2.1.1 Fan Stage Performance - An objective of the VP fan design for the RTA was to retain, if possible, the fan aerodynamic design from BMAD's 1975 Operational Aircraft studies. The fan aerodynamic characteristics of this fan design are given in Table I.

The initial work under this study was to assess the ability of the existing Hamilton Standard fan design to meet the BMAD and McAir RTA performance requirements. Partial fan aerodynamic performance maps which had been prepared for four blade angles associated with the operational aircraft were expanded from a speed range of 95-105% to 60-110% for Δ blade angles, as referred to an angle of 0.863 radians (49.5°) at the 0.75 blade radius, $\Delta\beta$ = 0, 0.07, 0.127, and -0.071 radians ($\Delta\beta$ = 0°, 4°, 7.3° and -4.1°). Two new maps were produced to cover 25% to 70% corrected speed for $\Delta\beta$ = 0 and $\Delta\beta$ = -0.30 radians (-17.2°). These maps were an extension of an existing design which employed a flow path, shown in figure 4-2, for the operational aircraft. It was judged that refinement of the flow path from the 9.5 BPR of the operational aircraft to the 13.5 BPR of the RTA was not warranted because it would not significantly affect the maps.

These blade angles were selected based on the fan performance required to meet the several operating conditions of the RTA. Fan root performance maps for engine supercharging were also developed for the same blade angles. The fan performance maps with adiabatic efficiencies, stall lines and choke lines are given in figures 4-3 through 4-14. Based on the expanded maps, DDA calculated the propulsion system performance for both the BMAD and McAir aircraft which is provided in table II.

Fan aerodynamic characteristics at a fan P_R = 1.181 and $w\sqrt{\theta}/\delta A$ = 176.7 kg/sec/m^2 (36.2 lb/sec/ft^2) for the rotor, by-pass stator and engine stator are given in table III.

Table I
Fan Stage Characteristics

		Rotor Blades	By-Pass Stators	Engine Stators
Number of blades		26	10	87
Airfoil		DCA	65/CA	65/CA
Solidity:	tip	0.83	0.83	1.67
	root	1.41	1.30	1.85
Thickness ratio:	tip	0.03	0.09	0.09
	root	0.12	0.09	0.09
Aspect ratio:	tip	2.73	0.75	1.10
	root	3.52	0.75	1.10
Radius Hub/Radius Tip		0.425		

DCA - Double Circular Arc
65/CA - 65 Thickness distribution on circular arc camber line.

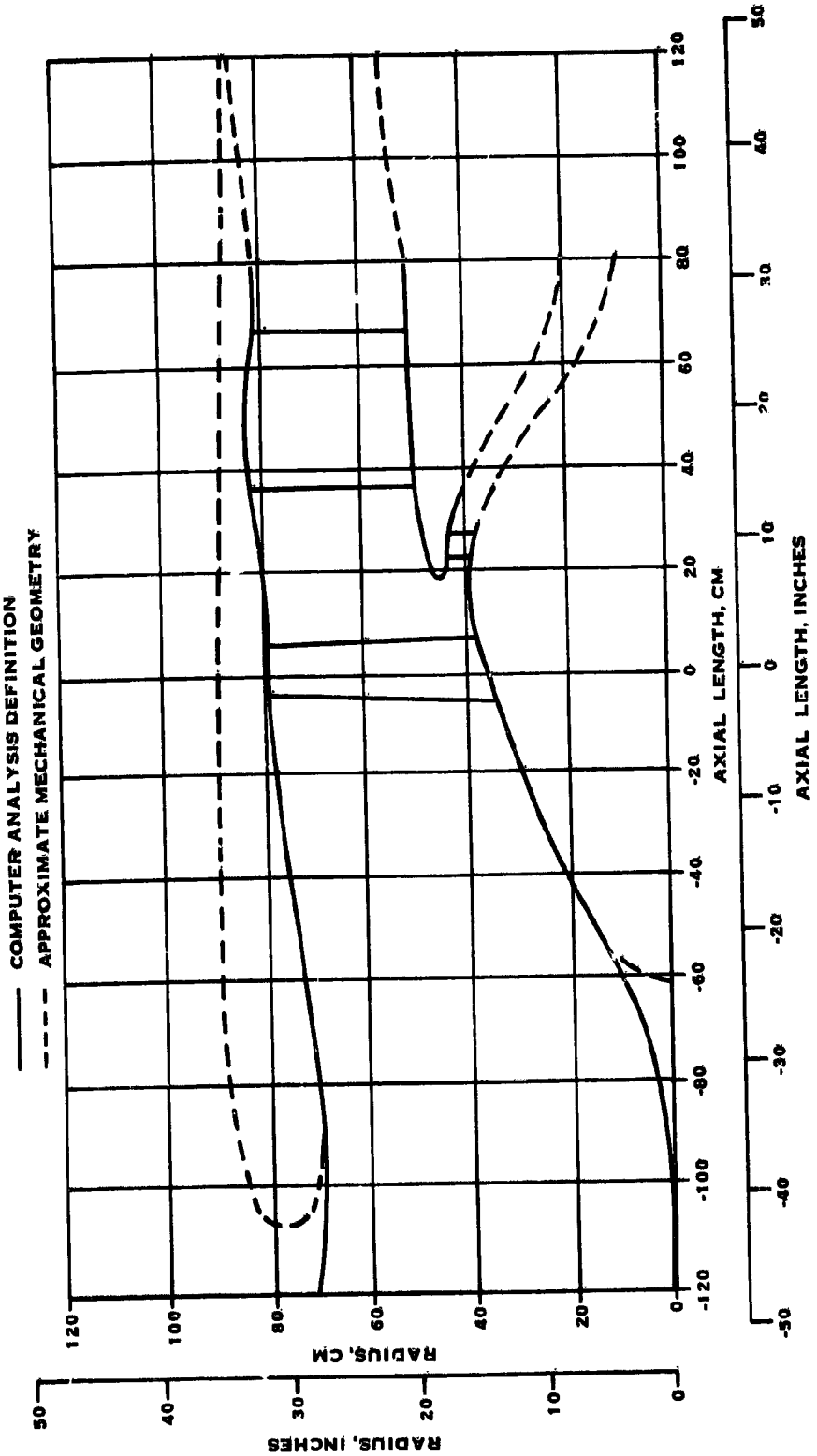

Figure 4-2. Lift/Cruise Fan Flowpath

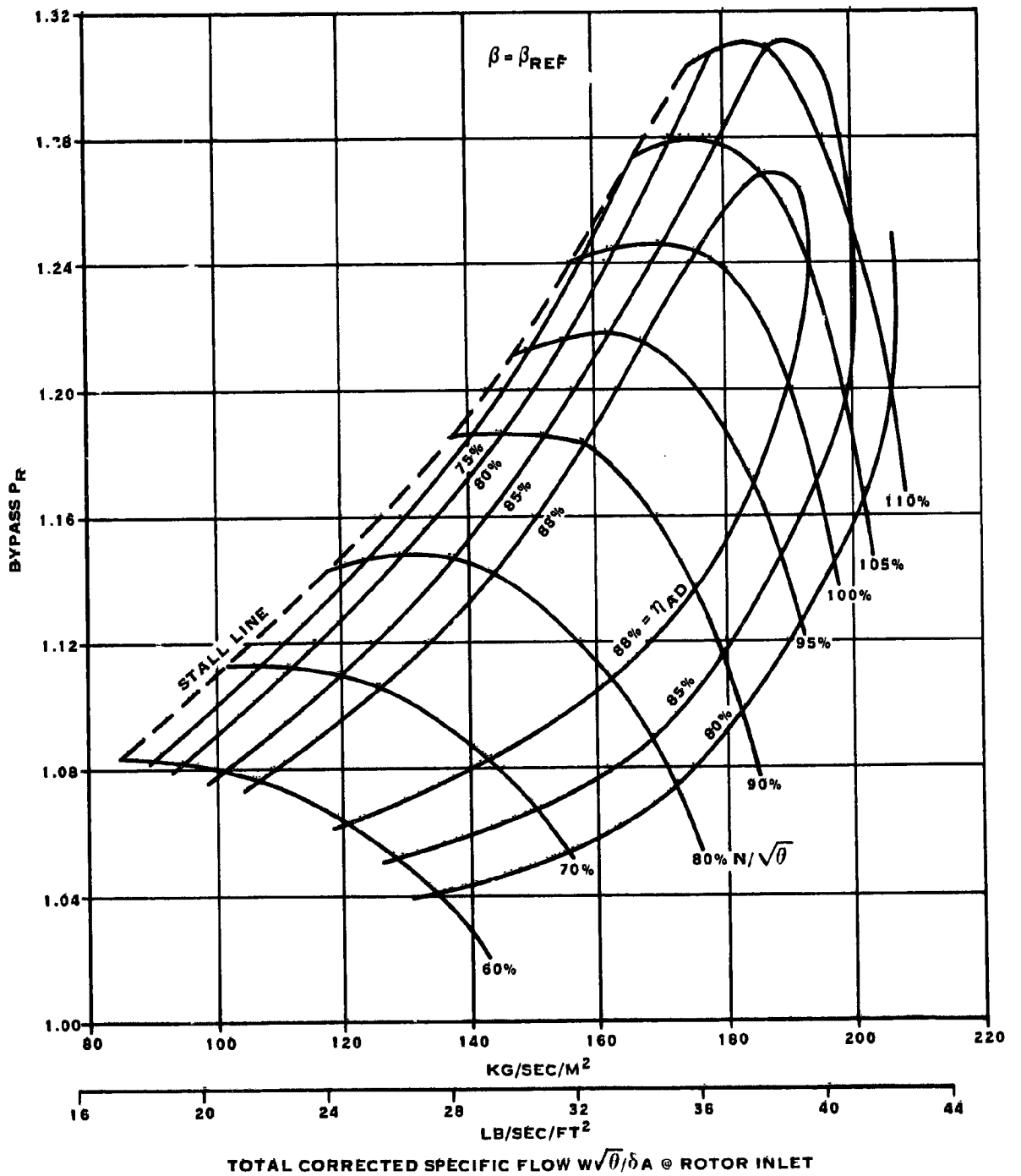

Figure 4-3. Lift/Cruise Fan Performance

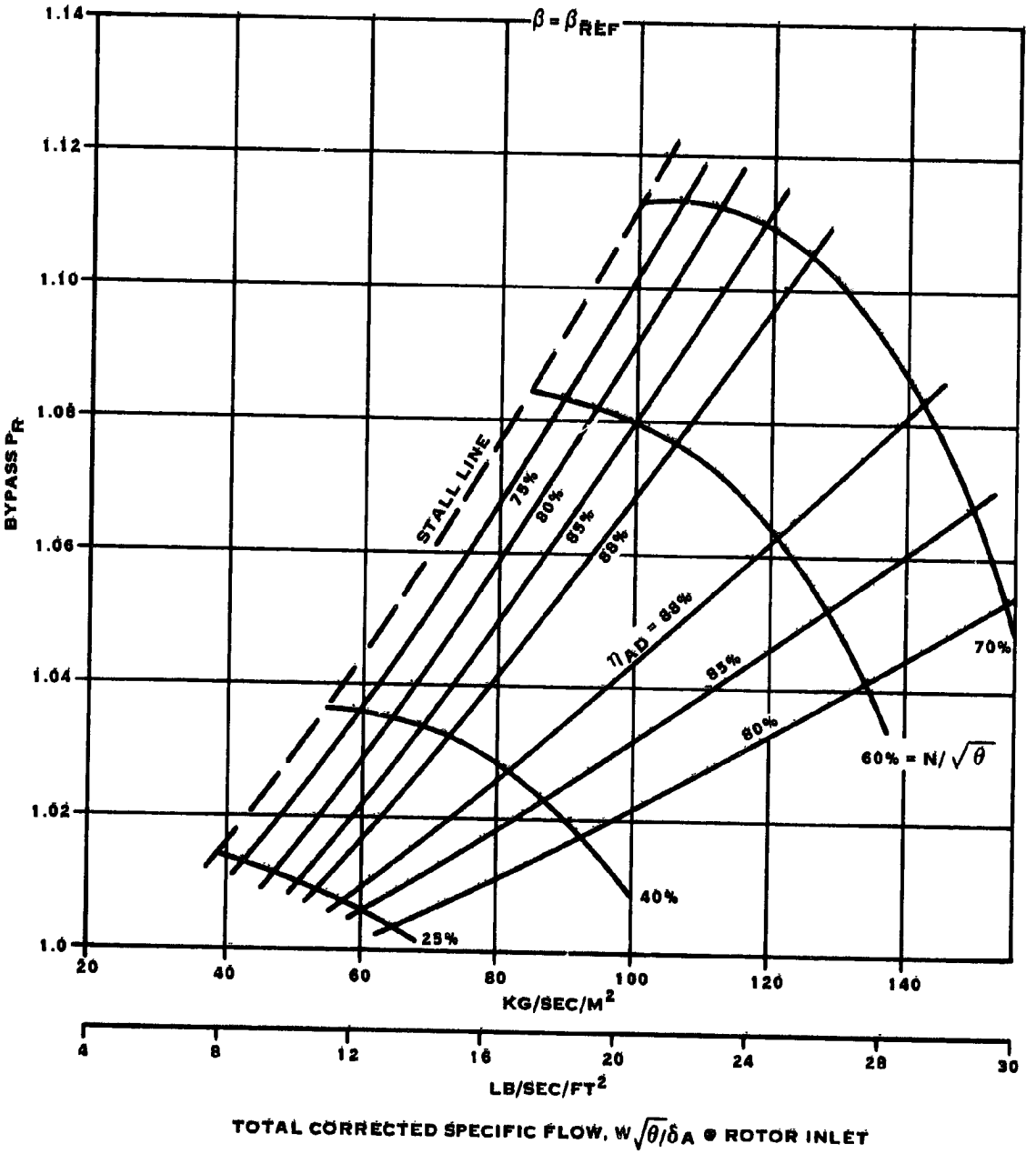

Figure 4-4. Lift/Cruise Fan Performance

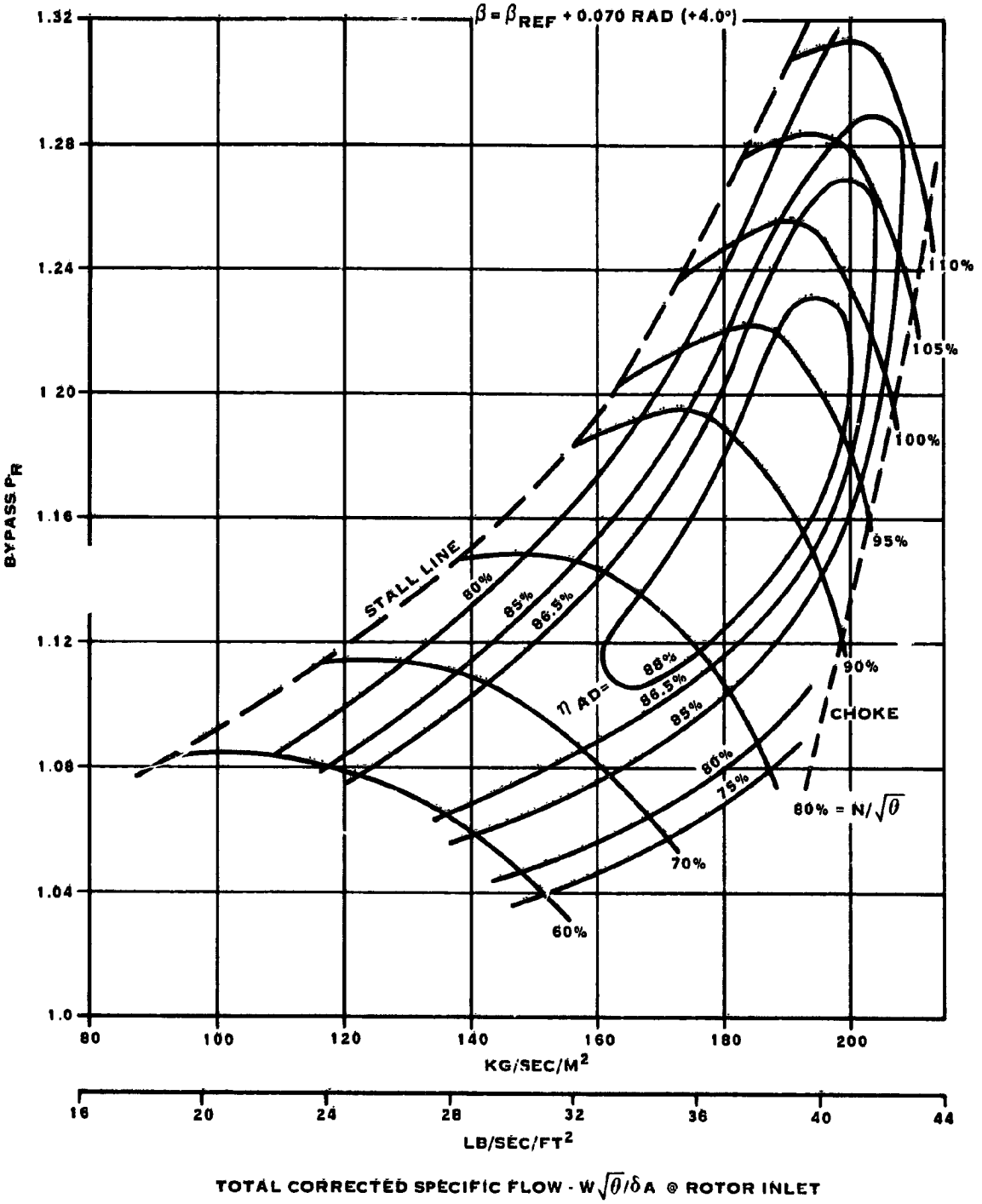

Figure 4-5. Lift/Cruise Fan Performance

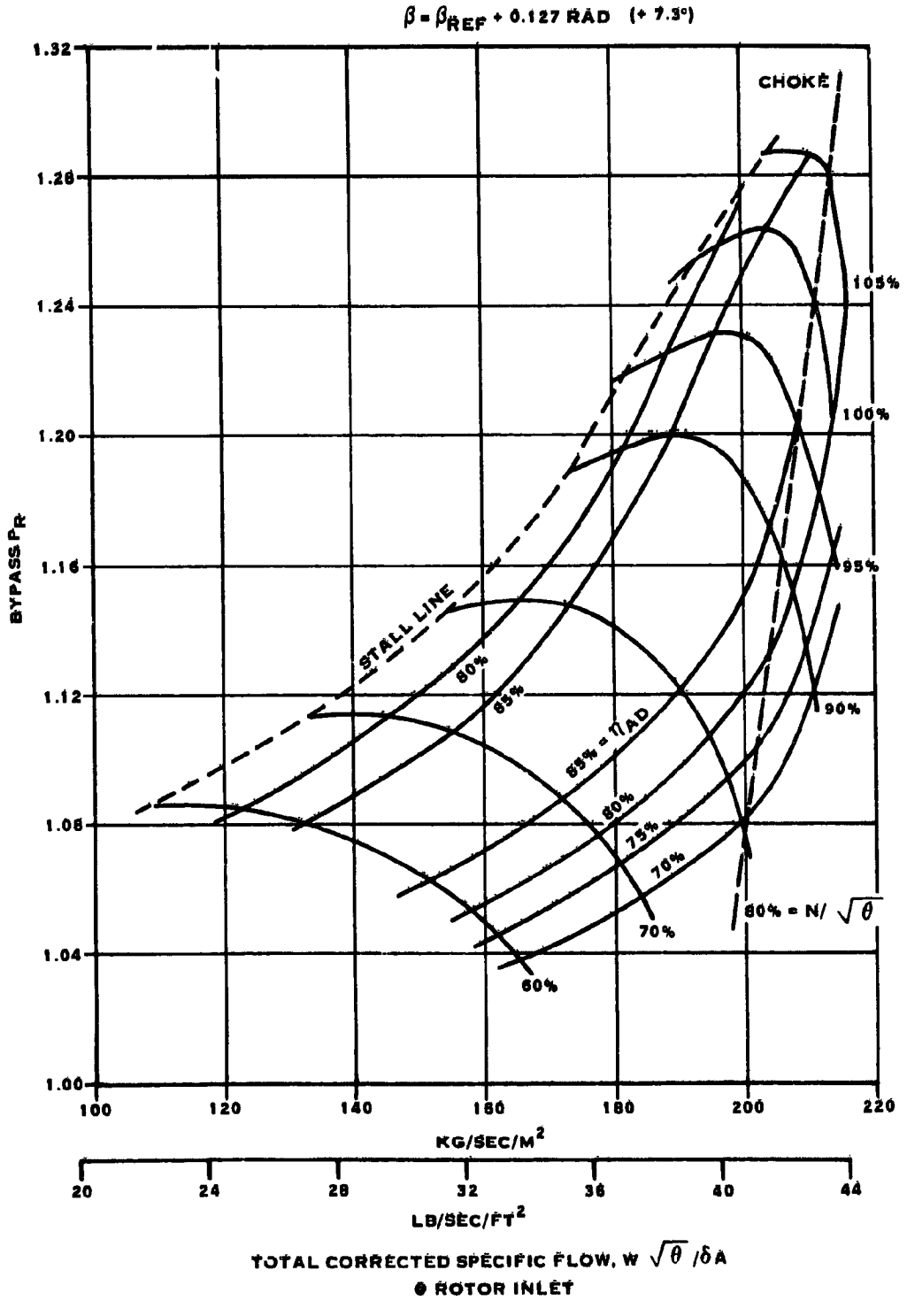

Figure 4-6. Lift/Cruise Fan Performance

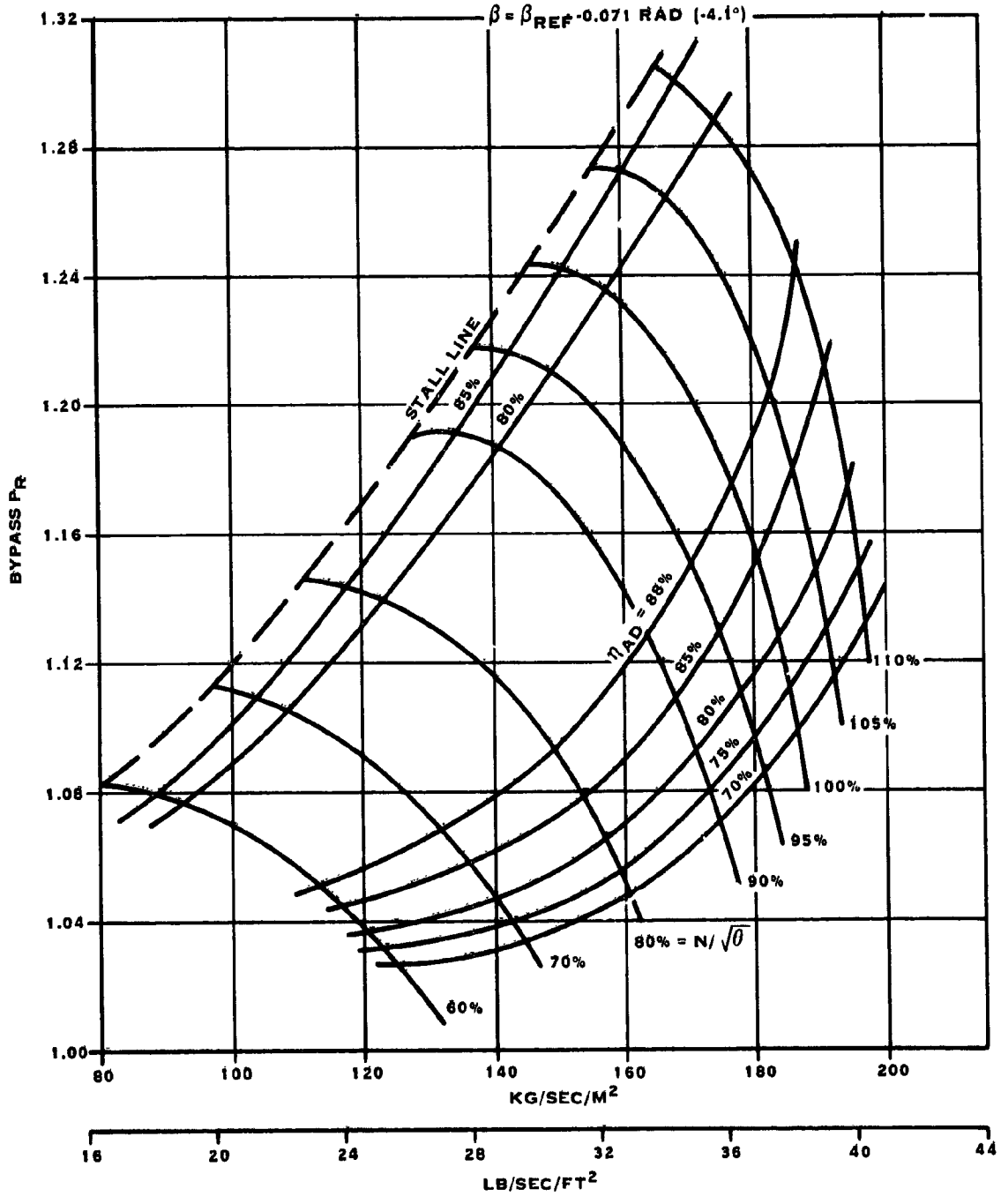

Figure 4-7. Lift/Cruise Fan Performance

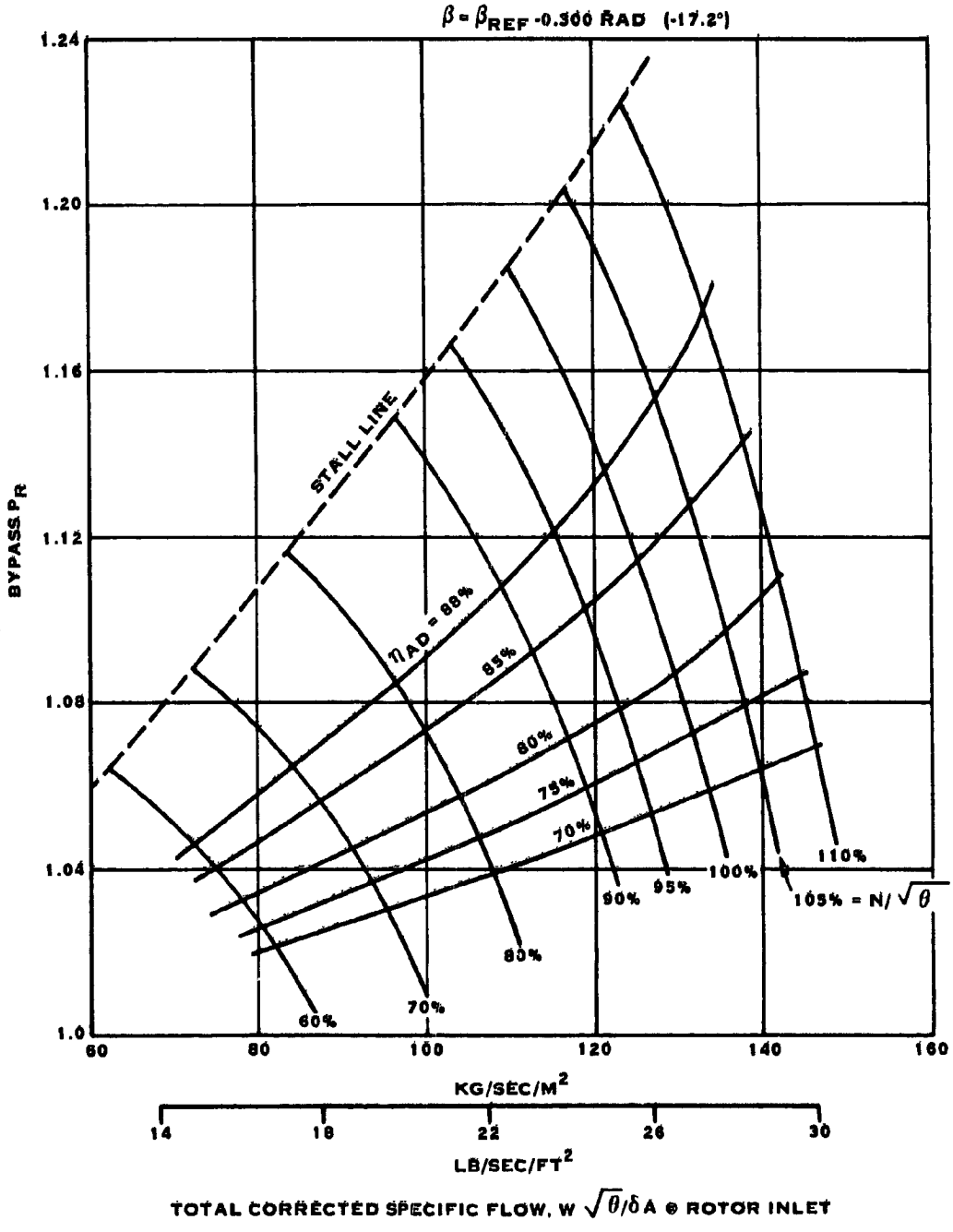

Figure 4-8. Lift/Cruise Fan Performance

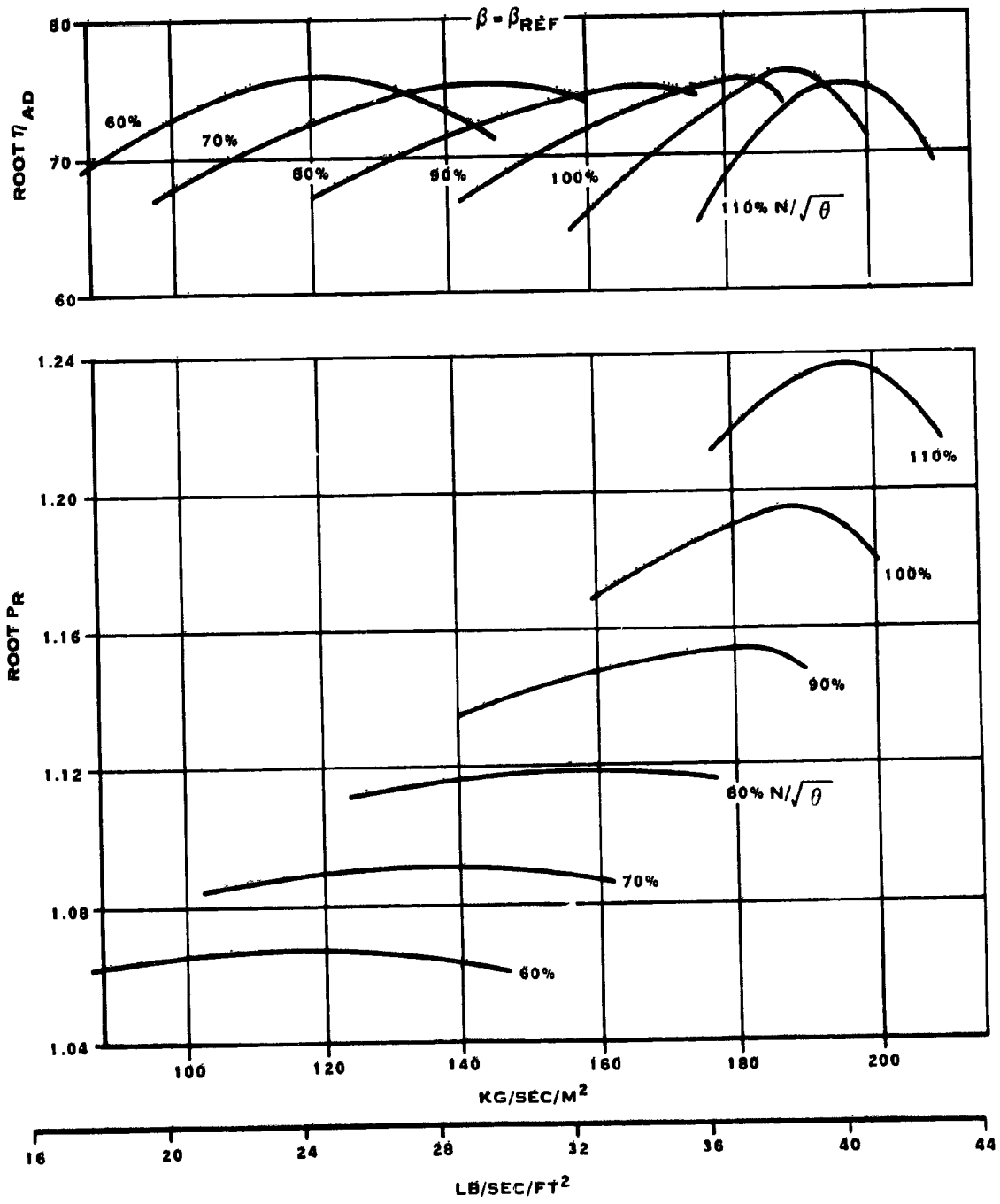

Figure 4-9. Lift/Cruise Fan supercharge performance

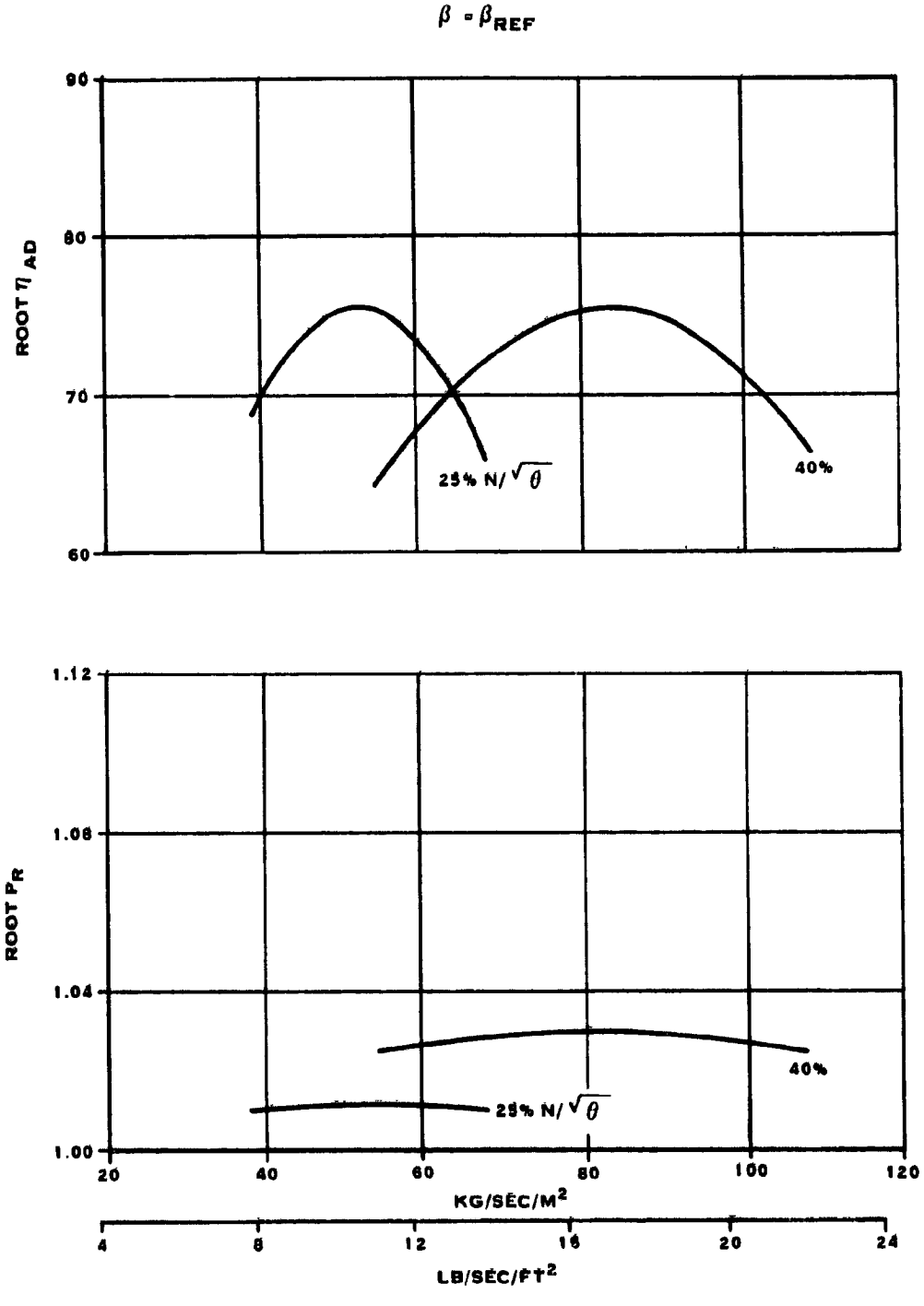

Figure 4-10. Lift/Cruise Fan Supercharge Performance

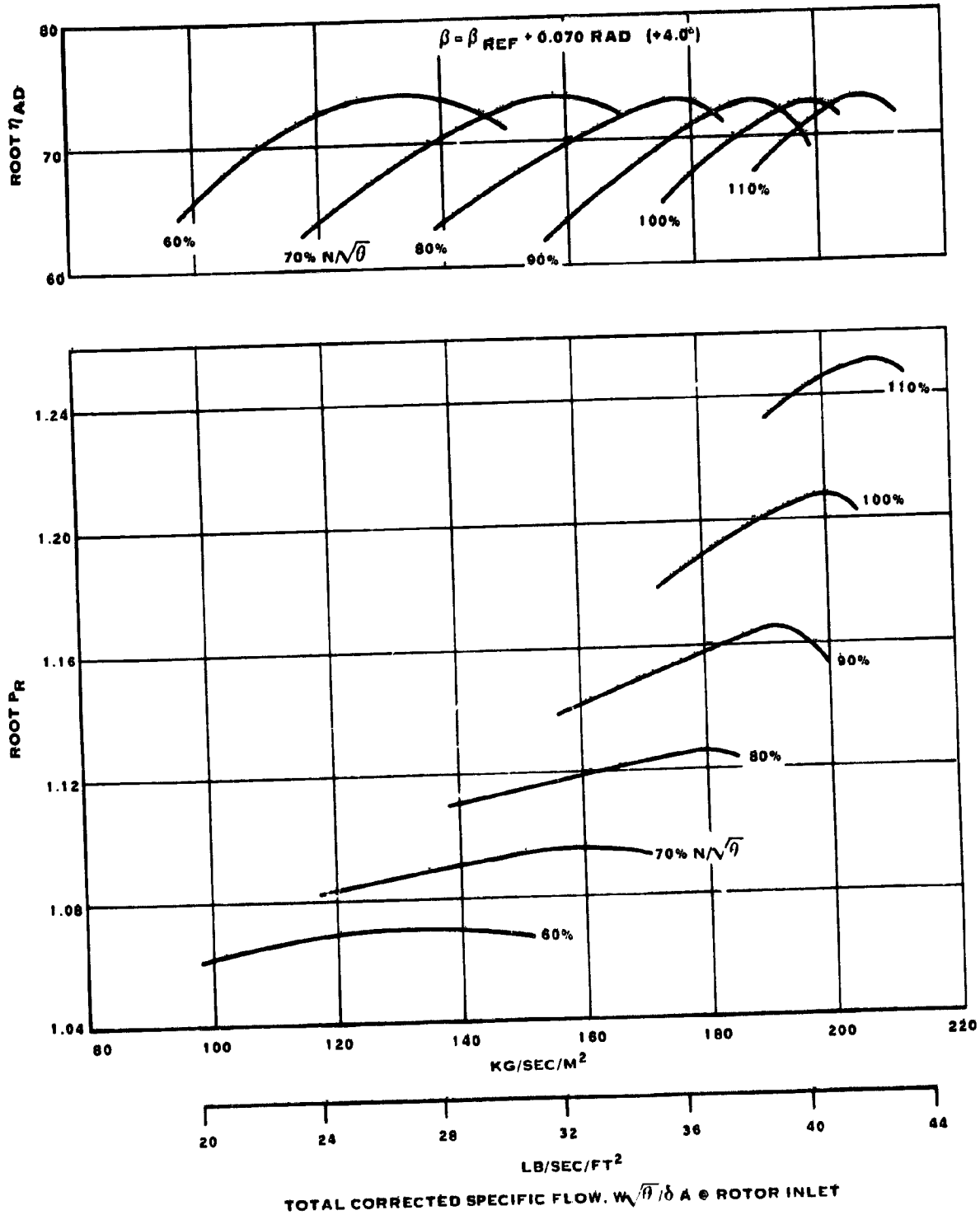

Figure 4-11. Lift/Cruise Fan Supercharge Performance

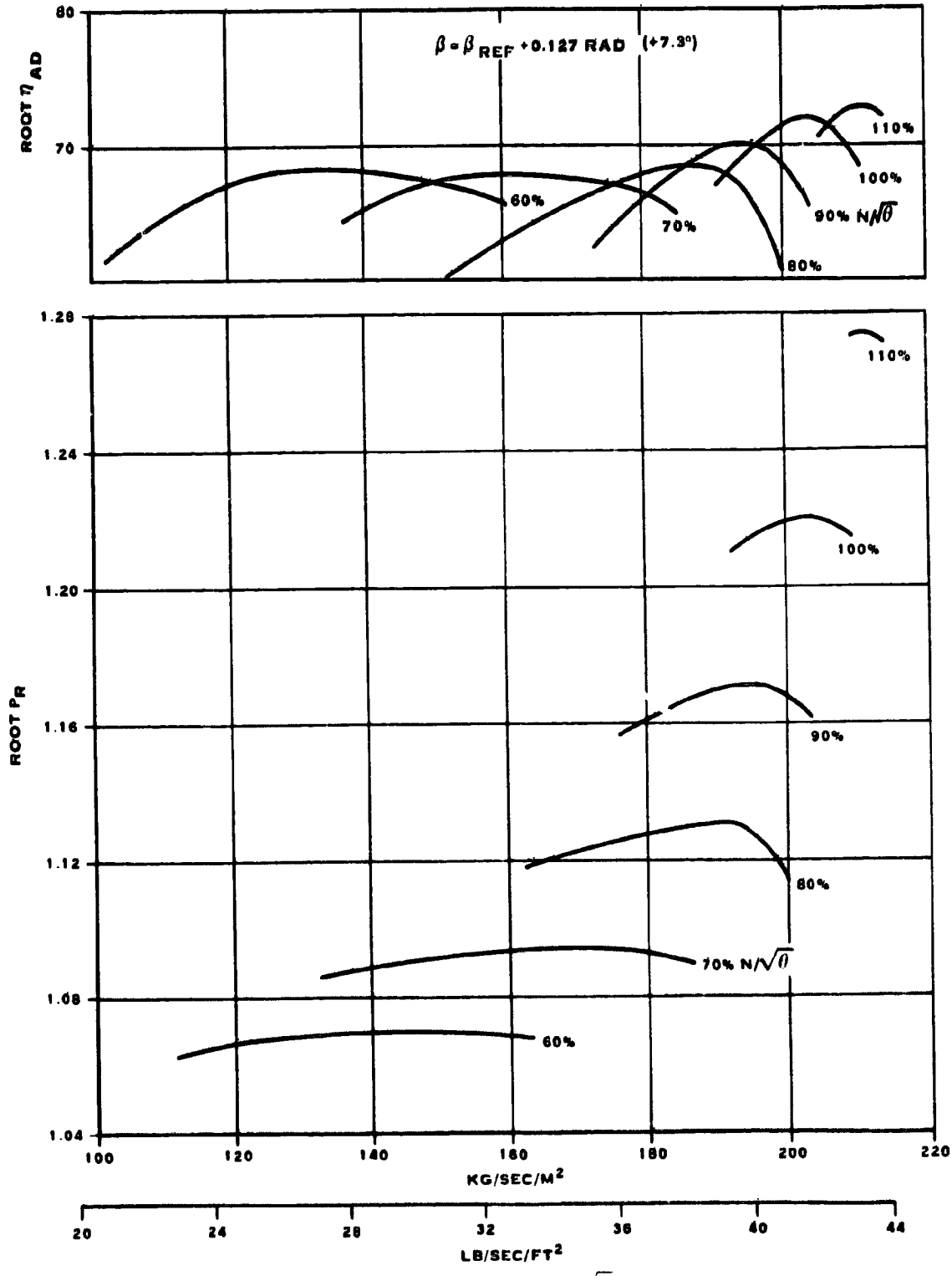

Figure 4-12. Lift/Cruise Fan Supercharge Performance

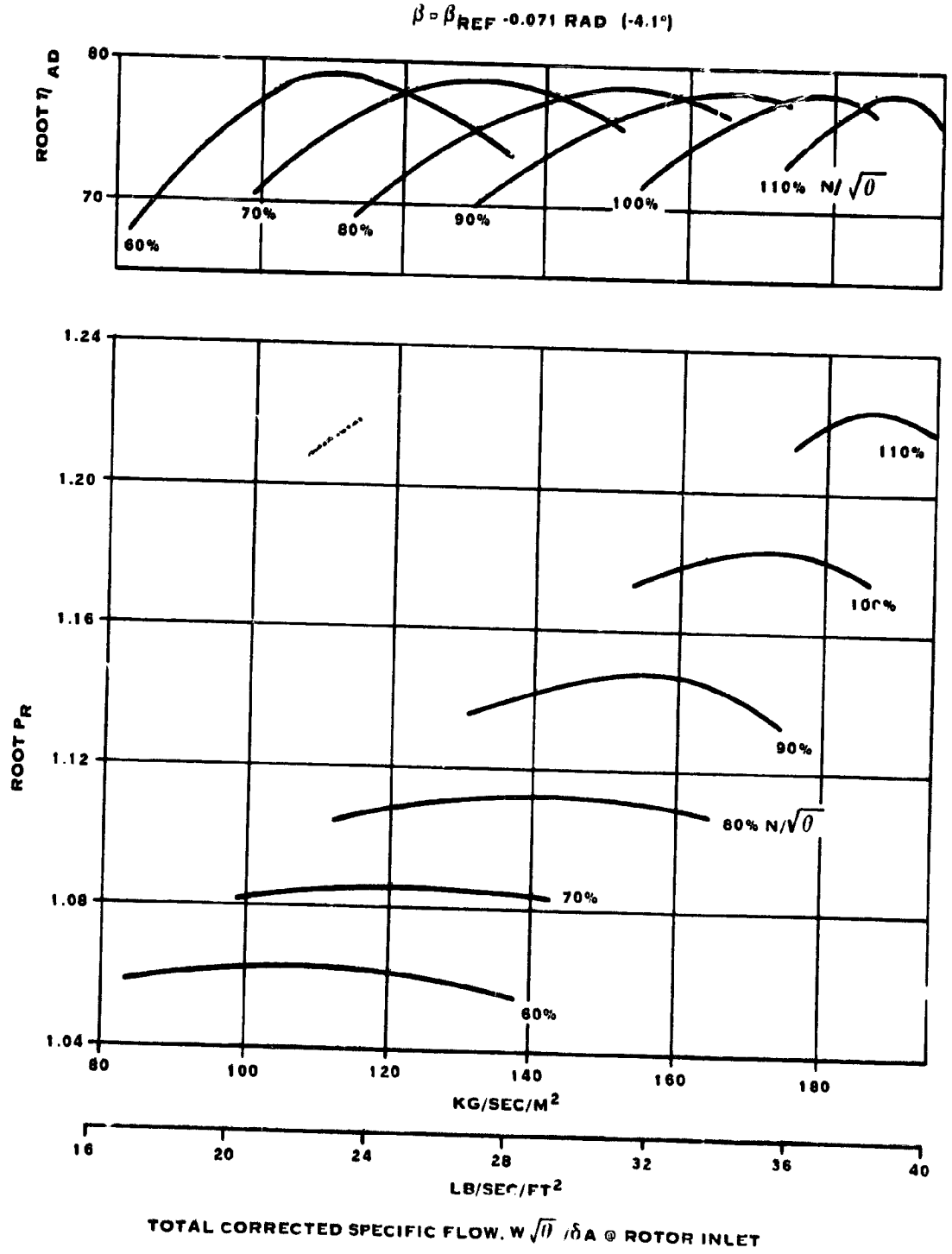

Figure 4-13. Lift/Cruise Fan Supercharge Performance

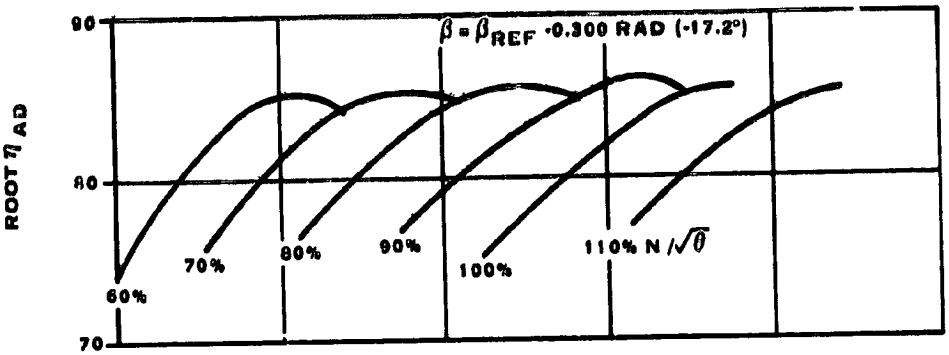

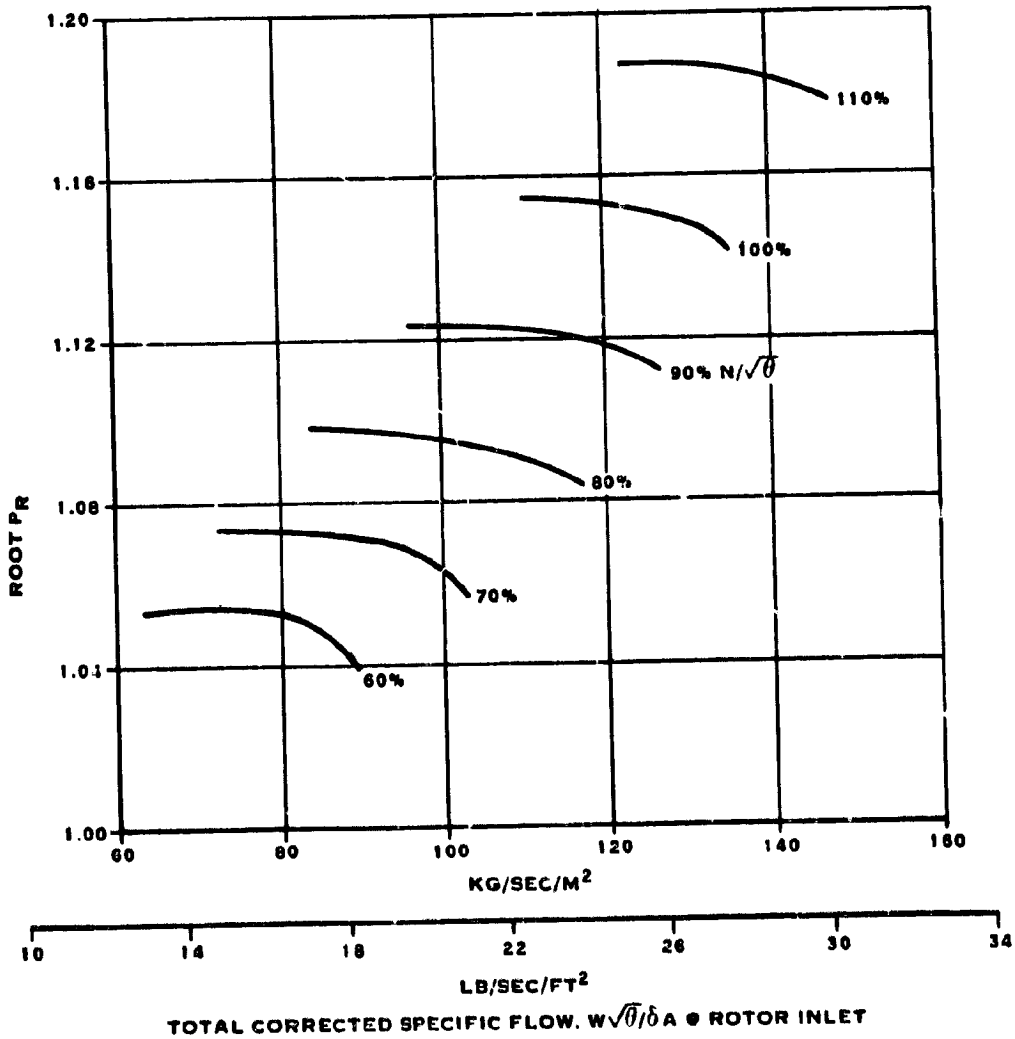

Figure 4-14. Lift/Cruise Fan Supercharge Performance

Table II
RTA Fan Performance

	Normal T.O./Land		Max. Control	
	McAir	BMAD	McAir	BMAD
Pressure ratio	1.181	1.175	1.221	1.213
Efficiency, %	88	88	88	88
Corr. specific flow, $kg/s/m^2$($lb/s/ft^2$)	176.7 (36.2)	175.2 (35.9)	194.3 (39.8)	191.9 (39.3)
Corr. tip speed, m/s(fps)	284 (932)	284 (932)	284 (932)	284 (932)
Supercharge pressure ratio	1.184	1.183	1.199	1.194
Supercharge efficiency, %	78	78	74	75
Power to fan, kw(SHP)	4552 (6105)	4392 (5890)	6046 (8108)	5784 (7756)
By-pass thrust, N(lbs)	38344 (8620)	39323 (8840)	47027 (10572)	47805 (10747)
Fan pitch, $\Delta\beta$, rad. (deg.)	-0.071 (-4.1)	-0.075 (-4.3)	+0.031 (+1.8)	+0.017 (+1.0)

Table III
Fan Aerodynamic Data

Normal T.O./Land Condition
$P_R = 1.181\ W\sqrt{\theta}/\delta A = 176.7$ kg/sec/m^2(36.2 lb/sec/ft^2)
$\Delta\beta = -0.071$ rad (-4.1°)

% Span	R/R_T	M_M	M_R	β	ϕ	P/P	T/T	Z	D_f
Rotor Inlet									
5.2	0.455	0.552	0.676	0	20.8	0.992	1.0	-	-
51.0	0.718	0.521	0.807	0	9.1	0.992	1.0	-	-
95.5	0.974	0.490	0.967	0	2.2	0.992	1.0	-	-
Rotor Exit									
5.0	0.509	0.526	0.528	35.9	11.6	1.187	1.064	0.158	0.412
49.8	0.741	0.466	0.620	24.3	7.1	1.173	1.052	0.032	0.341
95.3	0.976	0.483	0.792	20.9	0	1.186	1.060	0.073	0.275

% Span	R/R_T	M_M	M_A	α	ϕ	P/P	T/T	Z	D_f
By-Pass Stator Inlet									
7.5	0.651	0.566	0.632	26.4	0.8	1.205	1.060	-	-
48.9	0.826	0.467	0.504	22.0	2.4	1.172	1.052	-	-
93.9	1.016	0.425	0.460	22.5	3.8	1.186	1.060	-	-
By-Pass Stator Exit									
8.4	0.678	0.501	0.501	0	1.1	1.183	1.060	0.081	0.359
51.0	0.843	0.504	0.504	0	1.2	1.171	1.052	0.011	0.179
94.0	1.010	0.536	0.536	0	-0.3	1.180	1.060	0.041	0.072
Engine Stator Inlet									
0.8	0.477	0.463	0.619	41.5	-6.3	1.182	1.065	-	-
52.9	0.515	0.494	0.616	36.6	-7.7	1.198	1.063	-	-
99.2	0.548	0.504	0.607	34.0	-8.2	1.205	1.062	-	-
Engine Stator Exit									
1.1	0.470	0.450	0.450	0	-7.4	1.145	1.065	0.150	0.435
51.8	0.505	0.499	0.499	0	-8.8	1.191	1.063	0.025	0.348
98.9	0.538	0.472	0.472	0	-9.0	1.175	1.062	0.122	0.381

4.2.1.2 Distortion - The V/STOL lift/cruise fan sensitivity to distortion has been calculated and compared against measurements of inlet total pressure distortion for a one-fourth scale model V/STOL inlet. The results of this analysis show that the V/STOL RTA inlet total pressure distortion is not likely to induce surge or rotating stall of the lift/cruise fan. In addition, limited tests on a full scale V/STOL fan have indicated that full scale model distortion patterns are less severe than the one-fourth scale model tests indicated.

Fan sensitivity to inlet distortion is defined in terms of two variables; KR, radial distortion index and KΘ, circumferential distortion index. The definition of these indexes are given in figure 4-15. Combinations of KR and KΘ indicate the limits of distortion that will allow stall free operation of the fan. The distortion sensitivity analysis was performed for the V/STOL fan utilizing: (1) the parallel compressor method with dynamic stall delay for the circumferential distortion (KΘ) and, (2) the performance prediction program with ring average inlet total pressure gradients for the radial distortion (KR). The parallel compressor method used, is presented in AIAA Paper No. 74-233, authored by James A. Korn of DDA. The dynamic stall delay correction to the method, as presented, was modified as a result of consultations with Mr. Korn.

The distortion sensitivity calculations were made for a range of circumferential and radial distortion indexes. This analysis yields the maximum allowable values of KΘ and KR for stall free operation in the distorted flow field.

V/STOL inlet distortion profiles were obtained from Boeing's quarter scale model inlet tests. Two profiles of the windward sector of the inlet are shown in figure 4-16. For the high specific flow, representative of high power conditions, the inlet flow is attached and the distortion indexes, KΘ and KR, are low. However, for the low flow, representation of a part power approach to landing, the inlet is separated and the distortion indexes are high.

A summary of the distortion indexes for the quarter scale model is shown in figure 4-17 for two angle-of-attack/airspeed combinations. The inlet separation boundary can be clearly seen. Separation and high distortion indexes occur at flows below the separation boundary. The conditions which were analyzed in the distortion sensitivity study are indicated by the solid lines on figure 4-17.

The quarter scale inlet test was the forerunner to the Hamilton Standard variable pitch full scale VP fan demonstrator testing in the NASA Ames 40 x 80' tunnel. Although this test is not yet complete, early results have shown significantly improved inlet separation boundaries indicated by the dashed lines on figure 4-17.

Although the distortion measurements indicate that the highest distortion indexes occur with inlet separation at low airflows, no operation is anticipated in the low airflow region below the projected separation boundary for the full scale inlet. The two con-

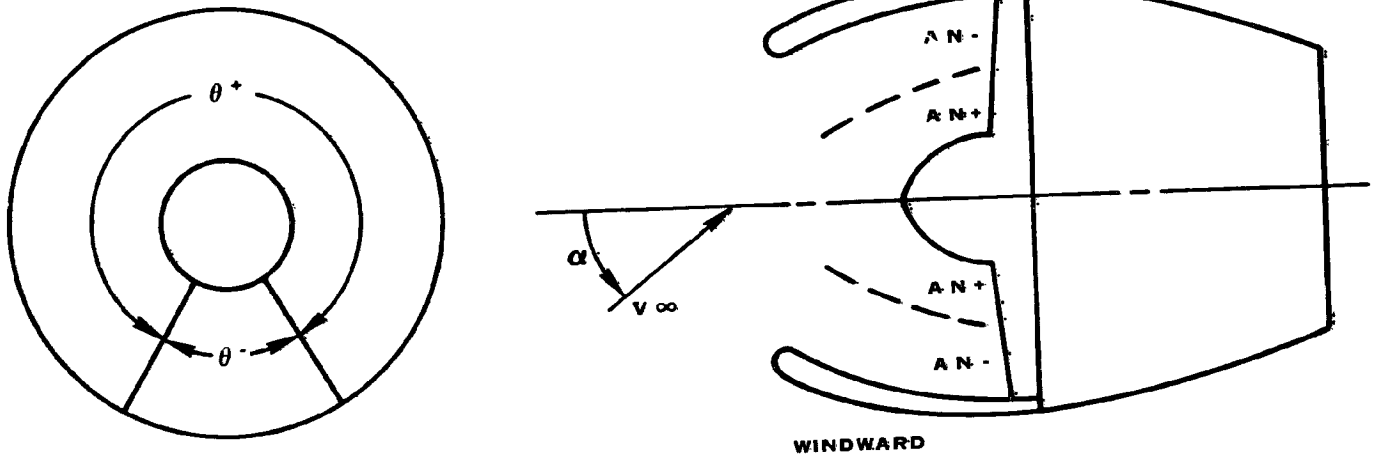

$$K\theta = \frac{\bar{P}_{T\theta+} - \bar{P}_{T\theta^-}}{P_{T\ AVG}}$$

$$KR = \frac{\bar{P}_{T\ AN+} - P_{T\ AN^-}}{P_{T\ AVG}}$$

- BARRED PRESSURES ($\bar{P}T\theta$) ARE ARITHMETIC AVERAGES OVER THE SECTOR INDICATED BY THE SUBSCRIPTS.
- θ^- = CIRCUMFERENTIALY DISTORTED SECTOR (120° FOR MEASURED DATA)
- AN = ANNULAR AREA OF DISTORTED FLOW (40% FOR MEASURED DATA)
- $P_{T\ AVG}$ = ARITHMETIC AVERAGE OF ALL INLET TOTAL PRESSURES

Figure 4-15. Distortion Geometry

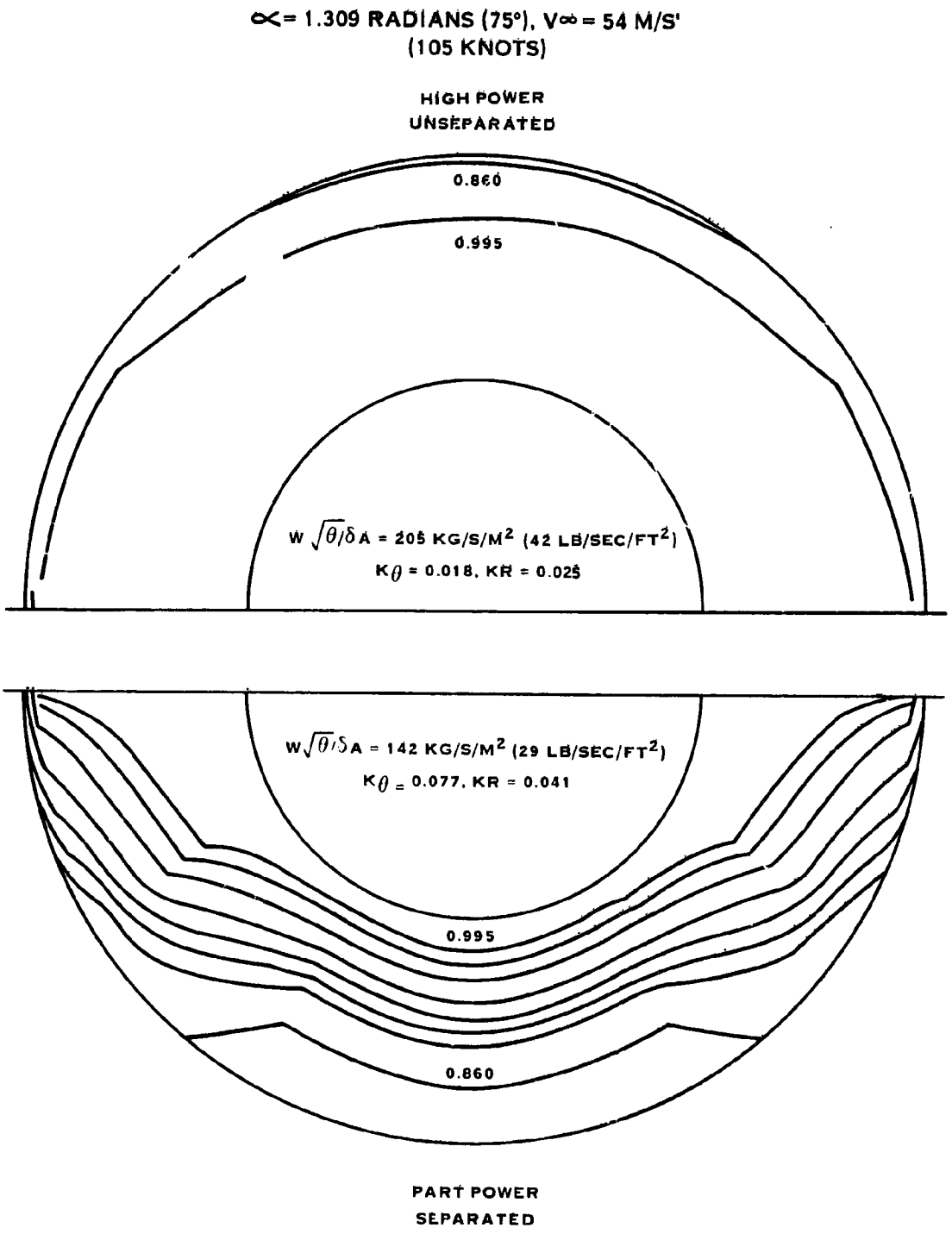

Figure 4-16. Representative Distortion Patterns

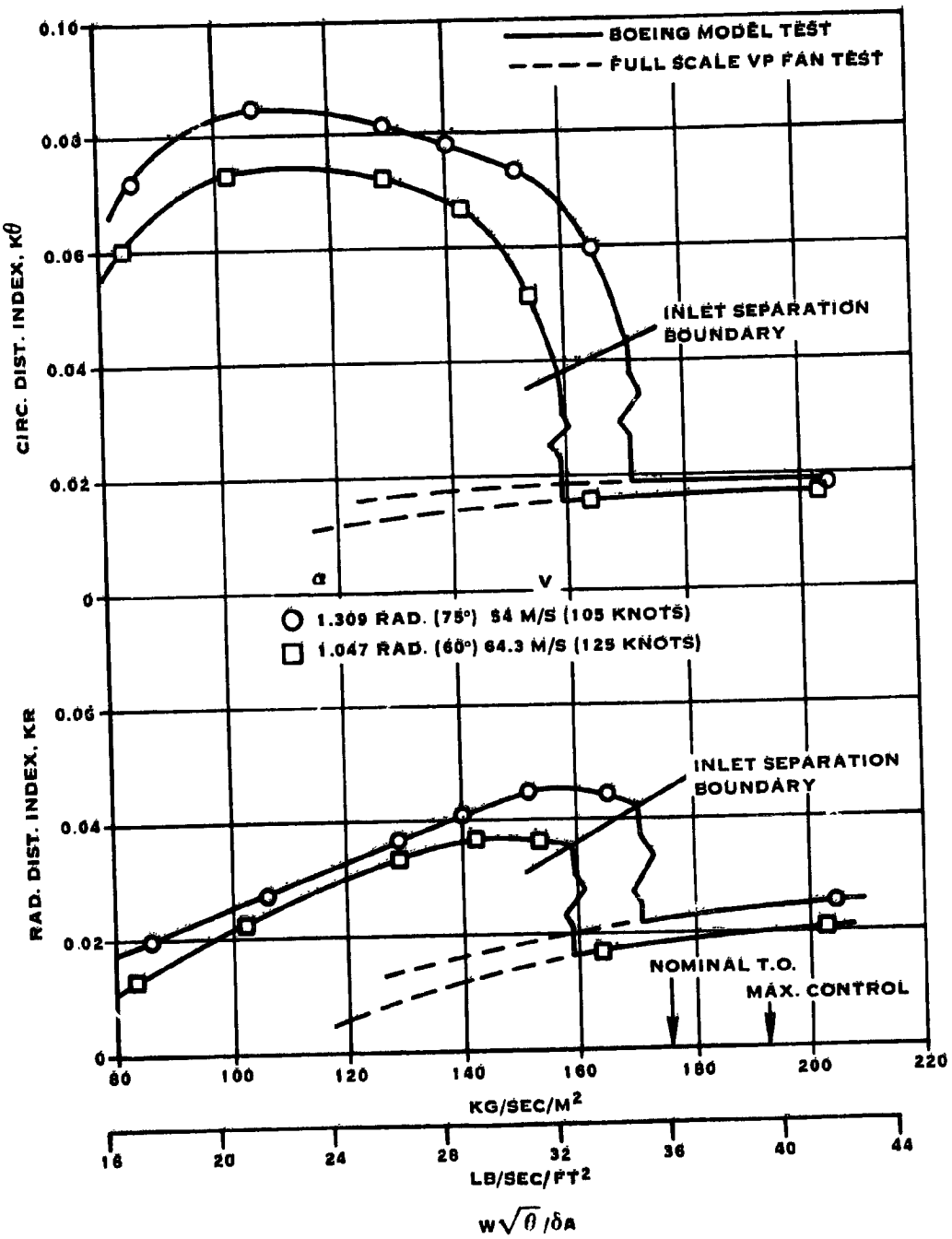

Figure 4-17. Inlet Distortion Indices

4.2.1.2 (Continued)

ditions which were selected for the distortion analysis, i.e., maximum control and normal takeoff operation for the RTA, are representative of high airflow conditions.

In the high airflow region the inlet sensitivity to radial distortion is more severe than at lower flows due to the fan tip being highly loaded, and sensitivity to circumferential distortion is also more severe than at lower air flows due to the characteristic of the fan speed lines. The calculated locii of KΘ vs KR for these conditions are shown in figure 4-18. The measured KΘ and KR values for the appropriate inlet corrected specific flows are also shown on figure 4-18. These two points fall well within the safe operating region for fan inlet distortion.

4.2.2 Mechanical Design

Design studies conducted during 1975 resulted in a fan concept and related weights for the Boeing V/STOL operational aircraft. The objective of this design study is to refine the fan rotor concept developed in the earlier studies to meet the requirements of the RTA. Rotor structural components, i.e., blade disk (cone) and actuator were analyzed for the RTA operating loads, including distortion and FOD. Component and system weights for the lift and lift cruise fans, incorporating the refined rotor, were calculated.

The fan rotor system components are illustrated in figure 2-3.

4.2.2.1 Blade - Preliminary blade analyses were performed to determine blade weight, stiffness, inertia, critical speeds, centrifugal loads, steady and cyclic stresses, flutter parameters, and to evaluate possible damage resulting from ingestion of a one kilogram bird.

Blade Description - A titanium spar, boron-aluminum shell blade (figure 4-19) was selected for this application. This construction offers a lightweight design while providing excellent strength and FOD resistance. During the 1975 studies the basic fan aerodynamic sizing had been accomplished and the number of blades, 26, selected for the operational aircraft. The RTA blade studied has a diameter of 157.48 cm (62-inch) and an average spinner diameter of 72.14 cm (28.4-inch). The average chord width is 15.00 cm (5.9-inch) and the integrated activity factor (power absorbtion characteristic) is 142 per blade. The blade spanwise geometry is defined in figure 4-20.

The boron/aluminum shell consists of a laminate of unidirectional boron/aluminum tape, diffusion-bonded together with an outer layer of titanium. The titanium skin is a unique feature which provides a corrosion/erosion barrier comparable to that of conventional turbofans.

Shell thickness varies from about 0.508 mm (20 mils) inboard to 1.524 mm (60 mils) over the outer half of the blade. Shell material properties and ply orientations, as well as spar width and chordwise location, are based on design philosophy of Hamilton

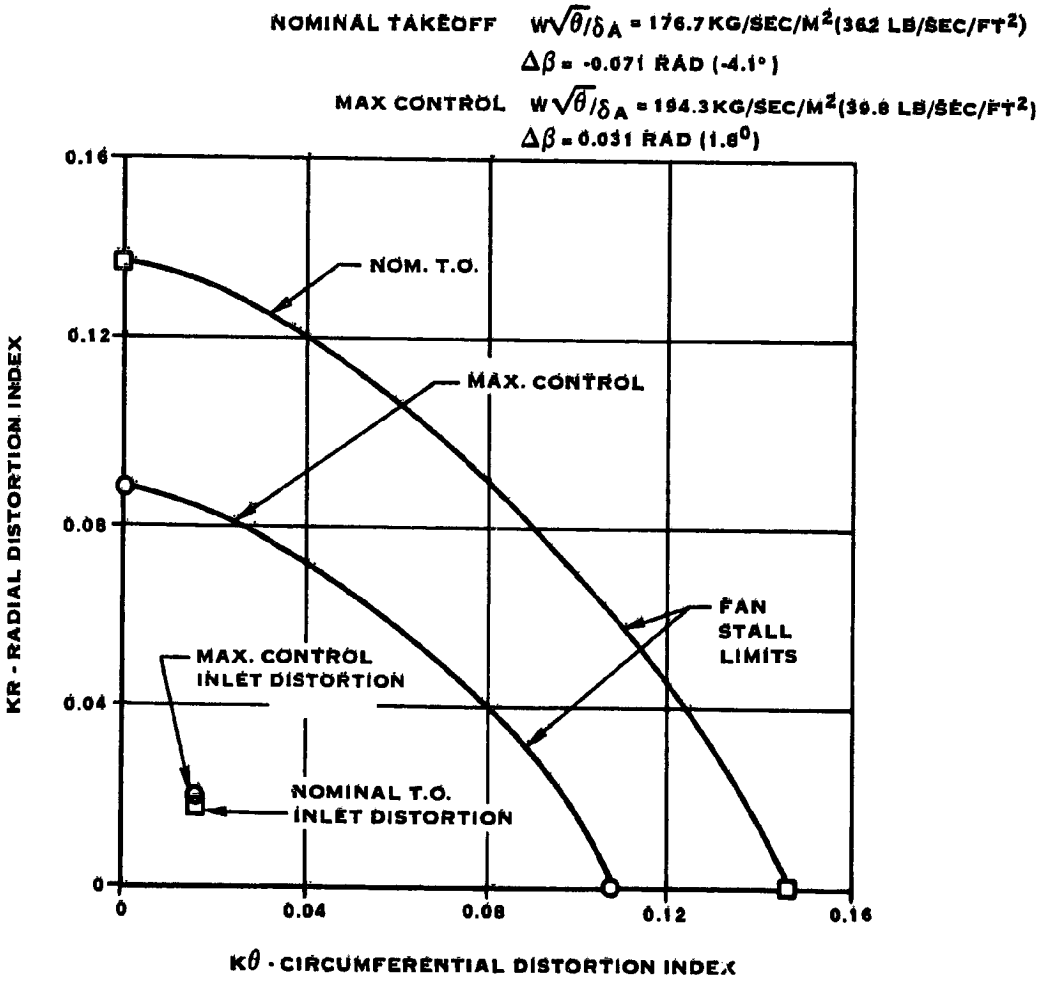

Figure 4-18. RTA Fan Distortion Sensitivity

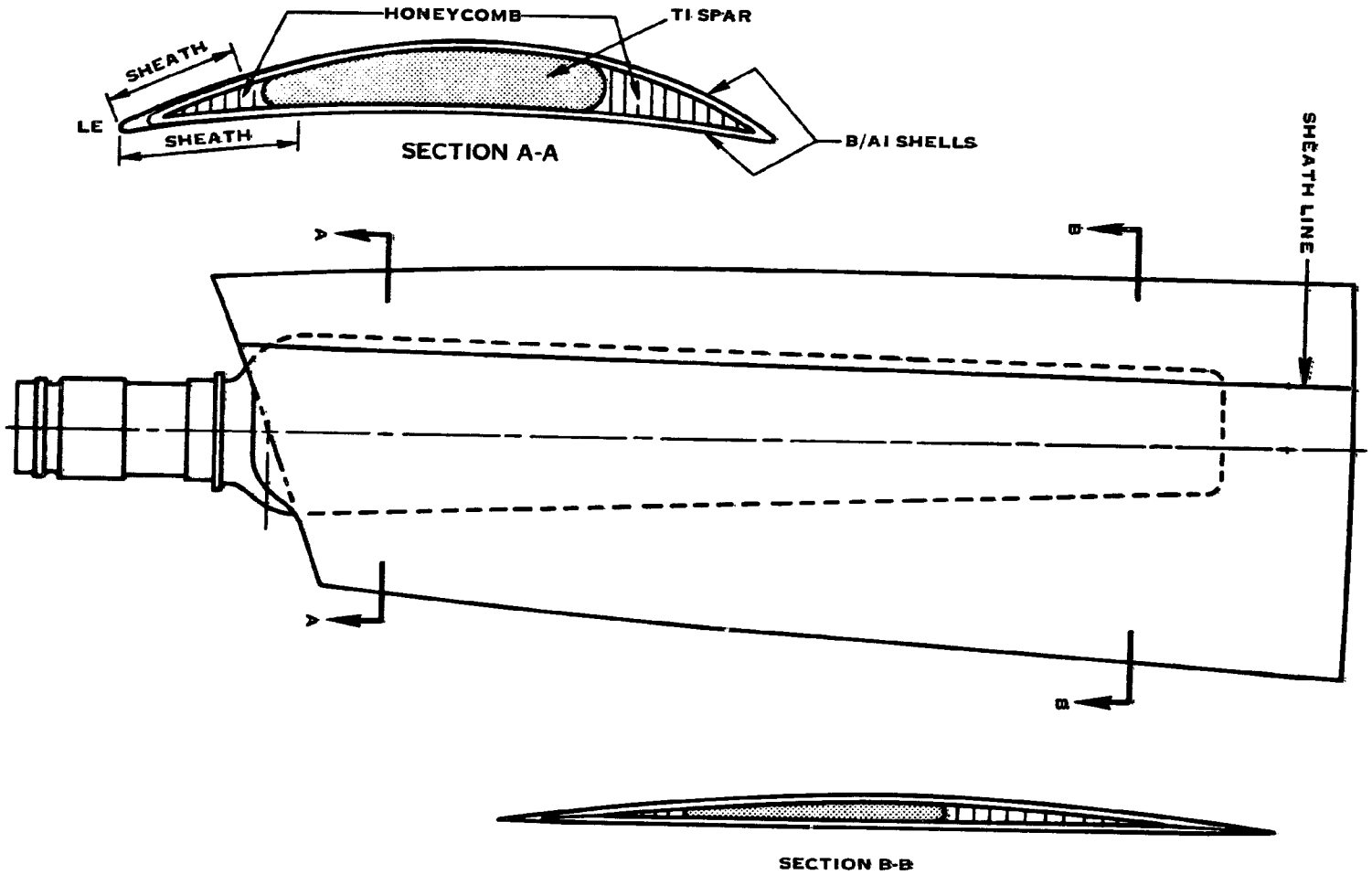

Figure 4-19. V/STOL Fan Blade Geometry

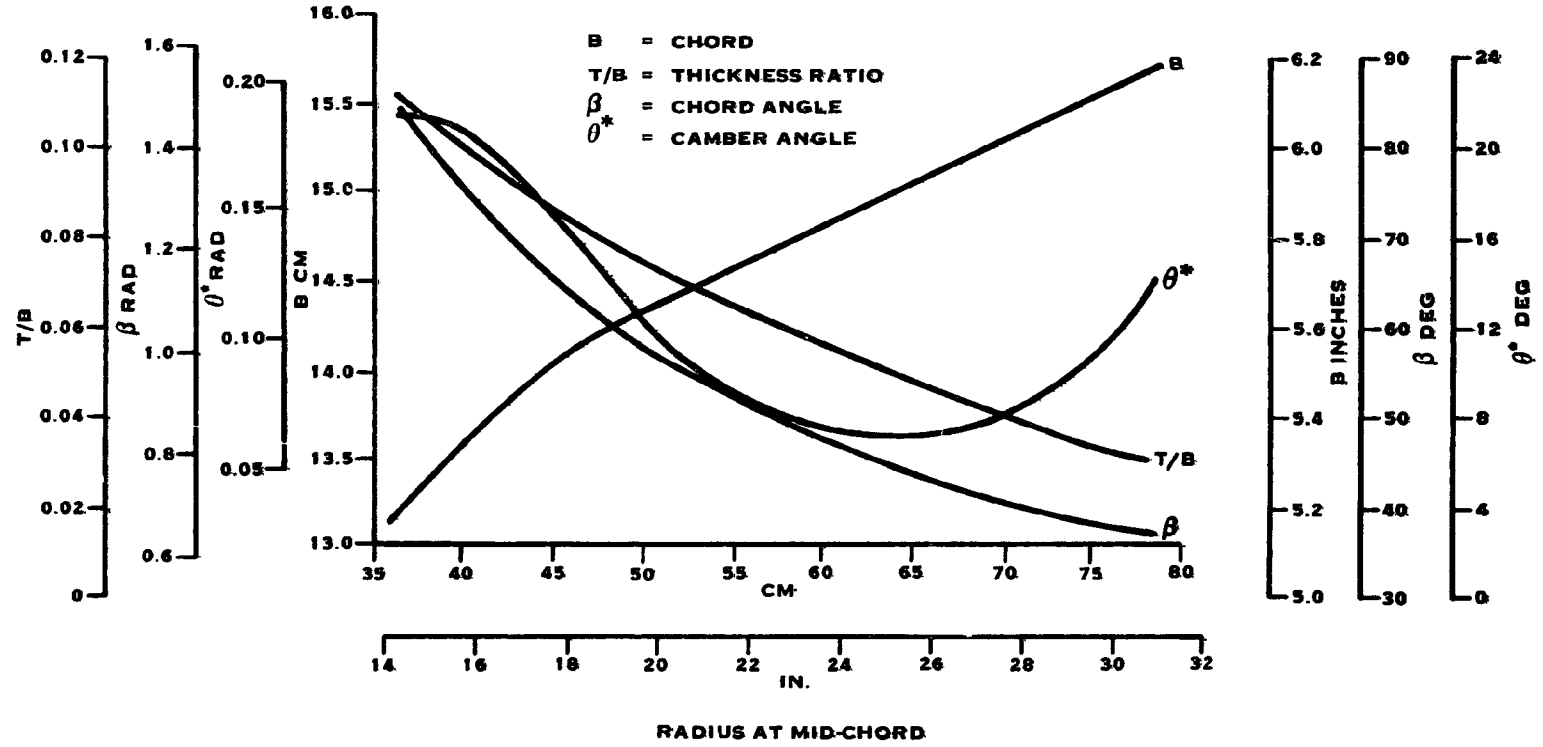

Figure 4-20. Fan Blade Spanwise Geometry

4.2.2.1 (Continued)

Standard's successfully tested FOD blade described in NASA report CR-135001. The spar extends inboard of the root airfoil region and blends into a cylindrical shank, compatible with the fan retention geometry. Hollow regions of the shell, forward and aft of the spar, are supported with aluminum honeycomb to provide maximum support for the shell and increase FOD resistance. A leading edge sheath of Inconel 625 provides continuity across the leading edge shell joint, while providing impact and erosion protection to this portion of the blade.

Natural Frequencies - Blade natural frequencies were calculated for the blade and results are presented on the Campbell plot shown in figure 4-21. A necessary input to the evaluation of fan critical speeds was the fan operating speed range. When this study was conducted, the airframe contractors' studies had not progressed to the point where they could define the fan operating range; therefore Hamilton Standard selected an operating speed range of 60-100% as representative of the V/STOL requirements, based on prior experience with V/STOL aircraft. It can be seen that the first mode, 2P, (P - excitations per revolution) critical speed crossover is in the operating range. A second mode, 4P crossover, also occurs within the operating range close to the maximum operating speed of 369.6 rad/sec (3530 rpm). Higher order crossovers for the second vibration mode are considered insignificant because their excitation levels are small, they occur at low power, and/or the response of the blade is small. While critical speeds within the operating range are undesirable, the flexibility afforded by the composite blade allows the critical speed crossovers to be relocated during the blade design to where they will not interface with fan operation.

Steady and Cyclic Loads and Stresses - The blade spar is the main structural member, while the blade shell provides the aerodynamic shape and carries the aerodynamic loads into the spar. To confirm the blade structural capacity the spar was analyzed for both steady and cyclic stressing. The condition selected for evaluation was during the take-off transition at 54 m/sec (105 kt) when both the steady and cyclic loads would be high. The analysis of steady stress considers both aerodynamic and inertia loads. The steady blade loads are summarized in table IV.

Table IV
Blade Steady Load Summary

	Metric	English
Rotor Thrust	28913 N	6500 lb
Rotor Speed	369.6 rad/sec	3530 rpm
Thrust/Blade	1112 N	250 lb
Blade Centrifugal Loads	111,200 N	25,000 lb

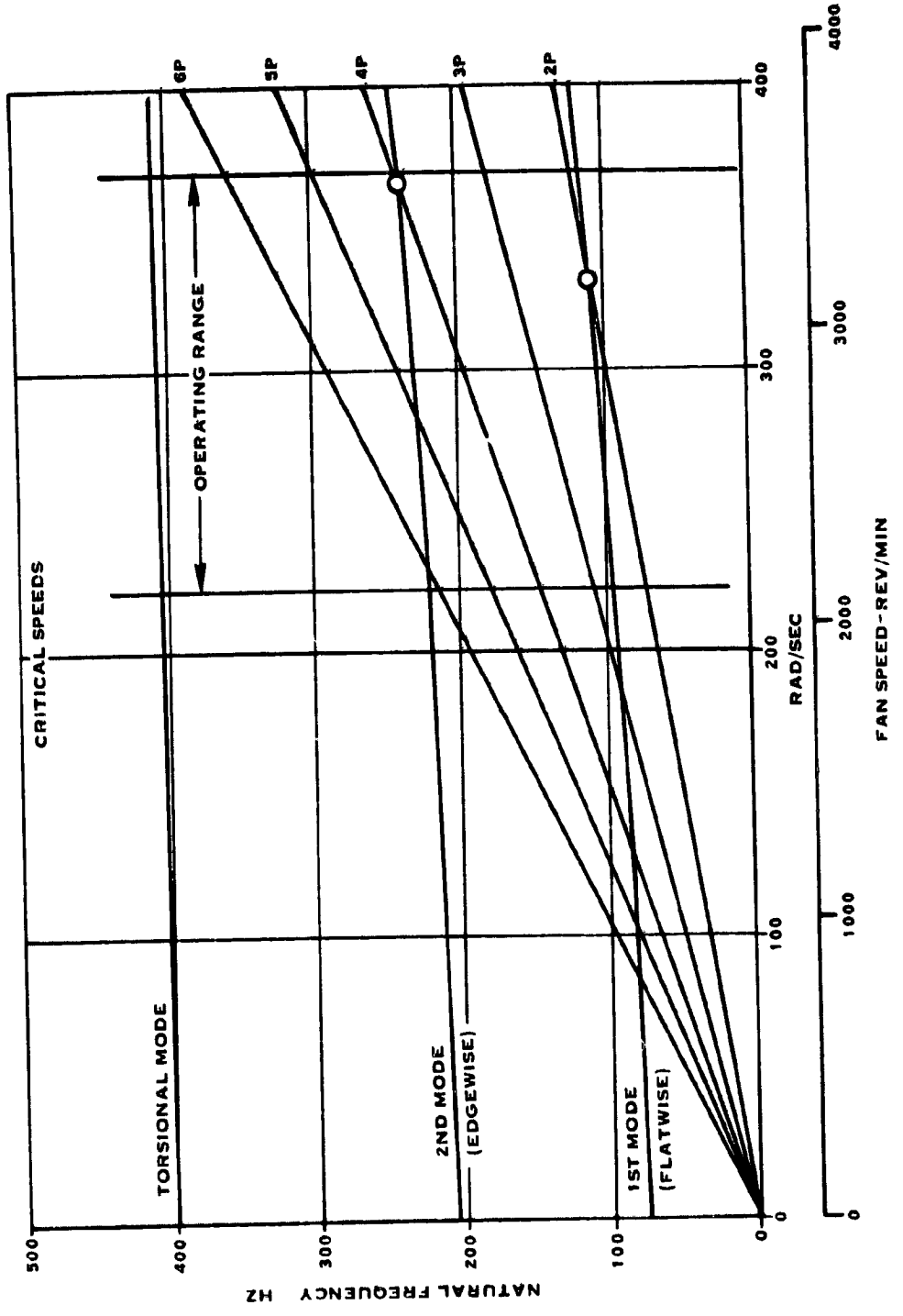

Figure 4-21. Blade Critical Speeds - 26 Blades (Campbell Plot)

4.2.2.1 (Continued)

Cyclic loads affecting the blade due to a once per revolution (1P) load variation were calculated for a separated fan inlet, as this was believed to be the worst case which could be experienced during transition. A separated inlet distortion profile obtained from Boeing inlet distortion testing was used to calculate the velocity profiles shown in figure 4-22 and input into the Hamilton Standard multi-azimuth blade airload calculation program. The multi-azimuth program calculated radial airload distributions of in-plane and out-of-plane loads at a once per revolution frequency. These rotation related loads were then used as excitation loads for a vibratory stress program. The 1P flatwise blade vibratory bending moment was calculated to be ± 99.42 N-M (±880 in.-lbs) at the 45.72 cm (18 inch) station. The 1P loads were increased by 50% to account for loading at multiple integers, i.e., 2P, 3P, 4P etc. The resulting moment of 149.13 N-M (1320 in.-lbs) was used to calculate a cyclic stress on both the pressure side and suction side of the spar.

These steady and cyclic stresses are related to spar material design fatigue strength found on the Goodman diagram presented in figure 4-23. A stress margin in excess of 1.0 exists for both points indicating sufficient spar strength at the most highly stressed station.

Blade Flutter - Fan blade bending flutter was analyzed to insure that the V/STOL fan blade would not be susceptible to large deflections due to momentary high air loads.

Blade flutter is brought on by the lower torsional rigidity of thinner blades. Since the center of pressure on an airfoil is near the quarter chord point, there will be some torsional deflection (twisting) of the blade tending to increase blade angles. If this deflection is large enough, the airfoil angle of attack will be increased to the point where the airfoil stalls, the air load drops, and the blade unwinds and returns to its original pitch and the cycle starts over again. If the blade is torsionally flexible enough, destructive vibrations will be set up.

Preliminary calculations were made to examine the bending and torsional flutter parameters of the V/STOL fan blade. Flutter parameter limits have been determined from design experience and development of many propeller and fan designs. The established design guides reflect conservative limits that will provide a fan blade design free from critical flutter properties. This analysis assessed the blade as having an adequate bending flutter parameter with 36% margin. The torsional flutter parameter was calculated having a value 15% below the design allowable. Torqional flutter is dependent on blade torsional frequency which is a result of blade structural characteristics. The detail design of the blade will provide local changes in the blade structure in order to increase the torsional frequency to bring this parameter to within acceptable design guides.

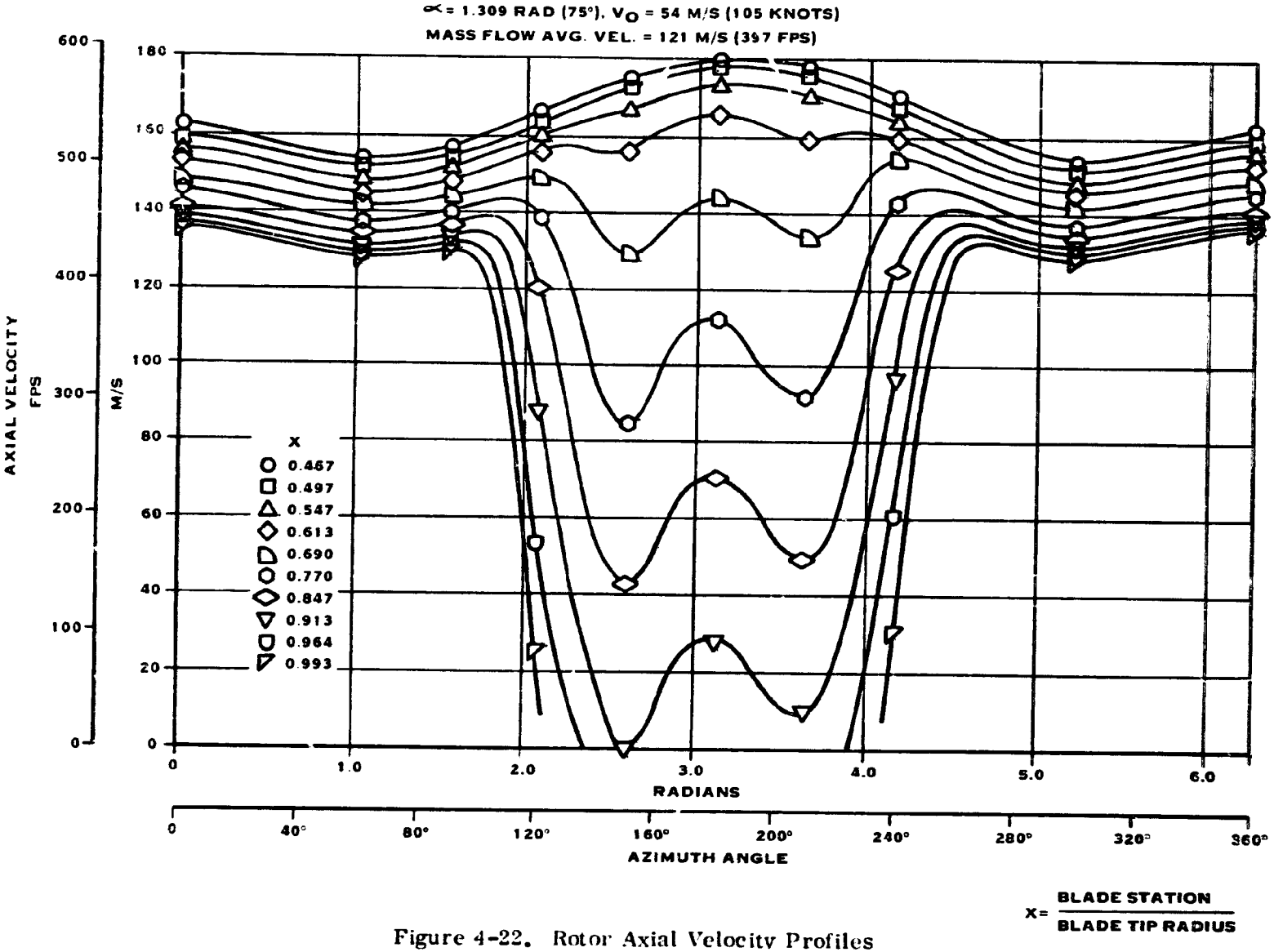

Figure 4-22. Rotor Axial Velocity Profiles

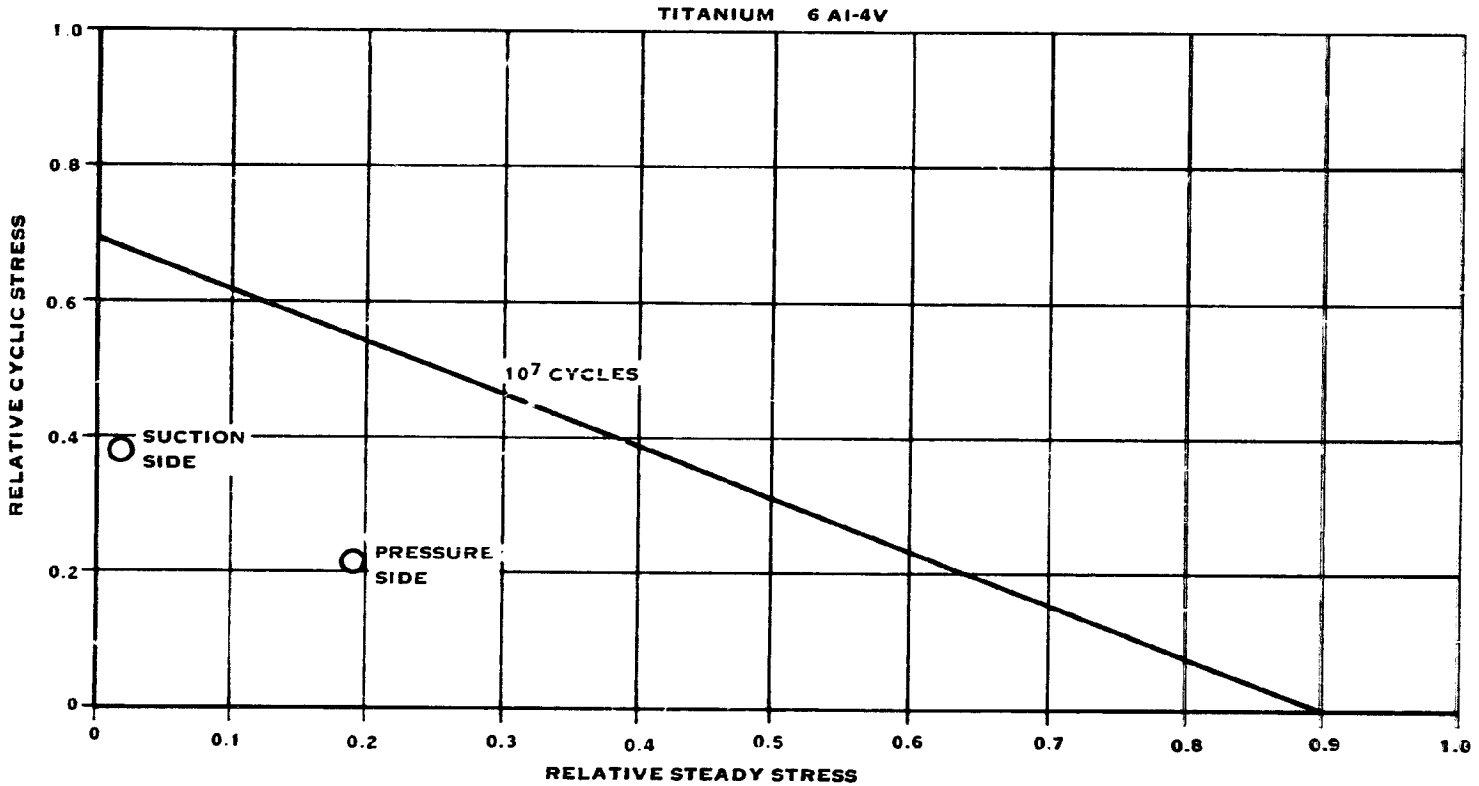

$$\text{RELATIVE STRESS} = \frac{\text{ACTUAL STRESS}}{\text{SELECTED MAXIMUM STRESS}}$$

Figure 4-23. Material Design Strength (Goodman Diagram)

4.2.2.1 (Continued)

FOD Analysis - The blade construction selected by Hamilton Standard for the V/STOL blade design has been experimentally demonstrated to have adequate impact resistance under both NASA and USAF contracts. Impact stressing associated with the fan blade for the V/STOL application was calculated and compared to impact stressing of experimentally tested blades to validate the V/STOL blades FOD tolerance.

The FOD resistance criteria for the Navy V/STOL operational aircraft is tolerance of 1 kg (2.2 lb) bird ingestion. This criteria was also adopted for the RTA fan. Stressing was calculated for the RTA fan blade using an impact analysis method developed by Hamilton Standard. This analysis indicated that stressing would be similar to that experienced by a boron aluminum composite fan blade tested at Hamilton Standard for NASA LeRC as reported in NASA CR-135001 and damage would be limited to minor local damage at the tip trailing edge. In the analysis of the 1 kg bird, the impact location on the blade was assumed to be at the 0.80 blade station. The values used in the analysis are listed in table V.

The impact analysis program treats the bird as though it were a cylinder. Bird dimensions are calculated for length to diameter ratio of 2, and an average bird density of 679.0 kg/M^3 (0.02453 lb/cu. in.). The relative impact velocity is determined from vector addition of the bird inlet velocity (equal to the aircraft forward velocity of 51.44 M/S (100 knots) in this case), and the tangential blade velocity due to rotation at the impact radius. The bird longitudinal axis lies normal to the relative impact velocity vector. The maximum slice width is calculated assuming the cylindrical end of the bird narrowly misses the leading edge of the adjacent blade. The slice thickness becomes dependent on the blade spacing times the sine of the angle between the relative impact velocity vector and the rotational velocity vector (figure 4-24). The blade spacing, in turn, is dependent on the circumference at the impact radius divided by the number of blades. These calculations result in a slice width of 3.30 cm (1.30 in.) or an equivalent mass of 167.8 g (0.37 pounds).

The cylindrical bird slice is divided into six equivalent rectangular segments, which impact the blade. The computerized analysis treats these segments as fluid jets impinging upon the pressure side of the blade and reacted by the blade inertia and stiffness. Time histories of impacting load, as well as blade reaction loads in the X, Y, and torsional directions, are calculated by the program. Corresponding time histories of three basic deflections, X, Y, and Θ, at the impact site are also generated. The X-deflection is taken parallel to direction of the blade natural flatwise mode of vibration, with the Y-deflection (primarily the edgewise deflection) normal to X. The torsional deflection is taken about the blade center of torsion at the impact station. Impact loads are determined as the forces required to turn FOD segments (treated as impinging fluid jets) through the impact angle. The time histories of load and deflection at the impact location, calculated and plotted by the computerized analysis, are shown in figures 4-25 and 4-26, respectively. The maximum deflection is in the flatwise (normal to surface) x-direction amounting to 7.37 cm (2.9 inches) at approximately 2.4 milli-seconds after initial impact.

Table V
FOD Impact Parameters Summary

	Metric	English
Bird Characteristics		
Mass	1 kgm	2.205 lbs
Density	0.679 grams/cm^3	0.02453 lbs/cu. in.
Length	19.576 cm	7.707 in.
Diameter	9.789 cm	3.854 in.
Coefficient of Restitution	0.0	0.0
Blade Parameters		
Radial Impact Station	70.21 cm	27.64 in.
Angle of Impact Station	0.62 radians	35.6 deg.
Blade Spacing	16.97 cm	6.68 in.
Damping Coefficient (same for all vibratory modes)	0.12	0.12
Angle of Flatwise Mode (X-axis)	2.647 radians	151.7 deg.
Angle of Edgewise Mode	1.141 radians	65.4 deg.
Impact Parameters		
Rotational Velocity Component	259.5 meters/sec	851.4 ft/sec
Fwd. Velocity Component (100 knots)	51.5 meters/sec	168.9 ft/sec
Resultant Relative Impact Velocity	264.6 meters/sec	868 ft/sec
Impact Angle	0.43 rad	24.4 deg.
Slice Size	3.30 cm	1.30 in.
Slice Weight	167.8 grams	0.37 lbs

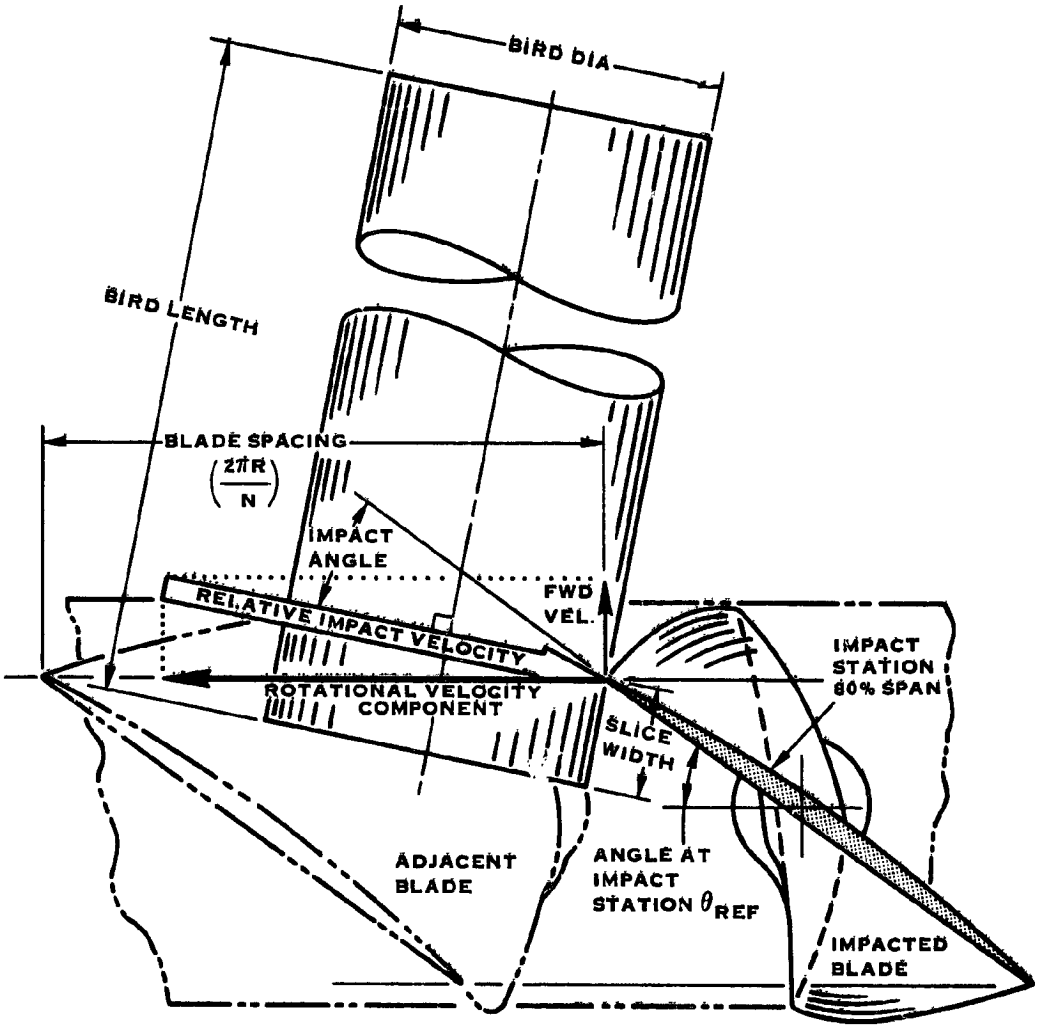

Figure 4-24. FOD Impact Geometry

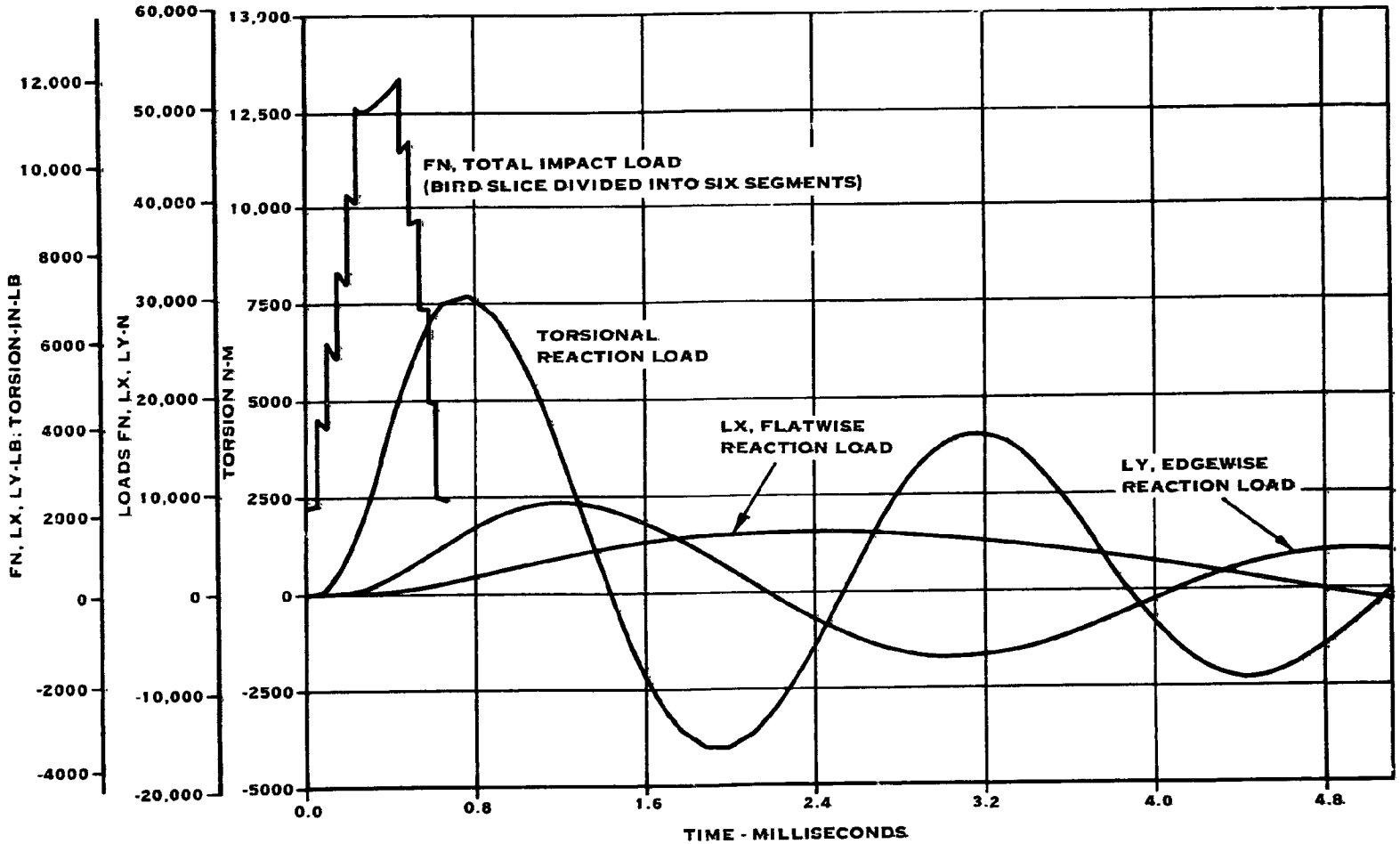

Figure 4-25. Blade FOD Impact Loads

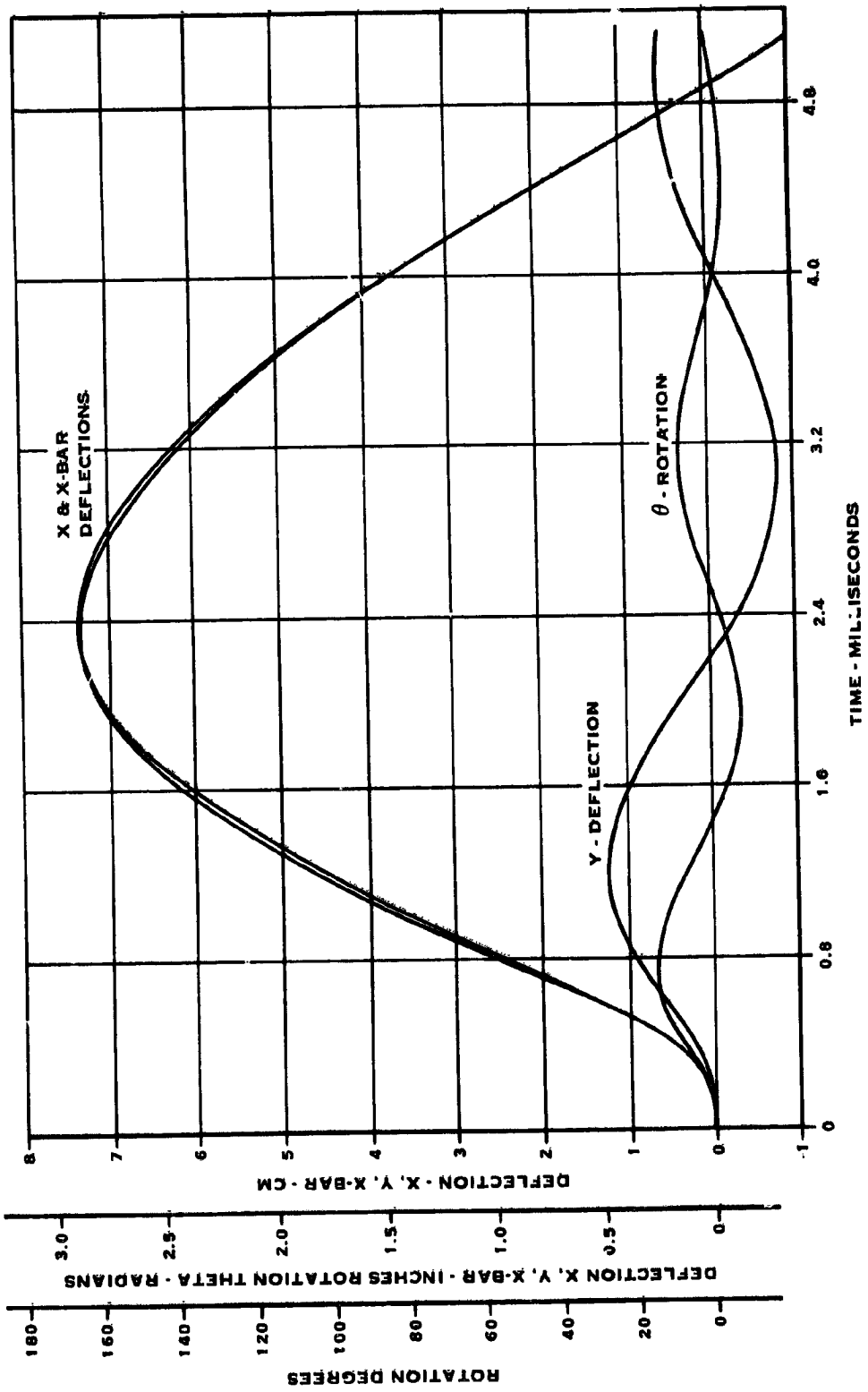

Figure 4-26. Blade FOD Impact Deflections

4.2.2.1 (Continued)

This deflection in the flatwise direction results in peak spanwise bending stresses at two locations along the blade span. These are generated by a second portion of the program which calculates the perturbation along the length of the blade due to localized impact. The spanwise stress distributions are calculated at specific time increments after impact and are plotted by the computer program in figure 4-27. As can be seen from the plot, there is a peak mid-blade bending stress of about 131 kN/cm^2 (190 ksi) at the 55.88 cm (22-inch) blade radius, which is a compressive stress on the suction side. A second peak of 158.6 kN/cm^2 (230 ksi) (a tensile stress on the suction side) occurs in the vicinity of the impact site.

Time histories of stress at both peak locations are plotted in figures 4-28 and 4-29 which also show comparative calculated curves for various impact conditions on FOD-tested, similar blades. The amount of calculated stress correlates with the degree of test damage occurring on the NASA test blade. Analysis of NASA test blade indicated damage for a given object would be comparable to damage on state-of-the-art titanium blades. Non-destructive inspection of the test blades showed that further operation was possible.

Calculation results, as shown in figures 4-28 and 4-29, indicate that stressing will be comparable to that of Hamilton Standard's boron-aluminum blades tested for NASA LeRC. The test blades experienced only minor damage to the trailing edge tip and were judged suitable for continued operation. Further improvement to the blade FOD tolerance is believed to be possible through refinement of the blade geometry during the detail design.

4.2.2.2 Disc Assembly - The disc assembly consists of the blade retention bearing, seal, pitch change trunnion and the disc itself.

Loads - The blade loads that act on the blade retention bearing and hence the disc are listed in table VI. (Max control condition)

Table VI
Blade Retention Loads

Blade and Attachment Centrifugal Load	=	133,440 N (30,000 lbs)
Steady Bending Moment	=	359.6 N-M (3183 in.-lb)
1P Vibratory Bending Moment	=	279.8 N-M (2477 in.-lb)*
NP Vibratory Bending Moment		139.9 N-M (1238 in.-lb)

* These are total loads at the 12.5 in. station in the retention and are therefore higher than those used for the blade.

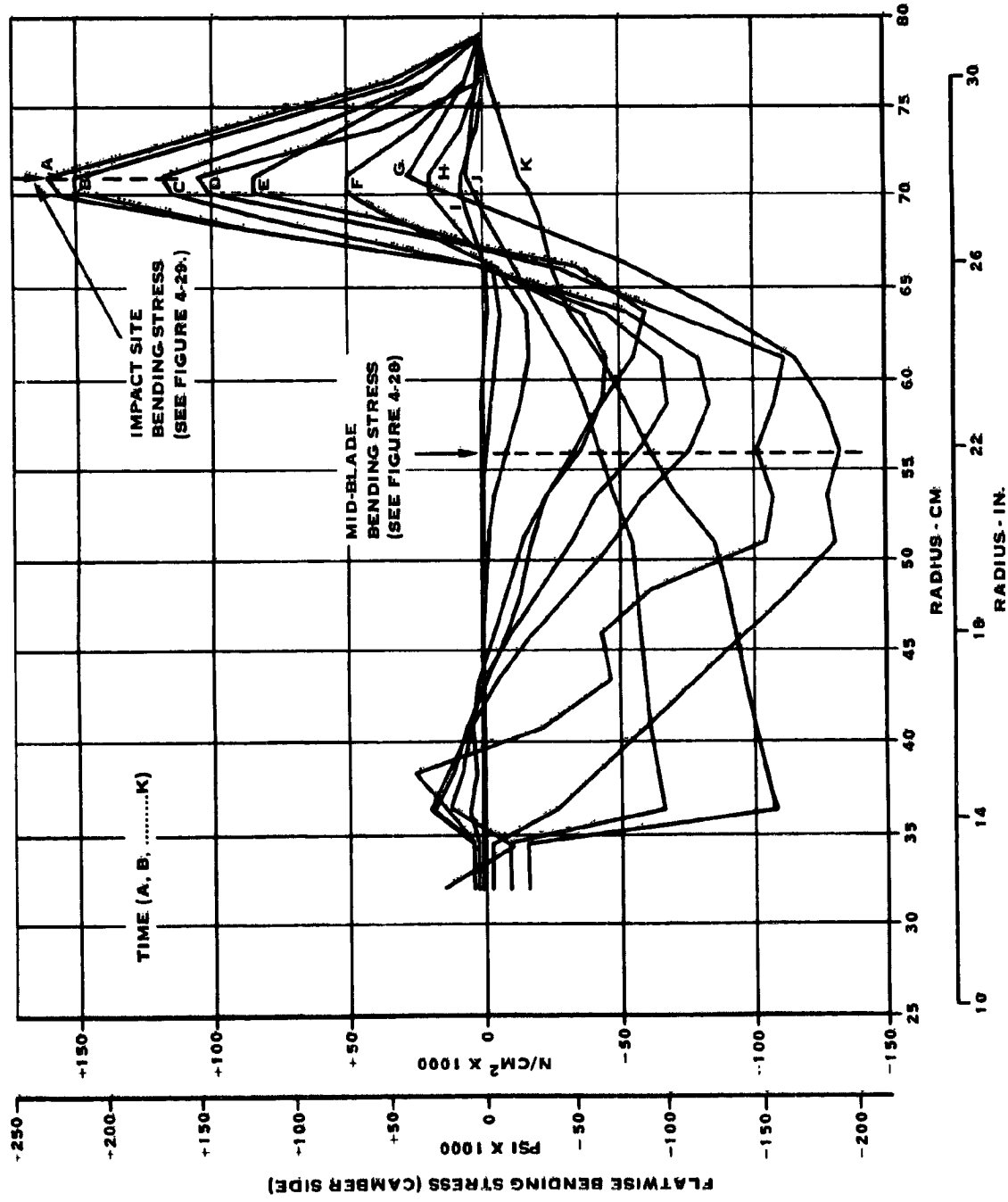

Figure 4-27. Blade Spanwise FOD Stresses

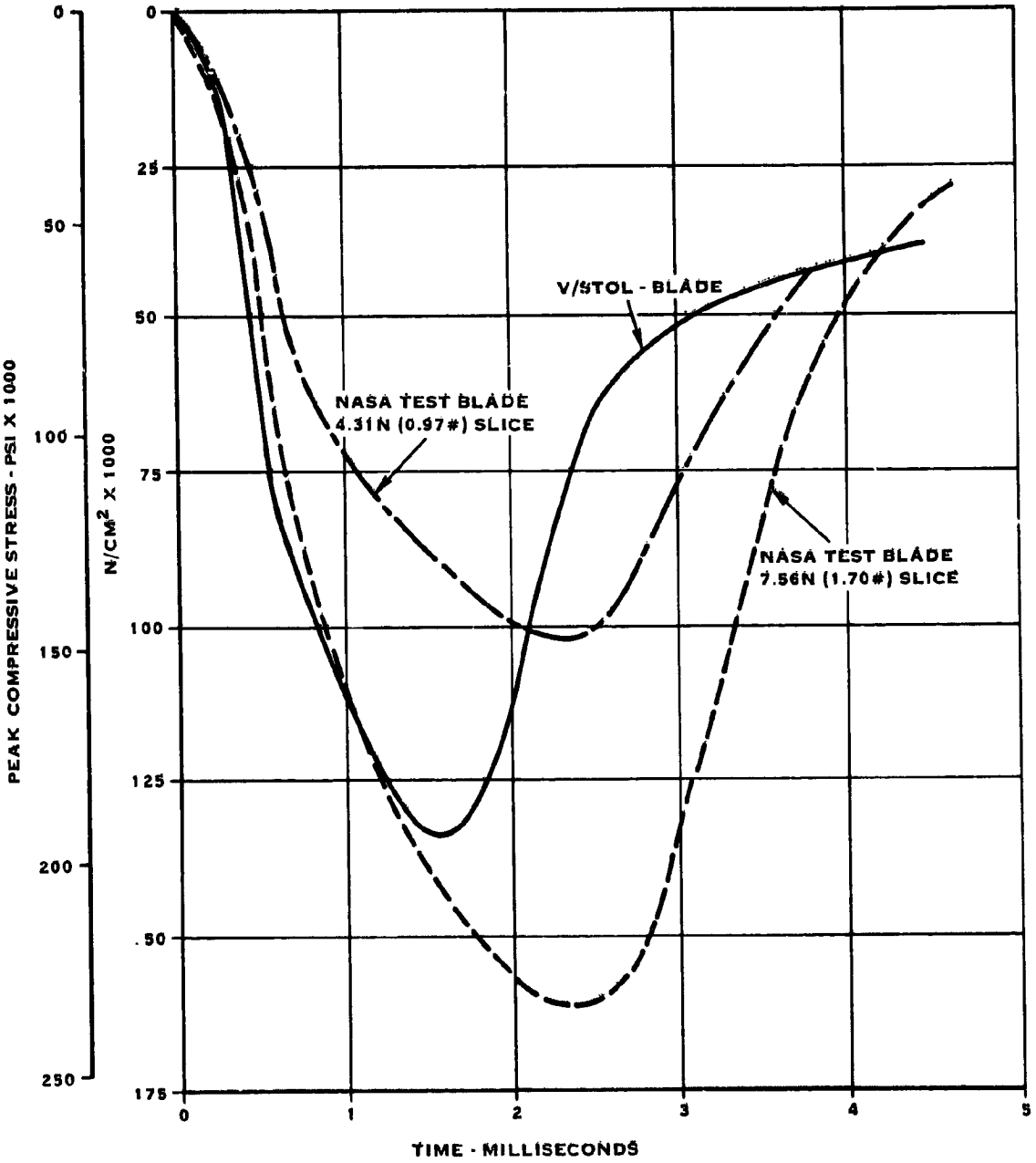

Figure 4-28. Mid-Blade Spanwise Bending Stress

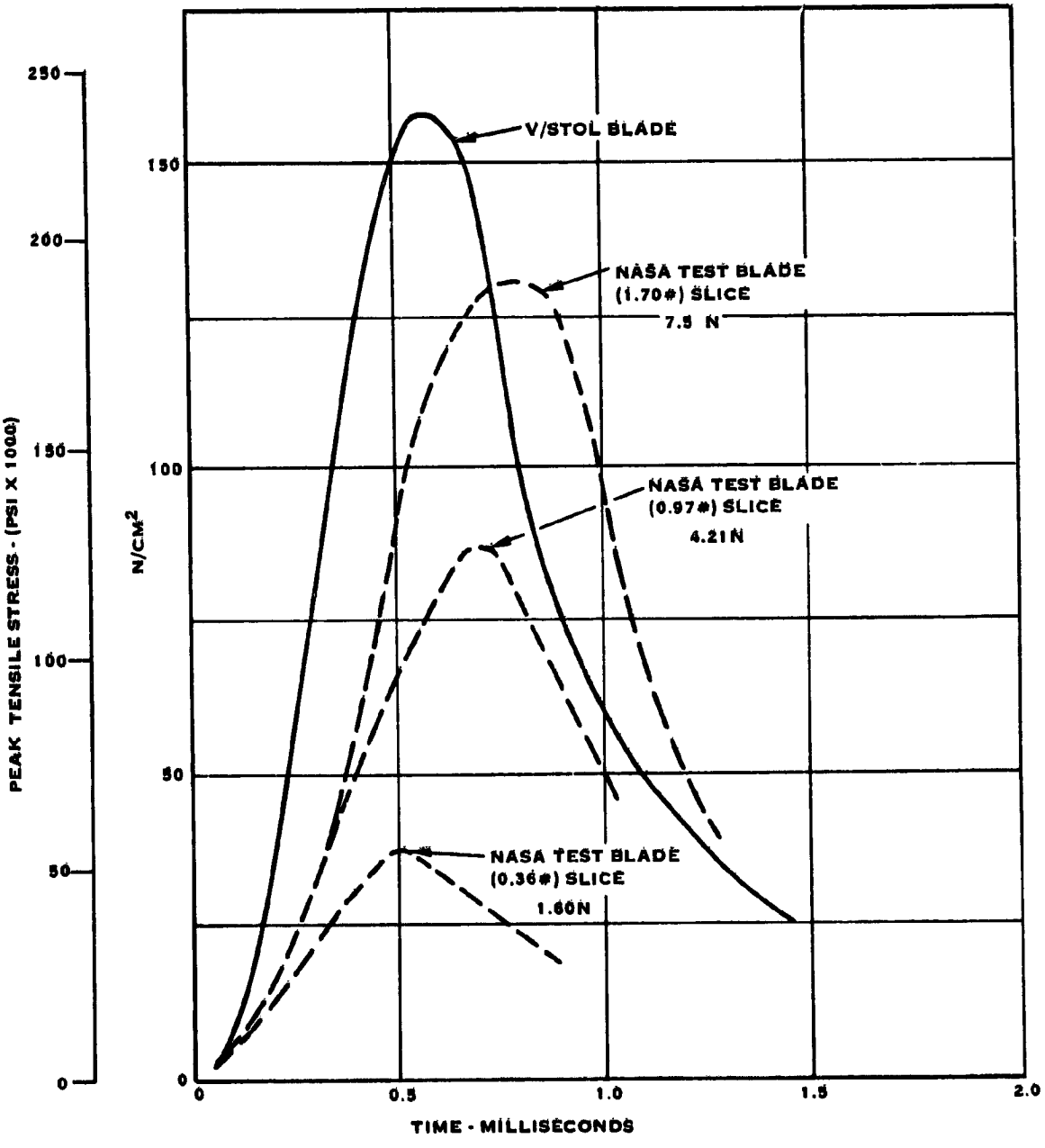

Figure 4-29. FOD Impact Station Spanwise Bending Stress

4.2.2.2 (Continued)

The requirement of variable pitch necessitates the use of a round retention and the inclusion of an anti-friction bearing. The retention that was selected for the V/STOL is a configuration that has been in service for more than six years and has successfully accumulated over one million flight hours. It is an angular contact ball bearing with an integral outer race in the steel disc and a split inner steel race on the titanium blade spar. The outer race is induction-hardened to RC 56 minimum in the region of the ball contact. The inner race is through-hardened to RC 56 minimum. Ball-to-ball contact is prevented through the use of separators.

The proposed lubrication system for the blade retention bearing consists of an ion-sputtered moly-disulfide (MOS_2) coating on the races and balls. The retention bearing dimensions are listed below:

Pitch dia. = 5.7099 cm (2.248 in.)

Ball dia. = 1.270 cm (0.5 in.)

No. of balls = 13

Initial contact angle 0.3698 to 0.6136 rad (21.19 to 35.16 deg)

With the above dimensions and loads, the retention bearing was analyzed.

The results are plotted on the contact stress Goodman diagram on figure 4-30, showing the relative position of calculated stresses and design allowables, and on a blow-up of the pertinent area on figure 4-31, with plots of previous design experience. The retention bearing stressing is satisfactory and within prior experience levels.

Disc - The single-piece disc concept, which has been utilized in Hamilton Standard's propeller and fan designs for nearly 15 years, will also be used on the V/STOL application. Steel, which has been the selected material for all previous designs, has been selected for the V/STOL application. Discs for variable-pitch fans have generally been designed for stiffness rather than strength in order to provide the retention stiffness required of a blade without part-span shrouds.

The disc is a fully machined component made from a D6AC vacuum melted steel forging. It is heat-treated to a hardness of RC 40-44 except in the blade retention area where it is induction-hardened locally to a minimum hardness of RC 56.

The stresses in the disc have been determined by a combination of ring, beam, and shell analysis methods. Partial stresses are calculated by each method due to different type loads and then added to determine the combined stress for various stations on the disc. The critically stressed area is the disc ring at the blade centerline. The loads imposed on the disc are the centrifugal force of the rotating disc by itself plus the steady and vibratory blade loads listed earlier. The normal bending and hoop stresses were calculated for each of these load cases and combined for a total steady stress plus and minus a total vibratory stress. These stresses are plotted on a modified Goodman diagram, figure 4-32, along with stress levels of several, recent applications. The disc design stresses are below the design allowable limits confirming an acceptable design.

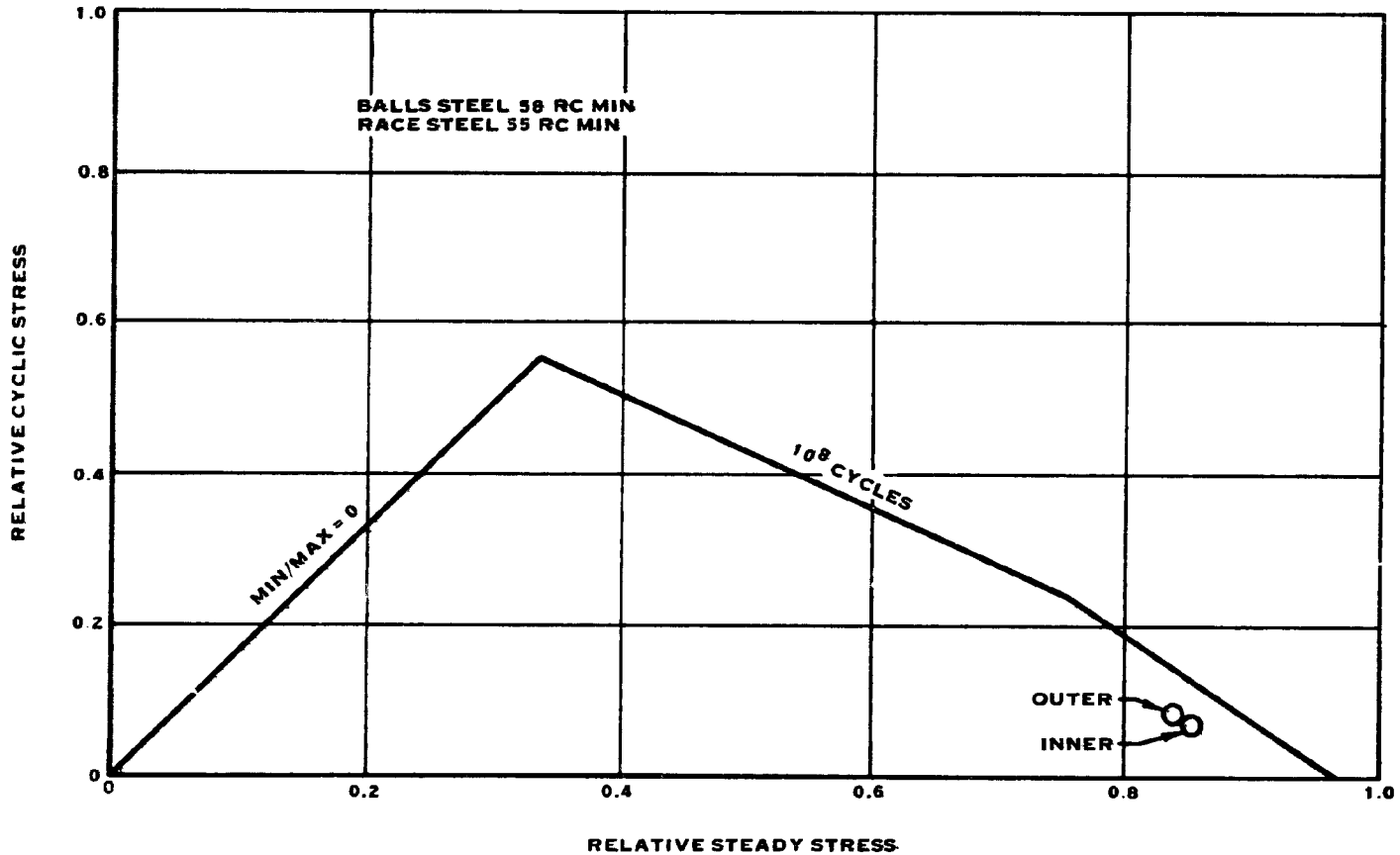

$$\text{RELATIVE STRESS} = \frac{\text{ACTUAL STRESS}}{\text{SELECTED MAXIMUM STRESS}}$$

Figure 4-30. Retention Contact Stress (Goodman Diagram)

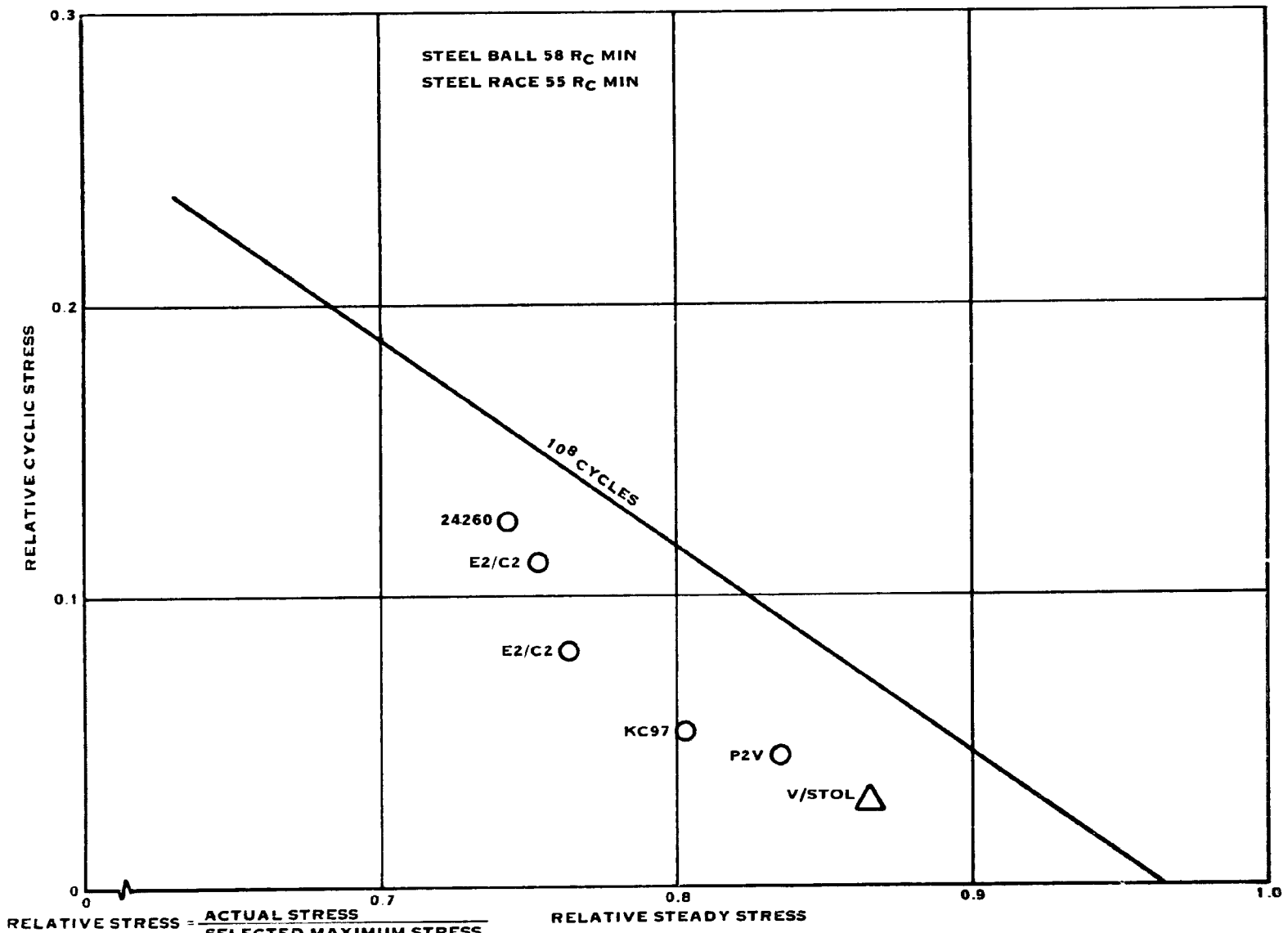

Figure 4-31. Blade Retention Stress Experience

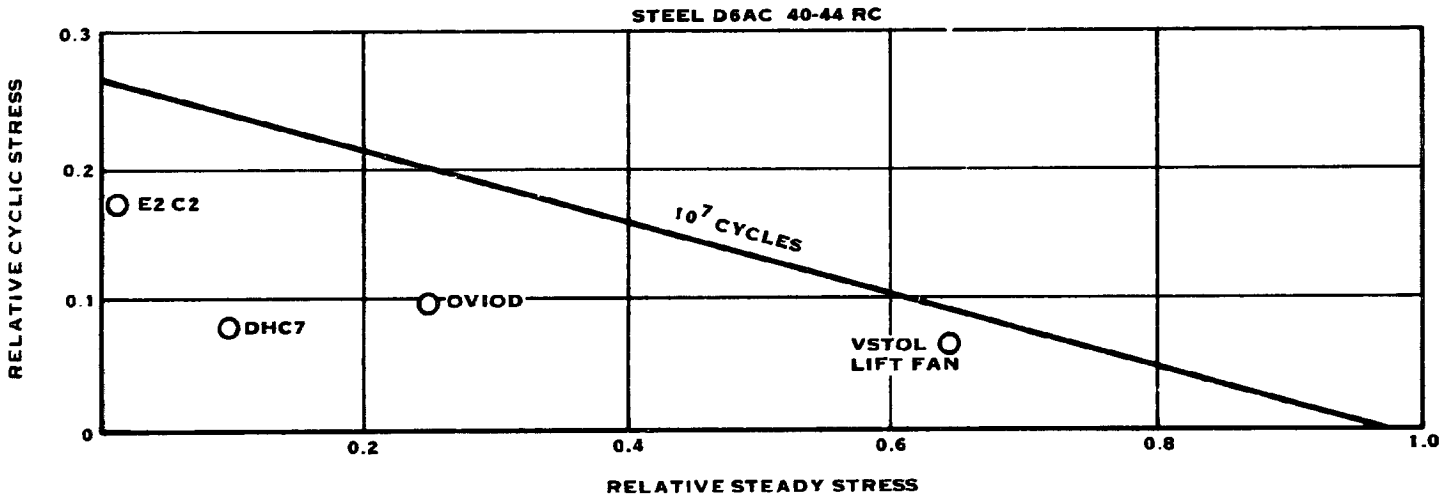

$$\text{RELATIVE STRESS} = \frac{\text{ACTUAL STRESS}}{\text{SELECTED MAXIMUM STRESS}}$$

Figure 4-32. Disc Stress Summary

4.2.3 Pitch Control System

The pitch control system draws heavily on proven concepts utilized on current aircraft applications. The pitch change concept was selected during the 1975 studies to provide the light weight, high reliability and safety necessary for a primary flight control system. It provides both hydraulic and mechanical redundancy to allow continued operation in the event of a hydraulic failure within or outside of the fan system or the failure of selected structural components.

The pitch change system employs a dualized linear hydraulic actuator that incorporates both hydraulic and structural redundancy. The actuator as illustrated in figure 4-33, is supported by the disc and connected to the blades by mechanical links. It also incorporates a splined torque restraint which removes circumferential loads from the blade links.

The control system which was defined by the 1975 design study is illustrated by the schematic presented in figure 4-34. It is powered by two independent aircraft hydraulic systems. Each system provides hydraulic power to one cylinder of the actuator via a beta regulator and transfer bearing. The beta regulator incorporates an electrically-controlled hydraulic servo valve (EHV) to modulate pressure to the actuator and a solenoid operated bypass valve to isolate the fan from a given hydraulic system in the event of a control system failure. Triple redundant electrical feedback is provided by linear variable displacement transducers (LVDT) attached to the actuator feedback arm.

Control system operation is monitored by a shutdown-abnormal-system (figure 4-34) which analyzes EHV position sensed electrically by LVDT's, hydraulic actuator position sensed by a triple-redundant LVDT, and a EHV comparator model. The shutdown system detects a control system failure and isolates the faulty hydraulic system via the solenoid-operated bypass valve.

The pitch change system characteristics are described in table VII.

Table VII
Pitch Change Characteristics

Time Constant:	0.1 second
Pitch Change Rate:	1.745 rad/sec (100°/second)
Blade Angle Range:	-0.5235 to + 1.5705 rad (-30° +90°) from design point
Flow Requirements:	0.69 liters/sec (11 gpm) per hydraulic system maximum flow rate at 2068.4 N/cm^2 (3000 psi).

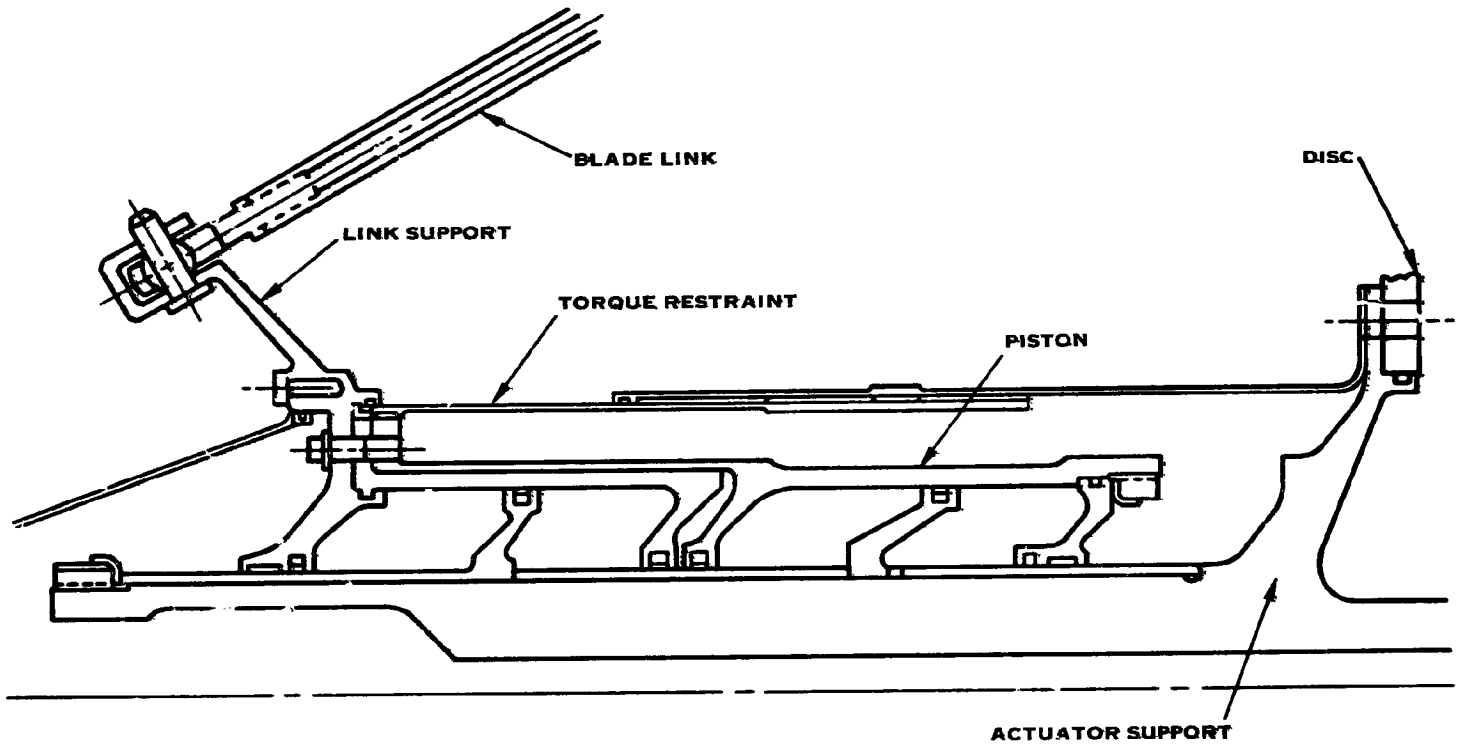

Figure 4-33. Actuator Concept

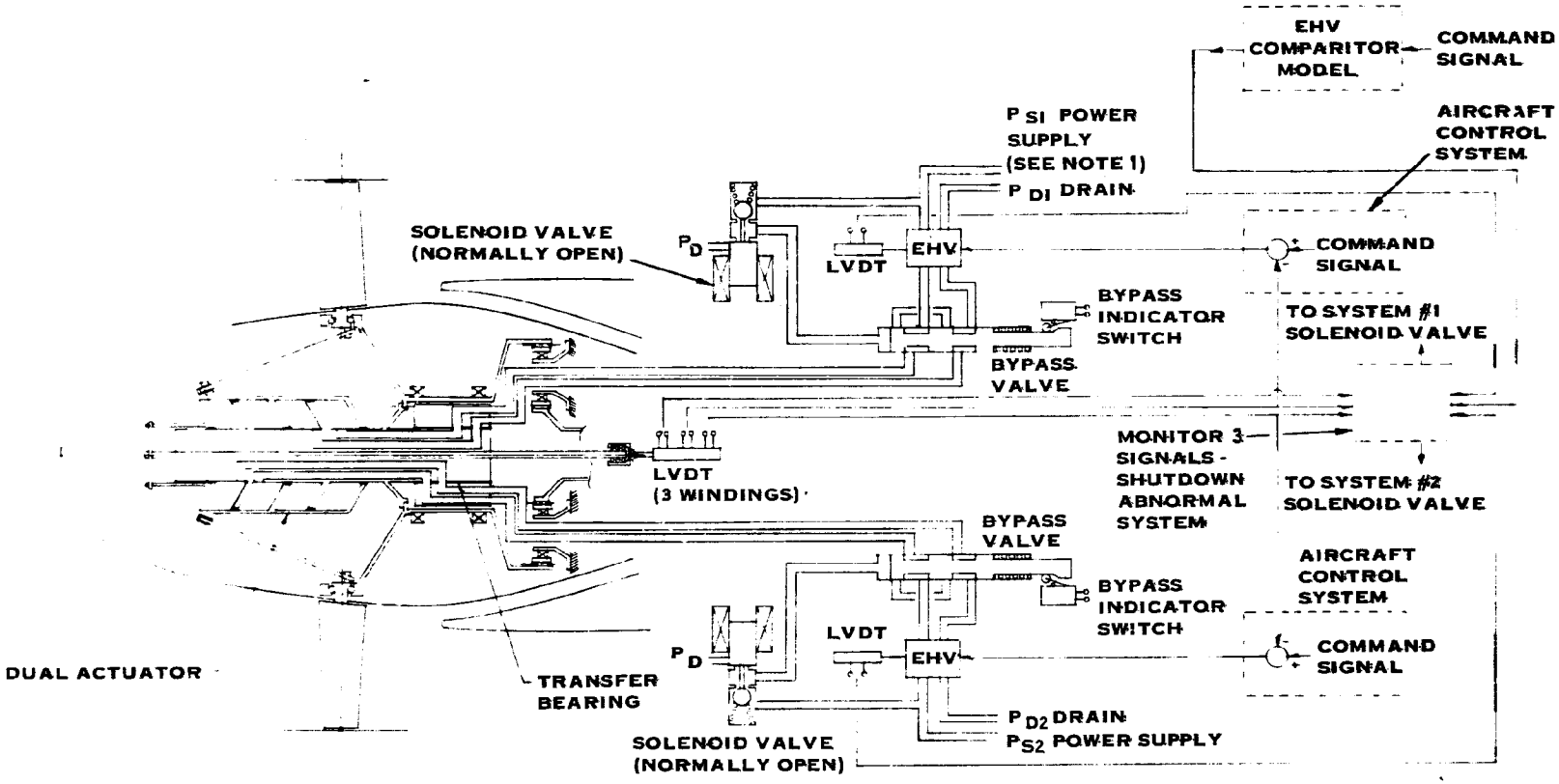

Note 1: Hydraulic pressure supplied from aircraft system.

Figure 4-34. Variable Pitch Control System

4.2.3 (Continued)

Elements of the actuation system were analyzed for structural capacity. The actuator loads are developed by the blades and are the result of centrifugal loads tending to rotate blade mass elements into the plane of rotation, retention friction and aerodynamic loadings. Because no load spectrum was available from the airframe contractors, loads were calculated for known conditions which could produce the maximum stress and an associated number of cycles assumed. These load conditions are presented in table VIII. The actuator piston and cylinder were not analyzed, but the component geometries were scaled from an existing similar design for the XC-142 main propeller. During its design, the XC-142 propeller actuator was analyzed for load conditions similar to the V/STOL fan.

Table VIII
Actuator Loads

	Load per Blade				
Condition	Steady		Cyclic		Cycles
Start - Stop	-60 N-M (-525 in.-lb)		± 50 N-M (± 525 in.-lb)		2×10^4
Hover	-80	(-712)	± 27	(± 239)	10^8
1 P	-92	(-814)	± 21	(± 186)	10^8
Bird Strike	273	(2420)	± 926	(± 8200)	1

Actuator elements which were analyzed include: blade link, blade pin, link support, torque restraint and center rod support. In all cases it was determined that the bird strike load determined the required structure. Table IX summarizes the results of the structural analysis.

Table IX
Actuator Design Margins

Item	Safety Margin* (bird strike)
Link	1.25
Pin	1
Link Support	20
Torque Restraint	11
Actuator Center Support (bending)	0.005

$$*\text{Safety Margin} = \frac{\text{Allowable Stress}}{\text{Actual Stress}} - 1$$

4.2.3 (Continued)

In all cases the member maximum stress during a bird strike is less than associated material design allowable. This assures a conservative design of the pitch control system, which will function satisfactorily during all modes of operation.

4.3 SYSTEM WEIGHT SUMMARY

The fan rotor is common to both the lift-cruise and lift fans. Mass, as tabulated below, were calculated for all rotor components.

Component	Mass	
Blades (26)	53.07	117 lbs.
Disc	50.80	112 lbs.
Spinner	12.7	28 lbs.
Pitch Change Actuator	29.03	64 lbs.
	145.60	321 lbs.

Weight for the gears and bearings were calculated during the gear study described in section 5.0. The gear weights resulting from this study are conservative because they are based on a structural analysis which assumed that the gearing would carry the maximum control power for the full life of the gearing. This was done because at the time of the study no time-load histogram of this data was available from the airframe contractors. The gear and rotor weights were combined with the weight values for the remainder of the system as calculated during the 1975 study to provide weight for the lift and lift-cruise fan shown below. Figure 4-35 provides a comparison of V/STOL design weights to actual weights of similar system components which have been fabricated for other applications.

Fan System Mass

	Lift-Cruise Fan		Lift Fan	
	(kg)	(lbs)	(kg)	(lbs)
Rotor	145.60	321	145.60	321
Beta Regulators (2 req'd)	4.99	11	4.99	11
Gear Reduction			186.88	412
Fan Case			121.11	267
Total	150.39	332	458.58	1011

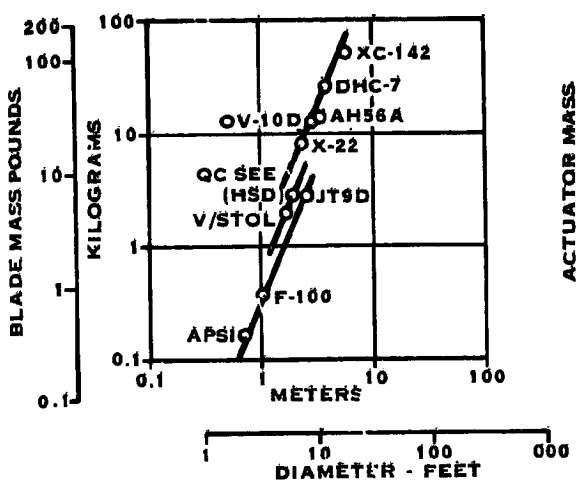

COMPOSITE BLADE MASS

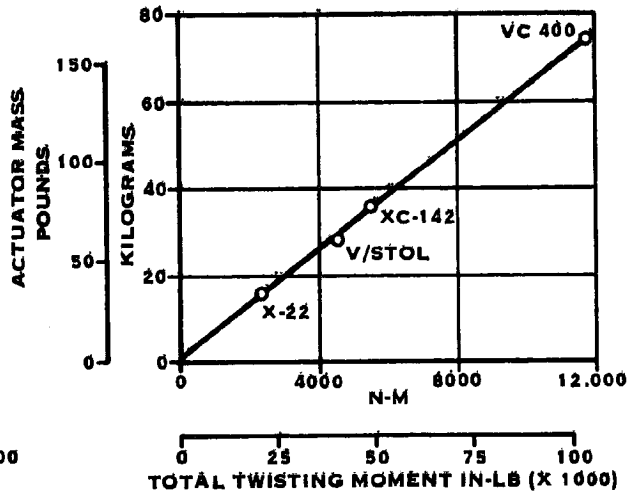

ACTUATOR MASS

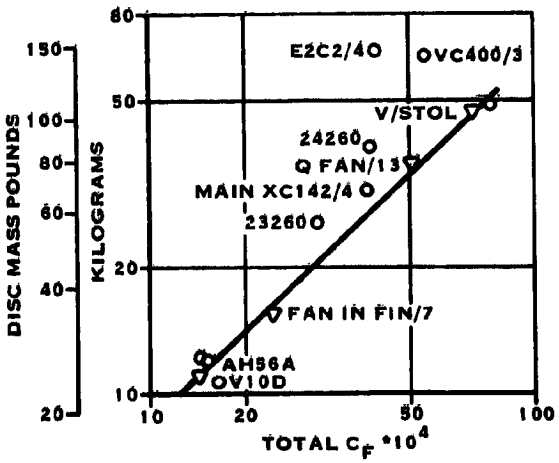

DISC MASS

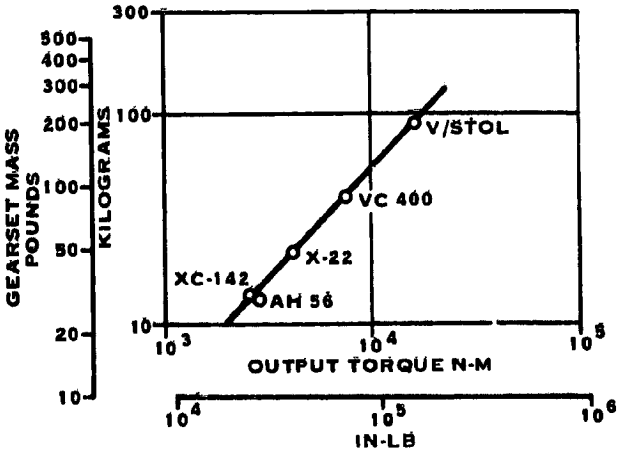

BEVEL GEARSET MASS

Figure 4-35. System Mass Experience

4.4 BEVEL GEARING STUDY

A bevel gear and cross shaft drive assembly is associated with both the lift and lift-cruise fans. During the 1975 studies, the cross shaft drive angle was 90° for both the lift and lift-cruise fans. It was intended at the onset of this program to evaluate the cross shaft drive systems with the objective of establishing commonality between the lift and lift-cruise fan bevel gearing in areas such as mounting arrangement, bearing type, size and placement. However, airframe studies had shown that the cross shaft drive angle for the lift fan should be different from the 90° angle for the lift-cruise fan eliminating the possibility of commonality. Study efforts were therefore directed at establishing a lift fan bevel gear mounting configuration having the lowest weight and best reliability.

Several tapered roller and roller-ball bearing configurations were evaluated for the gear arrangements shown in figure 4-36. Bearing loads were calculated for the fan and gearing data shown below.

Gear Ratio	3.33
Pinion	27 teeth
	1231 rad/sec (11755 rpm)
Gear	90 teeth
	370 rad/sec (3530 rpm)
Pitch	4.0
Pressure Angle	0.436 rad (25°)
Spiral Angle	0.436 rad (25°)

In addition to the gear loads the tail shaft bearings carry the fan loads shown below.

22895 N (5147 pounds) at maximum thrust

15746 N (3540 pounds) at mean thrust

443.3 N-M (327 ft-lb) 1P moment

1436 N (323 pounds) side load

Bearing loads were calculated for each bearing type and mounting configuration. Bearings were selected based upon catalogue sizing which would provide a 1500 hours actual B10 life based on vacuum-melt factors (life improvement factors due to higher cleanliness of the bearing material) of five for straight and tapered roller bearings and 10 for ball bearings. The loads and bearing weights are summarized in table X. For the input pinion configuration I, utilizing two tapered roller bearings was selected because it offered the lightest weight and most reliable system for the 1500 hours B_{10} life (2 bearings vs 3 bearings). For the tail shaft bearing configuration III also using three tapered roller bearings was selected. It, too, was selected for light weight and reliability.

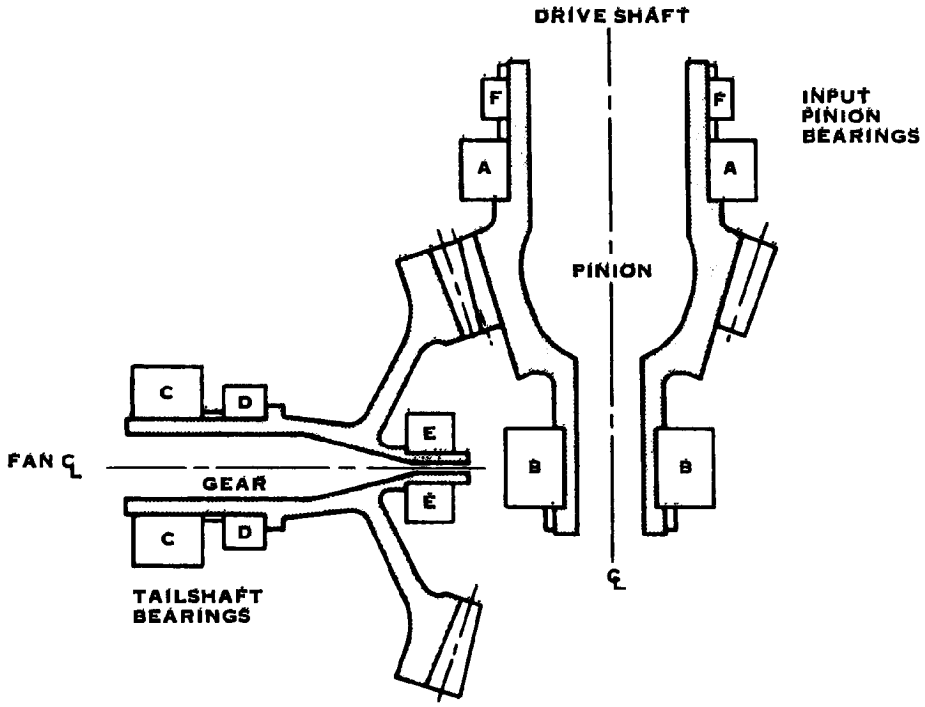

Figure 4-36. Lift Fan Bevel Gear Assembly

Table X. Lift Fan Drive Bearing Analysis

	CONFIG	BRG * POSITION	TYPE	DN	THRUST TAKEN	BRG WHEEL BASE	BRG RADIAL LOAD	BRG THRUST LOAD	BRG MASS	TOTAL BRG MASS	REMARKS
INPUT PINION	I	A	T ROLLER	1.44×10^6	B	7.50	3606 KG (7950 LB)	—	2.93 KG (6.46 LB)	8.37 KG (18.45 LB)	LIGHTEST ASSEMBLY WT LOW THERMAL MOTION AT MESH WITH THRUST AT B GOOD RELIABILITY (2 BRGS)
		B	T ROLLER	1.02×10^6	B		2502 (5516)	3160.6 KG (6968 LB)	5.44 (12.00)		
	II	A	BALL	1.44×10^6	B	9.20	3291.7 (7257)	—	5.08 (11.20)	15.28 KG (33.60)	HEAVIEST SINGLE BALL AT B IS LARGE TANDEMS WEIGHT PENALTY BRG A DESIGNED AS A DEEP GROOVE SPLIT INNER RACE CAN REACT GEAR THRUST IN CASE OF FAILURE OF BRG B FOR LIMITED LIFE
		B	TANDEM BALLS	1.92×10^6	B		2658.5 (5861)	4354.7 (9605)	10.16 (20.40)		
	III	A	T ROLLER	1.44×10^6	A	7.50	6545 (14.431)	3160.6 (6968)	7.62 (16.80)	8.78 (19.36)	OVERHUNG MOUNTING CONCEPT REQUIRES ADDITIONAL MOUNTING WEIGHT & ENVELOPE OUTBOARD
		B	T ROLLER	1.02×10^6	A		1100.3 (3065)	—	1.16 (2.56)		
	IV	A	T ROLLER	1.44×10^6	A	5.20	3308 (7293)	3206.7 (7268)	5.21 (11.50)	7.808 (17.24)	LIGHTEST BRG COMPLEMENT BUT MOUNTING WT FOR BRG F MAKES IT NOT LIGHTEST ASSY THRUST AT A CAUSES MORE THERMAL MOTION AT THE MESH LOWER RELIABILITY FOR 3 BRGS BRG F DESIGNED AS A DEEP GROOVE SPLIT INNER RACE FOR SOME ADDITIONAL WEIGHT CAN REACT GEAR THRUST FOR LIMITED LIFE IN CASE OF FAILURE OF BRG A
		B	ROLLER	1.02×10^6	A		3227.7 (7116)	—	2.19 (4.84)		
		F	BALL	1.02×10^6	A		—	116 (300)	0.408 (0.90)		
	V	A	BALL	1.44×10^6	A	5.20	3308 (7293)	3251.3 (7168)	6.71 (14.80)	9.308 (20.54)	BALL AT A IS INHERENTLY HEAVIER THAN A T ROLLER FOR COMBINED LOADS
		B	ROLLER	1.02×10^6	A		3227.7 (7116)	—	2.19 (4.84)		BRG F DESIGNED AS A DEEP GROOVE SPLIT INNER RACE FOR SOME ADDITIONAL WEIGHT CAN REACT GEAR THRUST FOR LIMITED LIFE IN CASE OF FAILURE OF BRG A
		F	BALL	1.02×10^6	A		—	90.7 (200)	0.408 (0.90)		
	VI	A	TANDEM BALLS	1.44×10^6	A	5.20	3308 (7293)	3251.3 (7168)	9.65 (19.88)	11.248 (24.82)	TANDEM BALLS ARE INHERENTLY HEAVIER THAN A SINGLE BALL BRG F DESIGNED AS A DEEP GROOVE SPLIT INNER RACE FOR SOME ADDITIONAL WEIGHT CAN REACT GEAR THRUST FOR LIMITED LIFE IN CASE OF FAILURE OF BRG A
		B	ROLLER	1.02×10^6	A		3227.7 (7116)	—	2.19 (4.84)		
		F	BALL	1.02×10^6	A		—	90.7 (200)	0.408 (0.90)		
TAILSHAFT BEARING	I	C	BALL	0.88×10^6	C	6.60	3527.7 (7766)	3514 (7747)	7.12 (15.70)	10.827 (23.89)	GOOD TOLERANCE OF SHAFT ANGULARITY GOOD CONTROL OF PRELOAD THRU SHORT PATH ROLLER AT E IS NOT OPTIMIZED FOR THE REQ'D BORE AND IS APPROXIMATELY 1 LB TOO HEAVY
		D	BALL	0.88×10^6	C		—	90.7 (200)	0.757 (1.67)		
		E	ROLLER	0.57×10^6	C		5701.6 (12570)	—	2.95 (6.52)		
	II	C	T ROLLER	0.88×10^6	C	6.60	3827.7 (7766)	3514 (7747)	5.04 (11.12)	12.92 28.51	HEAVIEST BALL AT E IS INEFFICIENT FOR THE HIGH RADIAL LOAD FROM THIS GEAR MESH
		E	BALL	0.57×10^6	C		5701.6 (12570)	—	7.88 (17.39)		
	III	C	T ROLLER	0.88×10^6	C	7.357	2606.8 (5747)	3514 (7747)	4.97 (10.96)	7.34 (16.54)	LIGHTEST BUT LESS TOLERANT OF SHAFT ANGULARITY LIFE IS REDUCED FOR ANGLES GREATER THAN 0.001 IN IN LESS CONTROL OF PRELOAD WITH LONGER LESS STIFF LOAD PATH OVER LENGTH OF HOUSING DESIGN STUDY IS REQ'D TO TRADE OFF ADDITIONAL WEIGHT REQ'D FOR HOUSING STIFFNESS VS BRG WEIGHT OVER CONFIG 1
		E	T ROLLER	0.57×10^6	C		6472.5 (14.269)	—	2.57 (5.68)		

*REF FIG. 3.14

SECTION 5.0
AIRFRAME AND CONTRACTOR SUPPORT

In addition to the interface activity described in section 3.0, detailed information generated during the preliminary design study was provided to McAir, BMAD, and DDA. This information consisted of the following:

- Fan performance maps (6) for five blade angles at speeds ranging from 20% to 110% speed.
- Supercharging performance (6 charts) for five blade angles and speeds ranging from 20% to 110%.
- Component weights (section 4.3).

Program planning data consisting of costs and schedules for the engineering, development and hardware associated with a two aircraft RTA program was also provided to DDA for their use under NASA contract NAS 3-20034.

Late in the study, MCAIR requested that the feasibility of a reduction in fan bypass stator exit Mach number be examined as a means of improving the gross thrust coefficient for the lift-cruise fan nozzle. High fan exit Mach numbers are inherent in low bypass fans when operating at high specific flow because of the lower density of the bypass air. Reduction of the Mach number by diffusion within the bypass nozzle was not possible because of the close proximity of the stator exit to the nozzles.

MCAIR's objective was to decrease the stator exit Mach number from the current value of 0.51 at take-off condition to about 0.30. A study was made to examine a Mach number reduction by means of diffusion through the bypass stators. The flowpath was modified and the stator solidity was increased producing a reduction in Mach number to about 0.40. However, there was a corresponding reduction of 25% in the fan stall margin and an efficiency reduction of 2% at the take-off and maximum control conditions.

While this approach to reducing stator exit Mach number appeared feasible, it has not been used in any previous applications and could be a technically challenging approach to implement. Therefore, additional studies were made to examine alternate means of reducing the stator exit Mach numbers. These studies included diameter changes, reduction in the rotor blade row convergence, increases in the rotor speed, moderate changes in the stator exit-to-inlet area ratio and raising of the operating line (reduction in the fan nozzle area). Each of these approaches are attempts to increase flow

5.0 (Continued)

area or reduce airflow with operation at higher fan pressure ratios with acceptable blade row diffusion factors. It was found that the stall margin loss was more rapid with these approaches than for diffusion through the stators.

It was concluded, therefore, that while technically challenging, diffusion through the fan exit stators was feasible and the best approach of those examined to reducing the stator exit characteristics.

The results of this work were discussed with McAir who concurred that further work in this area was unwarranted.

To support the lift fan drive train mechanical design, the power to drive the fan during transient start-up operation was analyzed.

The V/STOL propulsion system is designed so that the lift fan will be stopped during conventional forward flight. The lift fan drive train will contain a system to open the drive train channel so that power will not be transmitted to the lift fan. There are times when the lift fan will have to be engaged after the input drive system is already at governed speed, such as an approach to vertical landing. While engaging the lift fan, the coupling device will have to accommodate a speed differential between the constant speed input drive shaft and the nonrotating lift fan.

Figure 5-1 shows the power required throughout the start-up speed range. The indicated power is the steady state power required to drive the fan at the indicated rotational speed. Some additional power will be required to accelerate the fan depending on the acceleration rate.

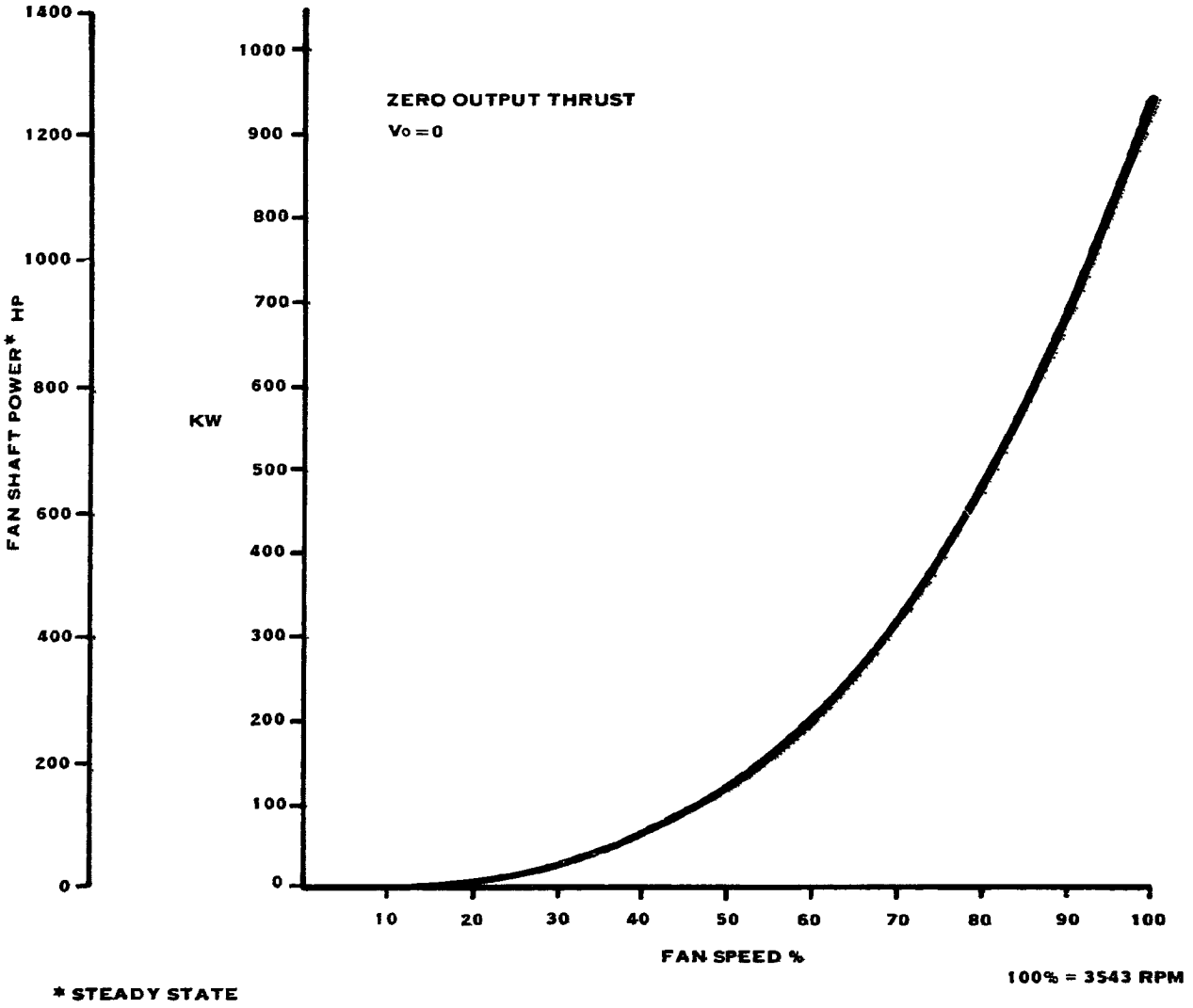

Figure 5-1. Lift Fan Power

INTERFACE DEFINITION

FOR

LIFT/CRUISE TURBOFAN ENGINE COMPONENTS

NASA/NAVY V/STOL RESEARCH AND TECHNOLOGY AIRCRAFT PROPULSION SYSTEM

HAMILTON STANDARD DIVISION
UNITED TECHNOLOGIES CORPORATION

DETROIT DIESEL ALLISON DIVISION
GENERAL MOTORS CORPORATION

JULY 1976
REVISION "B" JANUARY 1977

APPROVED:

R. M. LEVINIAN
HAMILTON STANDARD

S. M. HUDSON
DETROIT DIESEL ALLISON

CONTENTS

I. INTRODUCTION (REVISION B)

The Hamilton Standard (HS) Division of United Technologies Corporation and the Detroit Diesel Allison (DDA) Division of General Motors Corporation are engaged in concept definition studies of lift/cruise propulsion systems for a NASA/Navy V/STOL research aircraft under NASA contracts NAS3-19414 and NAS3-20033 with HS, and NAS3-20034 with DDA. These contracts require that the interfaces between the HS fan components and the DDA engine components be defined. This document defines the interface details which have been identified to date and the responsibility for components resulting from these interface details.

The refinement of details of the interfaces between the HS and DDA components defined herein will be recorded in revisions to this interface definition document as the program progresses. Any major interface changes from this document shall be identified in writing to the NASA Project Manager.

The lift fan interface definition agreed to between the airframe contractors and Hamilton Standard as part of HS's work under Contract NAS 3-20033 is incorporated into this document as Addendum A.

II. GENERAL DEFINITIONS AND RESPONSIBILITIES (REVISION A)

The V/STOL propulsion system consists of two turbofan engines, a remote lift fan and the associated gearing and shafting required to couple these components. Identical variable pitch fan rotors are used in the turbofan engines and the lift fan. This document deals with the interface between the Hamilton Standard variable pitch fan rotor and the Allison turboshaft engine, gearbox assembly and fan frame and case, which together form the turbofan engine

DDA is responsible for the gas turbine components and the resulting complete turbofan engine. Hamilton Standard is responsible for the single stage variable pitch fan and the actuators and controls associated with blade movement. This fan responsibility includes defining the overall fan stage performance and operating envelope, and providing the aerodynamic definition for rotating and stationary components within the stage. Hamilton Standard is also responsible for all mechanical components and functions of the fan rotor assembly and will therefore coordinate the aero-mechanical design. DDA will be responsible for the mechanical design of the stationary fan components since these will be integrated into the turbofan engine forward frame structure.

Signals for the positioning of the fan blade may come from the engine fuel control and the aircraft flight control. Hamilton Standard is responsible for the components required to condition these signals and convert them into blade angle settings on the variable pitch fan rotor. DDA will provide the power in the form of hydraulic pressure and flow for use in the HS actuators. The gearing, lubrication, accessory drives and aircraft structural interfaces are the responsibility of DDA. Overall lift/cruise turbofan engine performance is the responsibility of DDA.

III. REFERENCE DRAWINGS, DOCUMENTS AND SPECIFICATIONS (REVISION B)

DRAWINGS - The following drawings define the components and the associated interfaces which are the subject of this document:

HS DRAWINGS

SK 92249	Beta Regulator Envelope
SK 92250	Lift/Cruise Fan Installation
L-13081-8	Control Schematic
Preliminary Aero Lines - DB 4/14/75	

DDA DRAWINGS

SK 20163	PD370-25 A RTA Fan Engine Installation
SK 20148	RTA Engine-Fan Interface Definition
SK 20219	PD370-25A RTA General Arrangement
SK 20249	PD370-25E RTA General Arrangement
SK 20276	PD370-25E RTA Fan Engine Installation

DOCUMENTS - The following documents provide definition of the subject interfaces:

Statement of Work for NASA Contracts NAS3-19414, NAS3-20033 and NAS3-20034 with Hamilton Standard and DDA respectively.

A coordination memo system exists between HS and DDA which will be used to define interfaces for this program as the fan and engine component designs progress. Data such as rotor speeds, pressure profile, and flow rates will be coordinated using this system. These interface coordination memos will be included in this Interface Definition Document as an addendum.

SPECIFICATIONS -

The following specifications apply or may be used by reference to define the subject interface:

MIL-E-5007D - General engine requirements.

AS3694, 31 May 1973, "Transmission Systems, VTOL-STOL General Requirements for."

A DDA engine specification will be issued to cover the selected lift/cruise turbofan engine which will cover both the Hamilton Standard and DDA components as a unit. This specification will be issued after the engine design characteristics are established.

IV. INTERFACE DEFINITIONS (REVISION B)

The following table defines the responsible contractor for the various components of the lift/cruise turbofan engine and in turn the interfaces between mating Hamilton Standard and DDA components:

		RESPONSIBLE CONTRACTOR	REFERENCE DRAWING
1.0	**MECHANICAL INTERFACE**		
1.1	Fan - Engine Installation		
1.1.1	Fan Installation Drawing	HS	SK92250
1.1.2	Engine-Fan Interface Drawing	DDA	SK20148
1.1.3	Fan Engine Installation Drawing	DDA	SK20163 & SK20276
1.1.4	Fan Engine General Arrangement Drawings	DDA	SK 20219 & SK 20249
1.2	Fan-Engine External Envelope		
1.2.1	Fan External Envelope	HS	SK 92250
1.2.2	Engine External Envelope	DDA	SK 20163
1.2.3	Fan-Engine Envelope	DDA	SK 20163
1.3	Fan Drive		
1.3.1	Fan Drive Shaft Flange	DDA	SK 20148
1.3.2	Fan Wheel Rear Flange	HS	SK 92250
1.3.3	Fan Drive Shaft	DDA	SK20148
1.3.4	Fan Drive Shaft Bearings and Support	DDA	SK20148
1.4	Actuator		
1.4.1	Actuator Envelope	HS	SK92250
1.4.2	Transfer Bearing Envelope	HS	SK92250
1.4.3	Inner LVDT Envelope	HS	SK92250
1.4.4	Beta Regulator Envelope	HS	SK92249
1.5	Fan Parameters		
1.5.1	Fan Design Speed	HS	NA
1.5.2	Fan Blade Tip Clearance	HS	SK20148
1.5.3	Fan Speed Pickup	DDA	SK20148
1.6	L/C Rotor Assembly	HS	SK92250
1.6.1	L/C Rotor Component Weight and CG	HS	NA
1.6.2	L/C Rotor Component Polar Moment	HS	NA
1.6.3	L/C Power Requirements	HS	NA
1.7	L/C Gearbox Assembly	DDA	SK20219 & SK20249
1.7.1	Reduction & Bevel Gears & Cross Shaft	DDA	SK20219 & SK20249
1.8	Stationary Components		
1.8.1	Fan Duct Stator Definition	DDA	SK20148
1.8.2	Engine Inlet Stator Definition	DDA	SK20148
1.8.3	Fan-Engine Transition Definition	DDA	SK20148
1.8.4	Primary-Secondary Flow Splitter	DDA	SK20148

		RESPONSIBLE CONTRACTOR	REFERENCE DRAWING
1.0 MECHANICAL INTERFACE (Continued)			
1.9	Forward Frame		
1.9.1	Forward Frame Materials	DDA	SK20148
1.9.2	Forward Frame Temperatures	DDA	NA
1.9.3	Fan Blade Tip Seal Material	DDA/HS	SK20148
1.10	L/C Modules		
1.10.1	L/C Fan Module Definition	HS	SK92250
1.10.2	L/C Fan Turboshaft Engine Module Def.	DDA	TBD
2.0 AERODYNAMIC INTERFACE			
2.1	Component Design Responsibility	HS	NA
2.2	Fan Stage Maps	HS	NA
2.3	Engine Inlet Vane Aero Parameters	HS	NA
2.4	Fan Duct Stator Aero Parameters	HS	NA
2.5	Primary-Secondary Flow Splitter	HS	NA
3.0 ELECTRICAL INTERFACE			
3.1	Pitch Control Schematic	HS	L-13081-8
3.2	Electrical Connection Definition	HS	SK92250
3.3	Redundance Requirements	HS	NA
3.4	Wiring Definition		
3.4.1	Wiring Diagram	HS	NA
3.4.2	Amperage in Wires	HS	NA
3.4.3	Voltage in Wires	HS	NA
3.5	L/C Fan Control Modes	HS/DDA	NA
3.6	L/C Fan Instrumentation Requirements	HS	NA
3.7	L/C Fan Turboshaft Engine Control System	HS/DDA/AC	NA
3.8	Fan Speed Pickup	DDA	SK20148
4.0 HYDRAULIC INTERFACE			
4.1	Hydraulic Connections	HS	SK92250
4.2	Type of Oil	DDA	NA
4.3	Oil System		
4.3.1	Type & Size of Oil Supply Lines	DDA	SK20148
4.3.2	Oil Pressures	HS	NA
4.3.3	Oil Flow Rates	HS	NA
4.4	L/C Fan Oil Filter Requirements	HS	NA
4.5	Redundance Requirements	HS	NA
4.6	Fan Rotor Lubrication Requirements	HS	NA
4.7	Pump Drive Locations	DDA	TBD
4.8	Leakage Allowables	HS	NA

ABBREVIATIONS:

TBD - To be determined as the program progresses.

NA - Not applicable, this notation applies in this table to the form of transmitting data. The majority of the data so noted will be supplied in the form of interface coordination memo which will become a part of this interface document.

ADDENDUM A

LIFT FAN INTERFACE DEFINITION

ADDENDUM A

LIFT FAN INTERFACE DEFINITION

The lift fan interface which has been coordinated with the airframe study contractors, Boeing and McDonnell, is provided by the installation drawings noted below. These drawings will be updated during the fan detail design to define all mechanical interfaces.

Airframe Contractor	Drawing No.
Boeing	SK 92252
McDonnell	SK 92251

The beta regulator envelope as defined by drawing SK 92249 is common to both airframe contractors and DDA for the lift/cruise fan.

Additional data pertaining to the lift fan interface which will be established during the fan detail design is as follows:

1.0 Fan Operational Parameters

- 1.1 Fan Design Horsepower
- 1.2 Fan Design Speed

2.0 Fan Characteristics

- 2.1 Weight
- 2.2 Polar Moment of Inertia
- 2.3 Center of Gravity
- 2.4 Vibration Limits
- 2.5 Gear Ratio

3.0 Aerodynamic Characteristics

- 3.1 Fan Stage Maps

4.0 Electrical Interface

- 4.1 Wiring Diagram
- 4.2 Voltage Requirements
- 4.3 Power Requirements
- 4.4 Instrumentation Requirements

5.0 Hydraulic Interface

5.1 Pressure Requirements
5.2 Flow Requirements
5.3 Filtration Requirements
5.4 Pitch Control Schematic
5.5 Leakage Allowables
5.6 Heat Load
5.7 Type of Fluid